Palladium and Ruthenium Catalyzed Reactions

By

Bryan Jaksic

A thesis submitted to the Department of Chemistry
In conformity with the requirements for
the degree of Master of Science

Queen's University
Kingston, Ontario, Canada
(June, 2011)

Abstract

Part one of this thesis will discuss research which involves the direct comparison of the activity of commonly used precatalysts with the newly synthesized precatalyst, $Pd(\eta^5\text{-}C_5H_5)(\eta^3\text{-}1\text{-}Ph\text{-}C_3H_4)$, for Sonogashira cross-coupling reactions. Sonogashira reactions are important as they provide a simple method for the formation of substituted alkynes, a commonly found functionality within important organic molecules. These reactions are generally believed to be catalyzed by a $Pd(0)L_2$ species which are generated *in situ* from a palladium precatalyst and are often co-catalyzed by CuI although use of the latter is undesirable as it induces homocoupling in certain instances. The rate and quantity of active species generated is not known for the commonly used precatalysts and is a potential reason for decreased rates and yields. Norton *et al*. have recently demonstrated that the newly synthesized, easily handled compound $Pd(\eta^5\text{-}C_5H_5)(\eta^3\text{-}1\text{-}Ph\text{-}C_3H_4)$ is a superior precatalyst as it generates the active $Pd(0)L_2$ species more quickly than other commonly used palladium precatalysts. Part one of this thesis will discuss research which investigated the efficiencies of precatalysts used for Sonogashira cross-coupling reactions.

Part two of this thesis will discuss research into the syntheses of a novel series of ruthenium complexes and their utilization as ester hydrogenation catalysts. Reduction of esters to the corresponding alcohols is normally carried out using $LiAlH_4$, a stoichiometric type of reaction which produces large amounts of undesirable by-products. Ruthenium-based catalysts are known to hydrogenate a variety of functional groups and many catalytic systems have been developed for the hydrogenation of alkenes, ketones, etc. The recent literature also describes a small number of ruthenium catalyst systems which enable ester hydrogenation to the same types of alcohols produced by $LiAlH_4$ reduction albeit catalytically, a much "greener" type of chemistry. This paper will discuss the syntheses of a series of $Ru(acac)_2(phosphine)_{1\text{-}2}$ complexes and their utilization as ester hydrogenation catalysts.

Acknowledgements

I would like to begin by thanking Dr. Michael Baird for the opportunity to be a part of his research group. I have truly appreciated his guidance and patience. I would also like to thank Dr. Ruiyao Wang for the crystallographic work.

I would like to thank past and present group members for helping with my research whether it be starting the project or giving suggestions and guidance to further it. I would like to thank all the friends I've had the pleasure of getting to know at Queen's, you all made my time here more enjoyable.

I would like to thank my friends for all their support and understanding throughout the course of my studies. I would like to thank all the Barrhaven beauties who regularly made the trip to Kingston to visit and keep me from missing home too much, I love you all. To my brother Steve, the one person I will always be able to count on, thanks for being you. I would also like to thank H.A.F. for always having my back and all the hilarious times.

Finally, I need to thank my parents, Clare and Joe. Without their support, generosity, and love I would never be where I am today. I owe everything I have accomplished to you and one day I will pay you back for all you have done for me.

.

Table of Contents

List of Figures

List of Tables and Equations

List of Symbols and Abbreviations

acac	acetylacetone
Ar	aryl group
atm	atmospheric pressure
Å	Ångström
Bu^t	tert-butyl group
°C	degrees Celsius
Cp	cyclopentadienyl group (η^5-C_5H_5)
Cy	cyclohexyl group
δ	chemical shift
dba	dibenylideneacetone
DCM	dichloromethane
DMF	dimethylformamide
DMO	dimethyl oxalate
dppe	1,1'-bis(diphenylphosphino)ethane
dppf	1,1'-bis(diphenylphosphino)ferrocene
dppp	1,1'-bis(diphenylphosphino)propane
Et	ethyl group
eq	equivalents
g	grams
GC	gas chromatography
h	hour
L	ligand
M	moles/litre
Me	methyl group
mg	milligram

MHz	megahertz
min	minutes
μL	microlitres
mL	millilitres
mmol	millimoles
mol	moles
NEt_3	triethylamine
NMR	nuclear magnetic resonance
OAc	acetate
Ph	phenyl group
$P(n\text{-}C_8H_{17})_3$	trioctylphosphine
R	alkyl group
TFE	trifluoroethanol
THF	tetrahydrofuran
triphos	bis(diphenylphosphinoethyl)phenylphosphine

Part 1: Palladium Catalyzed Sonogashira Cross-Coupling Reactions

Chapter 1

Introduction

1.1 Cross-Coupling Reactions

Transition metal catalyzed cross-coupling reactions have been studied in depth with advancements in methodologies allowing for the synthesis of large complex organic molecules from smaller substituents.[1] These carbon-carbon bond forming reactions are found in most multistep syntheses for the production of compounds such as pharmaceuticals, simple organic molecules and precursors for natural products and are therefore some of the most important reactions in organic chemistry. In the general case, a coupled product, R-R', is generated through the reaction of an organometallic nucleophile (R-m) and an organic electrophile (R'-X) in the presence of a transition metal catalyst (C) (Figure 1).[1]

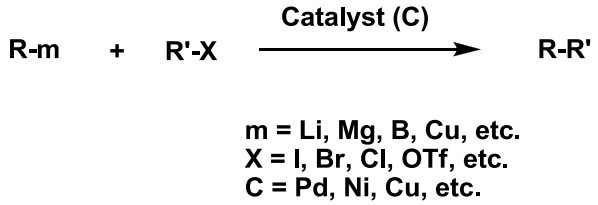

Figure 1. General cross-coupling reaction for C-C bond formation.

Due to the limitations of the organic groups R and R', which are reaction specific, many named cross-coupling reactions have been developed. The variation of m, X and C have produced cross-coupling systems capable of overcoming the limitations of the organic substrates.[1,2] Recent developments in catalysts and the availability of reagents has allowed for the expansion of cross-coupling reactions to include other bond forming reactions such as C-N, C-O and C-S bonds.

1.2 The Sonogashira Reaction

The formation of substituted alkynes is one of the important carbon-carbon bond forming reactions with the carbon-carbon triple bond being an important structural feature of organic molecules.[3-5]

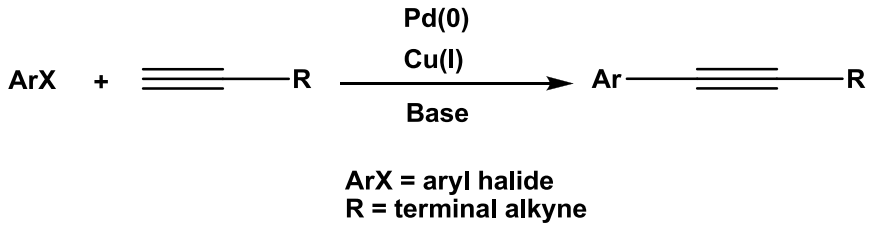

Figure 2. General Sonogashira cross-coupling reaction to produce substituted alkynes.

Alkynes are outstanding building blocks for unsaturated molecular scaffolds because of their conjugating π systems and rigid structure. They are a common functionality in natural products and have been isolated from plants and marine organisms. Furthermore, their unsaturated structure makes alkynes an attractive functional group for further derivation in many synthetic transformations such as the production of the contraceptive pill as well as enediyne antibiotics.[3-5]

1.2.1 The Development of the Reaction

As alkynes can be found in organic compounds that are involved in the syntheses of complex pharmaceuticals and natural products, the efficiency of the cross-coupling reaction to produce substituted alkynes becomes intriguing. The original method developed by Stephens and Castro[6] had significant limitations as it involved dangerous and difficult reactions that did not provide a viable industrial scale method for the production of substituted alkynes. The reaction involved pre-forming copper-acetylide compounds which can be explosive[3] and coupling them with organic halides in refluxing pyridine.[6]

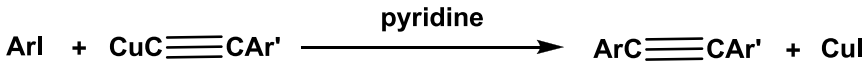

Figure 3. Stephens-Castro reaction to produce substituted alkynes.

In the early 1970's, Cassar[7] and Heck[8] independently published results stating a dramatic improvement for the method of substituted alkyne formation with both authors indicating the involvement of a palladium catalyst.

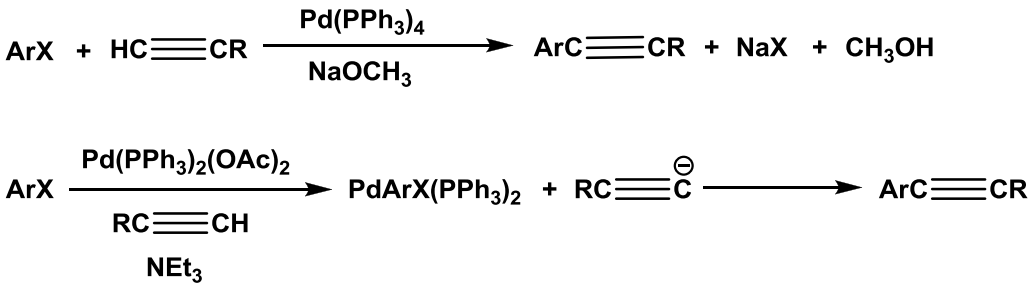

Figure 4. Improvements to the synthesis of substituted alkynes as reported by Cassar (top) and Heck (bottom).

The addition of a transition metal catalyst lead to more mild reactions as well as a wider substrate scope as the often difficultly synthesized and dangerous copper acetylide compounds no longer needed to be formed prior to reactions.[7,8]

The Heck and Cassar reactions were proof of concept that new catalyzed cross-coupling methodologies could also be applied to substituted alkyne forming reactions. Although catalytic, the discovery still had a large amount of limitations and also required harsh reaction conditions and lengthy reaction times to obtain yields greater than 90 %. The major limitation of the reaction under the specified conditions is that halides with strongly electron-donating substituents, or halides which are otherwise relatively unreactive do not react well with the palladium(0) catalyst.[9]

Also during the early 1970's, Kenichi Sonogashira discovered a superior catalytic method to produce a variety of substituted alkynes requiring more mild reaction conditions compared to the systems developed by Heck and Cassar. Unlike Heck and Cassar, the reaction conditions for

the Sonogashira system employed a co-catalyzed system, incorporating palladium and copper as co-catalysts. The copper was used as it presumably aids in the *in situ* formation of copper acetylides required for the rate determining transmetallation step.[10]

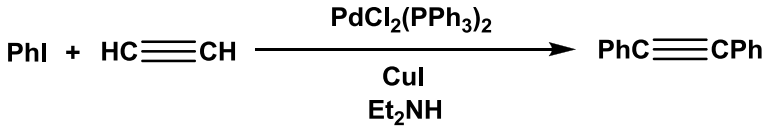

Figure 5. The original Sonogashira reaction.

The reaction involved an aryl halide coupling to a terminal alkyne in the presence of acetylene gas with a co-catalyzed system using $PdCl_2(PPh_3)_2$ and CuI. The availability of the catalysts and reagents, the simplicity of the procedure, and the mildness of the reaction conditions in comparison to other methods available made this reaction a highly useful technique for the formation of substituted alkynes.[10]

A significant amount of work has gone into the investigation of the Sonogashira reaction in terms of reaction conditions and substrates capable of partaking in the cross-coupling.[11,12] The literature states a variety of aryl halides capable of being coupled with a reactivity order determined to be ArI > ArBr > ArCl > ArF. There is a much larger variation of alkynes able to take part in the reaction with the only requirement being the presence of a terminal alkyne. Recent studies have demonstrated that co-catalyzed systems can be overcome through the variation of reaction conditions such as catalyst, phosphine and base used.[11,12] The general consensus of a Pd(0) active species has lead to the use of several different palladium(II) and palladium(0) precatalysts, most commonly $PdCl_2(PPh_3)_2$, $Pd(PPh_3)_4$, $Pd(OAc)_2$, or $Pd(dba)_2$, with the active species generated *in situ* through reduction or dissociation reactions.[11,12]

1.2.2 The Reaction Mechanism

The exact reaction mechanism is unknown but is generally agreed to proceed via the same basic mechanism as many other Pd-catalyzed cross-coupling reactions.[13] The generally

accepted catalytic cycle (Figure 6) begins with the generation of the catalytically active species $Pd(0)L_2$, followed by oxidative addition of the organic electrophile, then transmetallation with the copper acetylide complex, and ultimately reductive elimination to yield the coupled product and regenerate the catalyst.

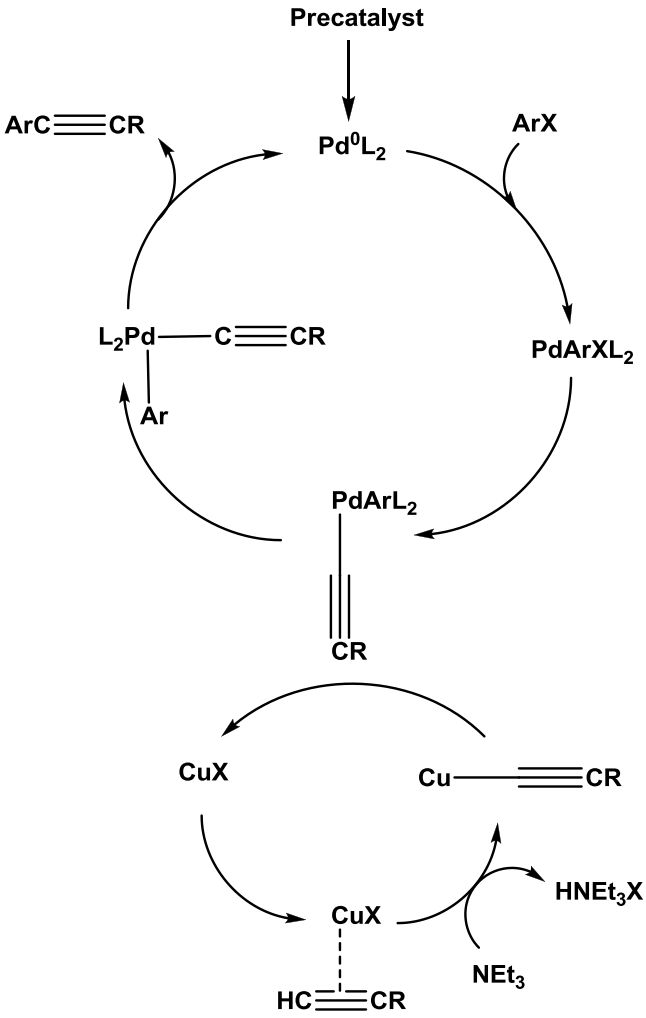

Figure 6. Generally accepted Pd/Cu co-catalyzed reaction mechanism for Sonogashira cross-coupling reactions.

1.2.2.1 Oxidative Addition

As previously mentioned, the catalytic cycle is not well understood with the oxidative addition product, $PdArXL_2$, being the only observable species in the cycle. As a result, the

oxidative addition step has been studied in depth. Oxidative addition of aryl electrophiles proceed via a 3-centered transition state (Figure 7) and can be the rate determining step when using less reactive organic electrophiles, such as aryl chlorides.[14-16] Two possible transition states were conceivable, proceeding via an ionic (top) or neutral (bottom) intermediate.[1b,17]

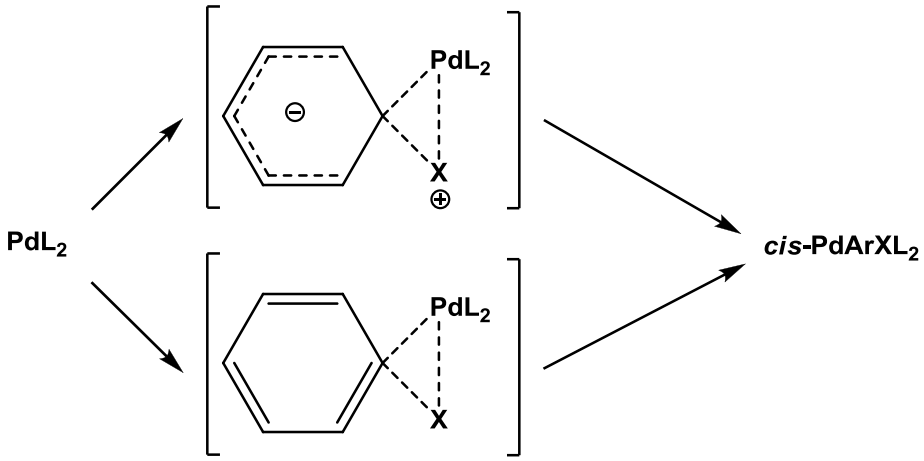

Figure 7. Potential transition states involved during oxidative addition.

Further studies carried out by Amatore and Pflüger[17] support the idea of a neutral transition state and lead to the conclusion of a concerted process to oxidative addition. This concerted addition is probably an associative reaction in which Ar-X first binds to PdL_2 as a σ complex, and then undergoes C-X bond breaking as a results of strong back donation from Pd(0) into the C-X σ* orbital.[19]

1.2.2.2 Transmetallation

The next step in the Pd-cycle connects with the cycle of the copper co-catalyst. Thus, a transmetallation from the copper acetylide formed in the Cu cycle would generate a $PdAr(C{\equiv}CR)L_2$ species (Figure 8), which gives the final coupled product after *trans/cis* isomerisation and reductive elimination with regeneration of the catalyst.[13,20]

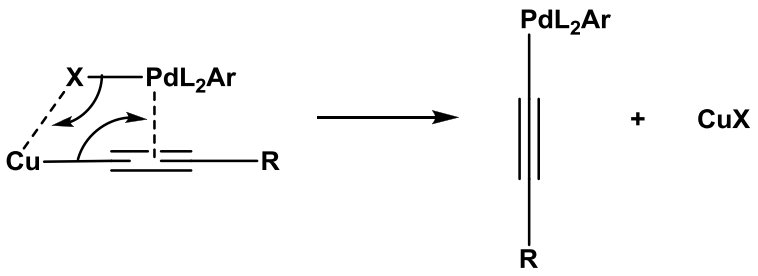

Figure 8. Proposed mechanism for transmetallation.

Seemingly simple, the actual Cu-cycle is still poorly understood.[20] A general accepted mechanism involves the base (generally an amine) abstracting a proton from the terminal alkyne, thus forming a copper acetylide in the presence of a copper(I) salt. It is known that the commonly used amines are not basic enough to deprotonate the free alkyne in order to generate the anionic nucleophile which would then form the copper acetylide. Therefore, it is hypothesized that a π-alkyne-Cu complex as shown in Figure 6 is involved in the cycle, thus making the alkyne proton more acidic for easier abstraction resulting in the desired copper acetylide formed *in situ*.[20]

1.2.2.3 Reductive Elimination

Reductive elimination is the final step of the catalytic cycle and is the process in which the catalysts, $Pd(0)L_2$, are regenerated by the release of the coupled product Ar-R from the Pd(II) complex $PdArRL_2$. Reductive elimination is essentially the reverse process of oxidative addition and may therefore occur through an analogous mechanism to the concerted oxidative addition step.[21] The accepted mechanism for reductive elimination (Figure 8) involves a three-centered transition state in which the aryl groups must be in the *cis* geometry for the elimination to occur.[19,21]

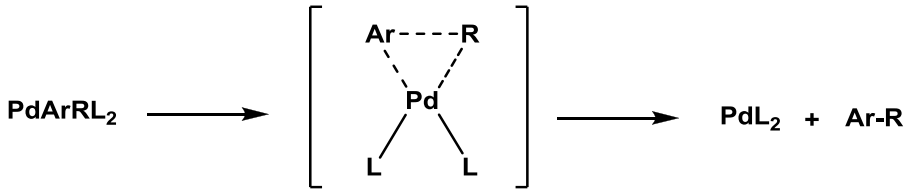

Figure 9. Transition state for reductive elimination.

1.3 The Copper-free Mechanism

Since the discovery of the Sonogashira reaction in 1975, several modifications have been reported including variation of the ligands, palladium sources, solvents, and bases in order to perform the coupling reactions more efficiently.[3,4,10,22-29] The presence of the copper co-catalyst facilitates the coupling reaction by the *in situ* generation of copper acetylide, but it can also induce a Glaser-type oxidative homocoupling of the terminal acetylene to yield a diyne (Figure 10).[22]

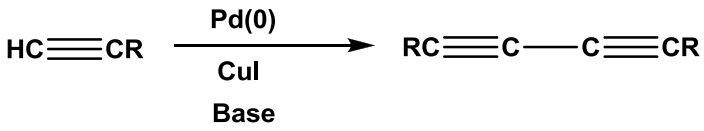

Figure 10. Diyne product from homocoupling of the terminal alkyne.

Several research groups have focused on suppression of the undesired bi-product by developing copper-free versions of the Sonogashira reaction.[22-24]

As is the case for the copper co-catalyzed catalytic cycle, the mechanism of the copper-free Sonogashira reaction is also not well understood. Two mechanistic pathways are feasible, but are often described in vague terms. The initial steps of oxidative addition and alkyne coordination are believed to be the same in both, but while one cycle is completed by subsequent deprotonation and reductive elimination, the other involves consecutive carbopalladation and hydride elimination (Figure 11).[22-24]

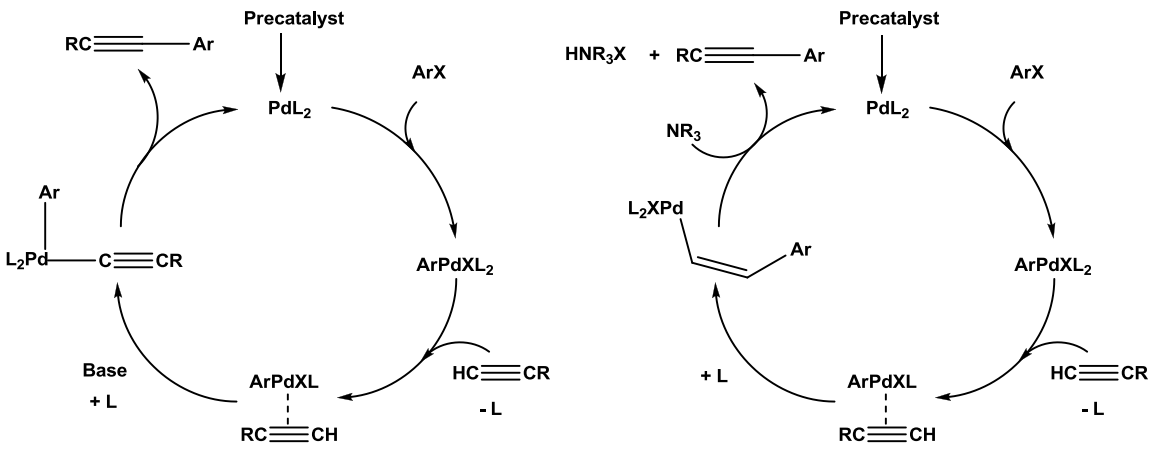

Figure 11. Two potential mechanisms for Cu-free Sonogashira cross-coupling reactions.

In the deprotonation mechanism (left), the base removes a proton from the coordinated alkyne, forming the palladium acetylide complex, from which the cross-coupled product is expelled. In the carbopalladation method (right), the Pd-R complex coordinated to the alkyne is added over the triple bond forming a coordinated alkene which the cross-coupled product is expelled and the catalyst regenerated through a ß-hydride elimination.[5] Martensson *et al.*[5] have recently concluded that both mechanisms occur with a mechanistic changeover when going from electron-poor to electron-rich alkynes. The changeover point is dependent on the nature of the amine base and its concentration. The preferred pathway for electron-rich alkynes involves the slow formation of the cationic Pd-alkyne complex while the electron-poor alkynes react via a proton transfer step to produce the Pd-acetylide intermediate.

1.4 Palladium(0) Precatalysts

1.4.1 Ligand Selection

The most widely used catalysts for cross-coupling reactions are of the type $Pd(0)L_2$ with steric and electronic properties of the ligands tuning the reactivity of the catalyst.[30] The rate of oxidative addition of RX to Pd(0) is directly related to the electron donating ability of the ligand employed. An electron rich Pd(0) centre experiences a greater driving force for oxidation and

therefore electron rich, strong σ-donors, such as PCy_3, $PMeBu^t_2$ and PBu^t_3, increase the rate of oxidative addition by increasing the electron density around the Pd centre. Strong σ-donation also increases the strength of the P-Pd bond, helping to stabilize Pd intermediates generated during the course of the reaction.[31] The reverse is true for reductive elimination, in that it is more difficult to reduce a Pd(II) centre with an increased electron density. Therefore, electron rich ligands generally result in a slower reductive elimination due to the increase in bond strength of the Pd centre to the substrates.[31]

Sterics have also been found to have an effect on the rate of both reductive elimination and oxidative addition. The rate of reductive elimination of R-R' from $Pd(R)(R')L_2$ is increased as the bulk of L increases.[31] This effect is generally believed to be caused by the need to reduce the steric congestion around the Pd(II) centre. Although a bulky L has a positive effect on the rate of reductive elimination, it often interferes with oxidative addition and transmetallation due to steric interactions with incoming reagents.

1.4.2 Catalyst Generation

The literature suggests a wide scope of palladium compounds are capable of producing successful results in cross-coupling reactions.[11,12] As a result, only the most successful and commonly used precatalysts will be studied for comparison. Palladium precatalysts are most commonly employed and dissociate or reduce *in situ* to produce the active $Pd(0)L_2$ species as the active species is often air-sensitive and therefore difficult to handle in common laboratory procedures.

1.4.2.1 $Pd(PPh_3)_4$

$Pd(PPh_3)_4$ was the first palladium catalyst used for a variety of cross-coupling reactions[1a,] and remains one of the most commonly used general precatalysts.[14,21] $Pd(PPh_3)_4$ must dissociate

into the active $Pd(PPh_3)_2$ species through a multi step procedure while in solution. Unfortunately, the tris species is the major species existing in solution with further dissociation being more difficult and much slower albeit required to produce the active bis species.[32]

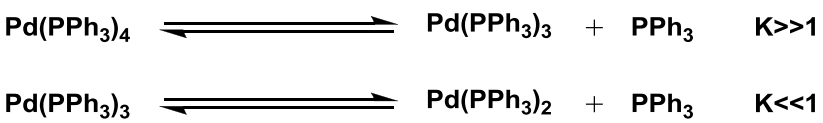

Figure 12. Dissociation of $Pd(PPh_3)_4$ in solution to produce the active palladium species.

Although commonly used for the Sonogashira reaction as well as a wide variety of cross-coupling reactions, $Pd(PPh_3)_4$ suffers from several drawbacks other then the already stated slow and incomplete formation of active species. The precatalyst is significantly air-sensitive, making common laboratory procedures and storage more difficult. The oxidative addition step becomes hindered when this precatalyst is utilized as the major tris species is much less active as well as the potential for the free PPh_3 generated during the dissociation to coordinate to the palladium species, impeding the addition of ArX. Also, it has been shown that the catalytic species produced in this case is not reactive enough to oxidatively add aryl chlorides or deactivated aryl bromides, preventing coupling with these aryl halides.[33]

1.4.2.2 $Pd(OAc)_2$

$Pd(OAc)_2$ is an attractive precatalyst for a variety of applications as it is air and moisture stable, making it easy to handle and store. $Pd(OAc)_2$ is a Pd(II) species and must first be reduced to the active Pd(0) catalyst before oxidative addition can occur.[34] It is generally accepted and assumed that the active species is formed by the reduction of the Pd(II) species by the addition of excess phosphine, but the rate and extent of the reduction remains unknown.

Studies have shown that a four-coordinate palladium species is initially formed by the addition of phosphine to the metal centre.[34a] This intermediate is not stable in solution and slowly undergoes a spontaneous intramolecular reaction to produce the active Pd(0) species capable of

oxidatively adding ArX. As the reduction involves the *in situ* formation of a variety of compounds of the general type OAc-PR_3, sterically demanding R groups make the attack unfavourable and severely limit the reduction of the Pd(II) precatalyst.[34b]

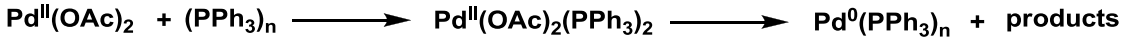

Figure 13. Production of the active Pd(0) species from $Pd(OAc)_2$ in the presence of phosphine as demonstrated by Amatore *et al*.

The amount of catalytically active Pd(0) species produced is directly correlated to the ability of the phosphine to reduce the Pd(II) species and thus, phosphine selection becomes extremely important.[32] This precatalyst becomes undesirable as an extra equivalent of phosphine is required to produce the stable Pd(0) species, becoming an economical issue when more complex phosphines are required. Also, it is generally unknown to what extent the active species is produced with the amount varying with the variation of the phosphine.[34]

1.4.2.3 $Pd(dba)_2$/$Pd_2(dba)_3$

Initial hypotheses suggested $Pd(dba)_2$ (dba = *trans*, *trans*-dibenzylideneacetone) would be a desirable precatalyst for cross-coupling reactions as it was assumed the dba ligands would be quite labile and therefore the active species would be easily generated with the addition of two equivalents of phosphine.[35] Studies performed by Amatore *et al*.[32,36] nullified the hypothesis by demonstrating that 6-8 equivalents of phosphine were required to displace both dba ligands and produce the active Pd(0) species.[32]

Subsequent studies investigating both monodentate (L) and bidentate (L-L) ligands found that while the first dba is easily displaced by a phosphine ligand, the second is much more difficult resulting in a $Pd(0)(dba)L_2$ or Pd(0)(dba)(L-L) species regardless of the ligand employed (Figure 14).[36]

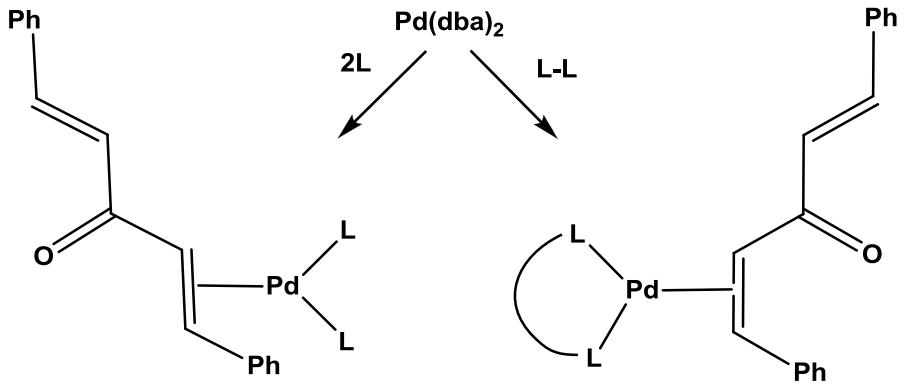

Figure 14. Dissociation of the first dba ligand from $Pd(dba)_2$ producing intermediates during the formation of the active PdL_2 species.

For monodentate phosphine ligands, the $Pd(0)L_2$ species is capable of oxidative addition while $Pd(0)dbaL_2$ is not. Therefore, the coordination of dba decreases the amount of the catalytically active species and affects the rate of oxidative addition. For bidentate ligands, both Pd(0)(L-L) and Pd(0)(dba)(L-L) are capable of oxidative addition, but Pd(L-L) is more reactive.[36] The difficulty of displacing both dba ligands and need for excessive amounts of phosphine make this precatalyst undesirable.

1.4.2.4 $PdCl_2(PPh_3)_2$

Original expectations of the quantitative generation of $Pd(0)(PPh_3)_2$ from $PdCl_2(PPh_3)_2$ were demonstrated to be incorrect as studies proved $PdCl_2(PPh_3)_2$ to be stable in solution.[16,37] This precatalyst is still often used as an alternative to other commonly used precatalysts as electrochemical reduction studies showed an equilibrium between three anionic Pd species, all being capable of partaking in the oxidative addition step with aryl halides to produce $PdArX(PPh_3)_2$.[37]

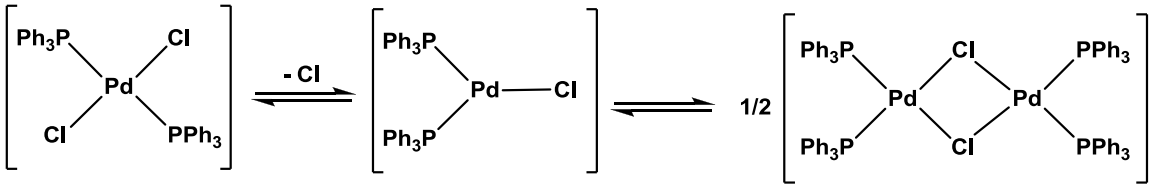

Figure 15. Electrochemical reduction of $PdCl_2(PPh_3)_2$ producing three anionic Pd species.

Despite $Pd(PPh_3)_2$ being stabilized by the halides resulting in a decrease in overall reactivity, the oxidative addition of ArX to the anionic Pd complex was demonstrated to experience an increased rate as compared to $Pd(PPh_3)_4$. The increased rate is attributed to the by-passing of ligand dissociation required in the $Pd(PPh_3)_4$ system.[37]

1.4.2.5 $Pd(\eta^5\text{-}C_5H_5)(\eta^3\text{-}1\text{-}Ph\text{-}C_3H_4)$

Recent studies within the Baird lab have led to the synthesis of an air and moisture stable palladium compound that is easily synthesized and manipulated.[38] NMR experiments have shown that the newly synthesized $Pd(\eta^5\text{-}C_5H_5)(\eta^3\text{-}1\text{-}Ph\text{-}C_3H_4)$ is a superior precatalyst as compared to other commonly used precatalysts in terms of generating the active $Pd(0)L_2$ species. It more rapidly generates the active $Pd(0)L_2$ species quantitatively in the presence of several phosphines including both mono and bi-dentate phosphines leading to the hypothesis that it may be a superior precatalyst for cross-coupling reactions.[38]

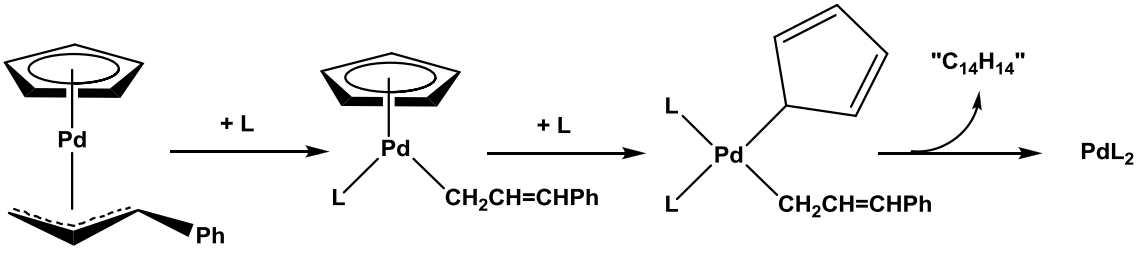

Figure 16. Reaction pathway producing the active palladium species from $Pd(\eta^5\text{-}C_5H_5)(\eta^3\text{-}1\text{-}Ph\text{-}C_3H_4)$ and two equivalents of phosphine.

1.5 Research Aims

1.5.1 Precatalyst Efficiency for Sonogashira Cross-Coupling Reactions

The objective of this thesis is to demonstrate an increased efficiency for Sonogashira cross-coupling reactions by employing the newly synthesized Pd(η^5-C_5H_5)(η^3-1-Ph-C_3H_4) (Figure 17) as the precatalyst. To demonstrate the increased efficiency, Pd(η^5-C_5H_5)(η^3-1-Ph-C_3H_4) will be compared to other commonly used palladium precatalysts ($PdCl_2(PPh_3)_2$, $Pd(PPh_3)_4$, $Pd(OAc)_2$ and Pd_2dba_3) under identical reaction conditions in the presence and absence of a copper co-catalyst. The reactions will be monitored by removing aliquots at specific intervals and running the samples through a GC to determine a percent yield. The data obtained will be plotted to obtain graphs of percent yield over time, i.e. a reaction profile. The profiles obtained will directly compare the efficiency of the precatalysts used with the aim of demonstrating that Pd(η^5-C_5H_5)(η^3-1-Ph-C_3H_4) is a superior precatalyst for the efficiency of conversion to the desired product over time.

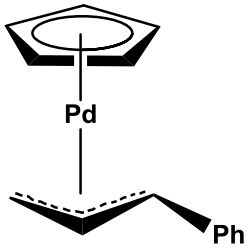

Figure 17. New precatalyst, Pd(η^5-C_5H_5)(η^3-1-Ph-C_3H_4), to be tested for Sonogashira reactions.

Norton *et al*. have demonstrated that the newly synthesized precatalyst Pd(η^5-C_5H_5)(η^3-1-Ph-C_3H_4) quantitatively generates the active species more quickly as compared to other commonly used precursors for Sonogashira reactions.[38] The ability of a system to generate the active species is a major factor for the rate and efficiency of a cross-coupling reaction,[11] a phenomena that is not well reported in terms of comparing precatalysts. It is hypothesized that the superiority of Pd(η^5-C_5H_5)(η^3-1-Ph-C_3H_4) to quantitatively generate the active species as

compared to other commonly used precatalysts will produce improvements in terms of yield and reaction time for cross-coupling reactions, more specifically the Sonogashira reaction.

A simple Sonogashira reaction was chosen as the standard reaction, eq. 1, along with very mild reaction conditions in order to monitor and compare the relative rates of conversion to the desired substituted alkyne.

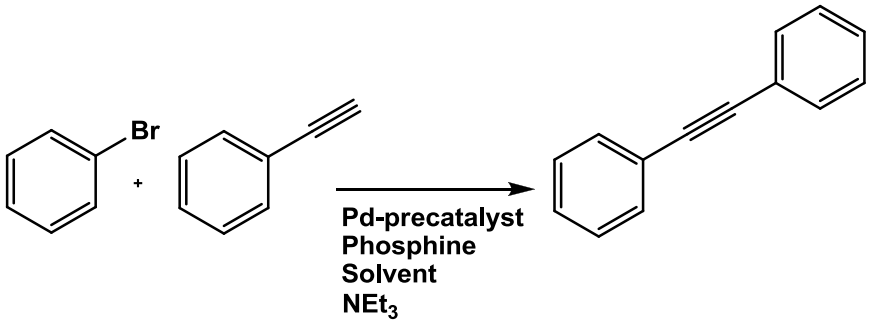

Figure 18. Coupling bromobenzene and phenylacetylene to produce diphenylacetylene will be monitored to compare the efficiency of the precatalyst.

The standard reaction chosen has been studied in depth by several other research groups with a wide variety of reaction conditions reported in literature. [3,4,10,22-29] The variation of reaction conditions from group to group is often quite large and therefore does not allow for a direct comparison of the results, but rather provides trends which will be compared to the results obtained in this project. The goal of this project is to demonstrate that, when compared to literature results, $Pd(\eta^5\text{-}C_5H_5)(\eta^3\text{-}1\text{-}Ph\text{-}C_3H_4)$ is a superior precatalyst for the generation of diphenylacetylene under identical or milder conditions.

To further the project, the reaction conditions using $Pd(\eta^5\text{-}C_5H_5)(\eta^3\text{-}1\text{-}Ph\text{-}C_3H_4)$ as the precatalyst will be optimized by varying the temperature, solvent and phosphine individually. Variation of the phosphine will not only provide an optimal phosphine but will also provide a reactivity series for a broad scope of phosphines for cross-coupling reactions which is currently not present in detail in the literature. The optimization of the standard reaction will provide a set of reaction conditions which will be utilized for a substrate scope. More difficult substrates in

terms of electronics and sterics will be tested with the hypothesis that using $Pd(\eta^5\text{-}C_5H_5)(\eta^3\text{-}1\text{-}Ph\text{-}C_3H_4)$ under optimal conditions will produce increased yields and more mild reaction conditions as compared to results stated in the literature. This research will provide reaction trends in terms of effectiveness of precatalysts, phosphines, solvents and temperatures which will allow for comparison to work published by other research groups with the goal of demonstrating $Pd(\eta^5\text{-}C_5H_5)(\eta^3\text{-}1\text{-}Ph\text{-}C_3H_4)$ to be an improvement for Sonogashira reactions over currently used precatalysts.

Chapter 2

Experimental

2.1.1 General Synthetic and Analytical Methods

All reactions were carried out under a dry, deoxygenated argon or nitrogen atmosphere using standard Schlenk line techniques or an MBraun Labmaster glove box. Anhydrous solvents such as THF and toluene were purchased packaged under nitrogen and were dried by passage through columns of activated alumina (Innovative Technology Solvent Purification System). The solvents were stored under an argon atmosphere over activated 4 Å molecular sieves for a minimum of 24 hours prior to use. DMF and triethylamine were purchased from Sigma-Aldrich and used directly from Sure/Seal bottles.

NMR spectra were obtained on a Bruker AV300 spectrometer. ^{31}P NMR spectra were run at 121.5 MHz with a delay of 2 seconds and are referenced with respect to external 85% H_3PO_4. ^{1}H NMR data are referenced to TMS via the residual proton signals of the deuterated solvents.

GC analyses were conducted on a Varian 3900 GC equipped with a CP-8400 autosampler, a CP-1177 injector, an FID detector and a Varian WCOT Fused Silica column (CP-Sil 8CB, 25 m x 0.32 mm ID, DF = 0.52). The GC method used was a total of 10 minutes with the column oven initially set at 140 °C. The temperature of the column oven was then increased at a rate of 10 °C/minute to 200 °C and held for 1 minute. Lastly, the column oven was increased at a rate of 60 °C/minute to 300 °C and held for 1.33 minutes to condition the column at the end of ever run. The injector port and FID detector were set to 250 °C. The data was plotted using Prism GraphPad 5.0 and the trend lines were developed by the program using the nonlinear regression function, one phase association.

2.1.2 Chemical Supplies

All chemicals were purchased from Sigma-Aldrich or Strem and used without purifications unless otherwise stated. Deuterated solvents were purchased from Cambridge Isotope Laboratories and stored over activated 4 Å molecular sieves. $PdCl_2$ was obtained as a loan from Johnson Matthey and was used as obtained. PMe_3, PMe_2Ph, $PMePh_2$, $PMeBu^t_2$, PEt_3, $P(CH_2Ph)_3$, PCy_3, PBu^n_3 and PBu^t_3 were purchased from Strem and were stored and used in the glovebox. Bidentate phosphines such as dppe, dppp and dppf were also purchased from Strem but were used directly on the bench top. PPh_3 obtained from Strem was recrystallized from EtOH and also handled on the bench top. $P(OC_6H_5)_3$ was synthesis according to the method described by Pietrusewicz *et. al*.[42] Other reagents such as Celite, silica gel (70-250 mesh, 60 Å), CuI, n-hexadecane, bromobenzene, chlorobenzene, phenylacetylene, diphenylacetylene, and bromoanisole were purchased from Sigma-Aldrich and used as obtained. A large quantity of $Pd(\eta^5\text{-}C_5H_5)(\eta^3\text{-}1\text{-}Ph\text{-}C_3H_4)$ was synthesized by a colleague in the Baird lab. 4-(Phenylethynyl)anisole was borrowed from a colleague in the Crudden lab. Palladium precursors such as $Pd(OAc)_2$ and $Pd_2(dba)_3$ were purchased from Strem and used without purification. Other palladium precatalysts such as $Pd(PPh_3)_4$ and $PdCl_2(PPh_3)_2$ were synthesized according to literature procedures as described in detail below.

2.2 Preparation of Reagents

2.2.1 Synthesis of *cis*-$PdCl_2(PPh_3)_2$

This compound was prepared according to the procedure described by Lord *et al*.[39] $PdCl_2$ (130 mg, 0.7 mmol) was stirred with PPh_3 (375 mg, 1.4 mmol) in DMF (20 mL) in air at 80 °C for 24 h. The resulting precipitate was collected by vacuum filtration, washed with cold DMF and

dried to give $PdCl_2(PPh_3)_2$ as a yellow powder. Yield: 450 mg, 90 %. . ^{1}H NMR ($CDCl_3$): δ 7.34-7.48 (phenyl protons), 7.63-7.72 (phenyl protons). ^{31}P NMR ($CDCl_3$): δ 24.0. Lit.[39]: ^{1}H NMR ($CDCl_3$): δ 7.34-7.70 (m, phenyl protons). ^{31}P NMR ($CDCl_3$): δ 23.9

2.2.2 Synthesis of $Pd(PPh_3)_4$

This compound was prepared according to the procedure described by Tellier *et al*.[40] $PdCl_2$ (0.36 g, 0.002 mol) and PPh_3 (3.16 g,0.012 mol) were placed in a 3-neck round bottom flask. After purging the system, DMF (50 mL) was added and the mixture was refluxed for 30 minutes. The mixture was allowed to cool to 80 °C and then a mixture of 0.5 mL NH_2NH_2 in 1.5 mL H_2O was added. The solution was stirred at 80 °C for an additional 2 hours and a yellow precipitate had formed. The precipitate was filtered and washed with methanol and ethyl ether, and dried overnight before being placed in the glove box. Yield: 2.01 g, 90%. ^{1}H NMR ($CDCl_3$): δ 7.31-7.92 (60 H, phenyl protons); ^{31}P NMR ($CDCl_3$): δ 30.7. Lit.[40]: ^{31}P NMR ($CDCl_3$): δ 29.8.

2.2.3 Synthesis of *trans*-$Pd(PPh_3)_2(C{\equiv}CPh)_2$

This compound was synthesized according to the procedure described by D`Amato *et al*.[41] A 2 M solution of NaOH in MeOH (0.032 g NaOH in 4 mL MeOH) was prepared and added to a round bottom flask containing a stir bar, $PdCl_2(PPh_3)_2$ (0.20 g , 0.28 mmol), CuI (5 mg, 0.026 mmol) and HC≡CPh (0.11 mL, 1.1 mmol). Upon stirring at room temperature for 3 h, a white precipitate formed and was collected by vacuum filtration and washed with cold MeOH. Yield: 227 mg, 91 %. ^{1}H NMR ($CDCl_3$): δ 6.25-6.35 (4 H, m, *o*-C_6H_5), 6.85-6.95 (6 H, m, *m,p*-C_6H_5), 7.31-7.90 (30 H, phenyl protons). ^{31}P NMR ($CDCl_3$): δ 27.0. Lit.[41]: ^{1}H NMR ($CDCl_3$): δ 7.33-7.81 (30 H, phenyl protons), 6.31-6.90 (10 H, phenyl protons). ^{31}P NMR ($CDCl_3$): δ 26.1.

2.2.4 Synthesis of $P(OC_6H_5)_3$

This compound was prepared according to the procedure described by Pietrusewicz *et al.*[42] Triphenyl phosphite was prepared by heating PCl_3 (2.6 mL, 0.03 mol) and phenol (9.4 g, 0.1 mol) in acetonitrile (40 mL) at 80 °C for 4 h. The solvent was evaporated under reduced pressure and the phosphite was used directly in the catalysis reactions as the ^{31}P NMR produced a single peak with the chemical shift matching the shift stated in the literature. Yield: 5.75 mL, 73 % . ^{31}P NMR ($CDCl_3$): δ 130.2. Lit.[42]: ^{31}P NMR ($CDCl_3$): δ 129.9

2.3 General Procedures for Sonogashira Cross-Coupling Reactions

A palladium precatalyst, phosphine and a stir bar were placed in a 10 mL test tube which was capped with a septum and then purged and filled with argon. Solvent was added (3 mL) and the mixtures were stirred at 50-100 °C with the length and temperature of premixing dependent upon results obtained by Norton *et al.*[35] Triethylamine, n-hexadecane, bromobenzene, phenylacetylene, and in certain trials CuI were added to the test tube. The reactions were monitored by the removal of aliquots at regular intervals for 24 h then running the sample through a GC to obtain a reaction profile. Reactions were duplicated and sometimes triplicated to ensure accuracy and reproducibility of the results obtained. Reactions were run in parallel with test tube (A) containing CuI (19 mg, 0.1 mmol) and test tube (B) being copper free. The precatalysts used require different amounts of phosphine to obtain the active Pd(0) species, with the ratios displayed in Table 1.

Table 1. Ratio of Pd-precatalyst:phosphine used to generate the active Pd(0) species.

Precatalyst	**Pd-precatalyst:P**
$Pd(OAc)_2$	1:3
$Pd_2(dba)_3$	1:4
Pd (η^5-C_5H_5)(η^3-1-Ph-C_3H_4)	1:2
$PdCl_2(PPh_3)_2$	1:2
$PdCl_2(PPh_3)_2$*	1:0

$Pd(PPh_3)_4$*	1:0

*No phosphine was added

The reactions were started in the morning and monitored throughout the day. The reactions ran overnight with aliquots removed the next morning to determine the yields after 20-24 h. This sampling method left gaps within the plots as can be seen in many cases. In certain cases the plots appeared to be levelling off in terms of yield. By starting the reactions much later in the day the gaps were filled in as can be seen in Figure 20 and it was determined that the plots were proceeding at a slow rate rather than levelling off.

2.3.1 Precatalyst Comparison using PPh_3

2.3.1.1 Presence of CuI

A stir bar, precatalyst (0.05 mmol) and PPh_3 with the desired ratio were added to a test tube. Once purged, THF (3 mL) was added and the reaction was stirred at 50 °C for 1 h. Triethylamine (0.4 mL, 2.8 mmol), bromobenzene (0.11 mL, 1.1 mmol), phenylacetylene (0.10 mL, 1 mmol), n-hexadecane (0.1 mL, 0.34 mmol) and CuI (19 mg, 0.1 mmol) were added to the test tube. The reaction was monitored for 24 h by removing 0.2 mL aliquots at specified intervals. The aliquots were diluted in a 10 mL volumetric flask using THF or toluene and then ran through the GC. Using n-hexadecane and a calibration curve, GC yields of diphenylacetylene were calculated and plotted to obtain a reaction profile for each precatalyst.

2.3.1.2 Absence of CuI

The procedure for 2.3.1.1 was repeated with the omission of CuI from the reaction flask.

2.3.1.3 1 mol % of Precatalyst

All reactions for procedure 2.3.1.1 and 2.3.1.2 were repeated using 1 mol % of precatalyst (0.01 mmol) rather than the previously used 5 mol % (0.05 mmol). The amount of

triethylamine was reduced (0.15 mL, 1.1 mmol) as well as the amount of PPh_3 to maintain the proper ratio of Pd-precatalyst:P where required.

2.3.1.4 Repeat of 2.3.1.3 at 100 °C

All reactions of 2.3.1.3 were repeated using 1 mol % of precatalyst at 100 °C. Due to the increased temperature, the solvent was changed to DMF to overcome the low boiling point of THF. The premixing was done at 50 °C and, upon completion, the temperature was increased to 100 °C at which point the other reagents were added and the reaction was monitored.

2.3.2 Precatalyst Comparison using PBu^t_3

2.3.2.1 Presence of CuI

Reactions were only performed using $Pd(OAc)_2$, $Pd_2(dba)_3$ and $Pd(\eta^3\text{-}1\text{-}Ph\text{-}C_3H_4)(\eta^5\text{-}C_5H_5)$ to avoid the complications of a mixed phosphine reaction. A stir bar, precatalyst (0.01 mmol) and PBu^t_3 with the desired ratio were added to a test tube. Once purged, THF (3 mL) was added and the reaction was stirred at 50 °C for 1 h. Triethylamine (0.15 mL, 1.1 mmol), bromobenzene (0.11 mL, 1.1 mmol), phenylacetylene (0.10 mL, 1 mmol), n-hexadecane (0.1 mL, 0.34 mmol) and CuI (19 mg, 0.1 mmol) were added to the test tube and the reaction was maintained at 50 °C . The reaction was monitored for 24 h by removing 0.2 mL aliquots at specified intervals. The aliquots were diluted in a 10 mL volumetric flask using THF or toluene and then ran through a GC. Using n-hexadecane and a calibration curve, GC yields of diphenylacetylene were calculated and plotted to obtain a reaction profile for each precatalyst.

2.3.2.2 Absence of CuI

The procedure for 2.3.2.1 was repeated with the omission of CuI from the reaction flask.

2.3.2.3 Repeat of 2.3.2.1 and 2.3.2.2 at 100 °C

All reactions were repeated using 1 mol % of precatalyst at 100 °C. Due to the increased temperature, the solvent was changed to DMF to overcome the low boiling point of THF. The premixing was done at 50 °C and, upon completion, the temperature was increased to 100 °C at which point the other reagents were added and the reaction was monitored.

2.3.3 Optimization of $Pd(\eta^3\text{-}1\text{-}Ph\text{-}C_3H_4)(\eta^5\text{-}C_5H_5)$

2.3.3.1 Solvent Effect

All reactions were performed using 1 mol % of $Pd(\eta^3\text{-}1\text{-}Ph\text{-}C_3H_4)(\eta^5\text{-}C_5H_5)$ at 50 °C. The reactions were carried out using PPh_3 and PBu^t_3 with all other reaction conditions unchanged. The solvents investigated were THF, toluene and DMF. A stir bar, precatalyst (0.01 mmol) and phosphine (0.02 mmol) were added to a test tube. Once purged, solvent (3 mL) was added and the reaction was stirred at 50 °C for 1 h. Triethylamine (0.15 mL, 1.1 mmol), bromobenzene (0.11 mL, 1.1 mmol), phenylacetylene (0.10 mL, 1 mmol), n-hexadecane (0.1 mL, 0.34 mmol) and CuI (19 mg, 0.1 mmol) in certain cases were added to the reaction. The reactions were monitored for 24 h.

2.3.3.2 Temperature Effect

All reactions performed in DMF and toluene from 2.3.3.1 were repeated using 1 mol % of $Pd(\eta^3\text{-}1\text{-}Ph\text{-}C_3H_4)(\eta^5\text{-}C_5H_5)$ at 100 °C in the presence and absence of CuI. Due to the increased temperature, THF was not used as its boiling point is well below 100 °C. The premixing was done at 50 °C and upon completion the temperature was increased to 100 °C at which point the other reagents were added and the reaction monitored for 24 h.

2.3.3.3 Phosphine Comparison

All reactions were performed only using 1 mol % of $Pd(\eta^3\text{-}1\text{-}Ph\text{-}C_3H_4)(\eta^5\text{-}C_5H_5)$ in the presence and absence of CuI as well as at 50 °C and 100 °C. The phosphine was varied while

always maintaining a 1:2 ratio of Pd-precatalyst:P even for bidentate phosphines as suggested by Norton *et al*. The phosphines tested are stated in section 2.1.2.

2.3.3.4 Isolated Yields

The reaction of interest was repeated under identical conditions without the removal of aliquots throughout the experiment. Referencing the time for completion from the previous monitored attempt, the reaction was stopped and filtered through a Celite plug. The desired compound was isolated by column chromatography (95:5, hexanes:EtOAc, on silica gel). In all cases the isolated yield was within 10% of the GC yield.

2.4 Miscellaneous Reactions

2.4.1 Comparing $Pd(\eta^3\text{-}1\text{-}Ph\text{-}C_3H_4)(\eta^5\text{-}C_5H_5)$ and $PdCl_2(PPh_3)_2$

2.4.1.1 Chlorobenzene Coupled with Phenylacetylene

The reactions were performed in the presence and absence of CuI at 100 °C. A stir bar, DMF (3 mL), precatalyst (0.01 mmol), and for $Pd(\eta^3\text{-}1\text{-}Ph\text{-}C_3H_4)(\eta^5\text{-}C_5H_5)$, PBu^t_3 (10 mg, 0.02 mmol) were added to a test tube. Upon premixing at 50 °C for 1 h the temperature was increased to 100 °C and chlorobenzene (0.11 mL, 1.1 mmol), phenylacetylene (0.1 mL, 1 mmol), triethylamine (0.15 mL, 1.1 mmol), n-hexadecane (0.1 mL, 0.34 mmol) and CuI (19 mg, 0.1 mmol) in certain cases were added to the test tube. The reactions were monitored for 24 h.

2.4.1.2 Bromoanisole Coupled with Phenylacetylene

The reactions were performed in the presence and absence of CuI at 100 °C. A stir bar, DMF (3 mL), precatalyst (0.01 mmol), and for $Pd(\eta^3\text{-}1\text{-}Ph\text{-}C_3H_4)(\eta^5\text{-}C_5H_5)$, PBu^t_3 (10 mg, 0.02 mmol) were added to a test tube. Upon premixing at 50 °C for 1 h the temperature was increased to 100 °C and bromoanisole (0.11 mL, 1.1 mmol), phenylacetylene (0.1 mL, 1 mmol), triethylamine (0.15 mL, 1.1 mmol), n-hexadecane (0.1 mL, 0.34 mmol) and CuI (19 mg, 0.1 mmol) in certain cases were added to the test tube. The reactions were monitored for 24 h.

2.4.2 Investigation of $Pd(PPh_3)_2(C{\equiv}CPh)_2$

2.4.2.1 Reductive Elimination of Diphenyldiacetylene from $Pd(PPh_3)_2(C{\equiv}CPh)_2$

The reactions were performed in the presence and absence of CuI at room temperature, 50 °C and 100 °C. A stir bar, $Pd(PPh_3)_2(C{\equiv}CPh)_2$ (0.25 g, 0.3 mmol), n-hexadecane (0.1 mL, 0.34 mmol) and DMF (3 mL) were placed in a test tube. The reaction was stirred and the production of diphenyldiacetylene was monitored by removal of aliquots at specified intervals which were then diluted using toluene and a 10 mL volumetric flask and the samples were run through the GC.

2.4.2.2 Use of $Pd(PPh_3)_2(C{\equiv}CPh)_2$ as a Precatalyst for the Standard Reaction

The reactions were performed in the presence and absence of CuI at 50 °C and 100 °C. A stir bar, $Pd(PPh_3)_2(C{\equiv}CPh)_2$ (8.32 mg, 0.01 mmol) and DMF were placed in a test tube. The reaction was premixed for 30 min at 50 °C, and then bromobenzene (0.11 mL, 1.1 mmol), phenylacetylene (0.10 mL, 1.0 mmol), triethylamine (0.15 mL, 1.1 mmol), n-hexadecane (0.1 mL, 0.34 mmol) and CuI (19 mg, 0.1 mmol) in certain cases were added to the test tube. The reactions were monitored for 24 h.

Chapter 3

Results and Discussion

3.1 Discussion of Cross-Coupling Results

The preliminary reaction conditions used for this project were based on a similar reaction study by Thorand *et al*.[29] in which aryl halides and phenylacetylene were coupled in the presence of $PdCl_2(PPh_3)_2$ and CuI to produce substituted alkynes in high yields. Initial reactions in this project were carried out as described in subsections 2.3.1.1 and 2.3.1.2 using 5 mol % of precatalyst for the standard reaction of coupling bromobenzene with phenylacetylene to produce the desired product diphenylacetylene (eq. 1).The investigation involved comparing the efficiencies of $PdCl_2(PPh_3)_2$, $Pd(PPh_3)_4$, $Pd(OAc)_2$, Pd_2dba_3 and $Pd(\eta^3\text{-}1\text{-}Ph\text{-}C_3H_4)(\eta^5\text{-}C_5H_5)$ as precatalysts for eq. 1 with the results obtained displayed in Figure 19.

$$\mathbf{C_6H_5Br + C_6H_5C{\equiv}CH \longrightarrow C_6H_5C{\equiv}CC_6H_5 + HBr} \qquad \textbf{(eq. 1)}$$

The results obtained from subsection 2.3.1.1 were very promising as $Pd(\eta^3\text{-}1\text{-}Ph\text{-}C_3H_4)(\eta^5\text{-}C_5H_5)$ produced diphenylacetylene at a rate equal to or greater than other commonly used precatalysts in the presence of CuI. Even more promising were the results obtained when CuI was omitted from the reactions. As can be seen in Figure 19, other commonly used precatalysts generated a maximum yield of 27% while $Pd(\eta^3\text{-}1\text{-}Ph\text{-}C_3H_4)(\eta^5\text{-}C_5H_5)$ produced nearly quantitative yields after 24 h in the absence of CuI. Ngassa *et al*.[43] reported a 72 % yield for a system coupling the same substrates while using 6 mol % of $PdCl_2(CH_3CN)_2$ with the addition of phosphine at 90 °C in the absence of a co-catalyst. Although the reaction conditions were more vigorous in the Ngassa *et al*. study, yields obtained using $Pd(\eta^3\text{-}1\text{-}Ph\text{-}C_3H_4)(\eta^5\text{-}C_5H_5)$ in the absence of CuI were greater than those obtained by Ngassa *et al*. Several other research groups have developed copper-free conditions for Sonogashira reactions, but in all comparable situations the conditions needed to achieve yields greater than 90% for eq. 1 were much harsher.[4,25-27,43]

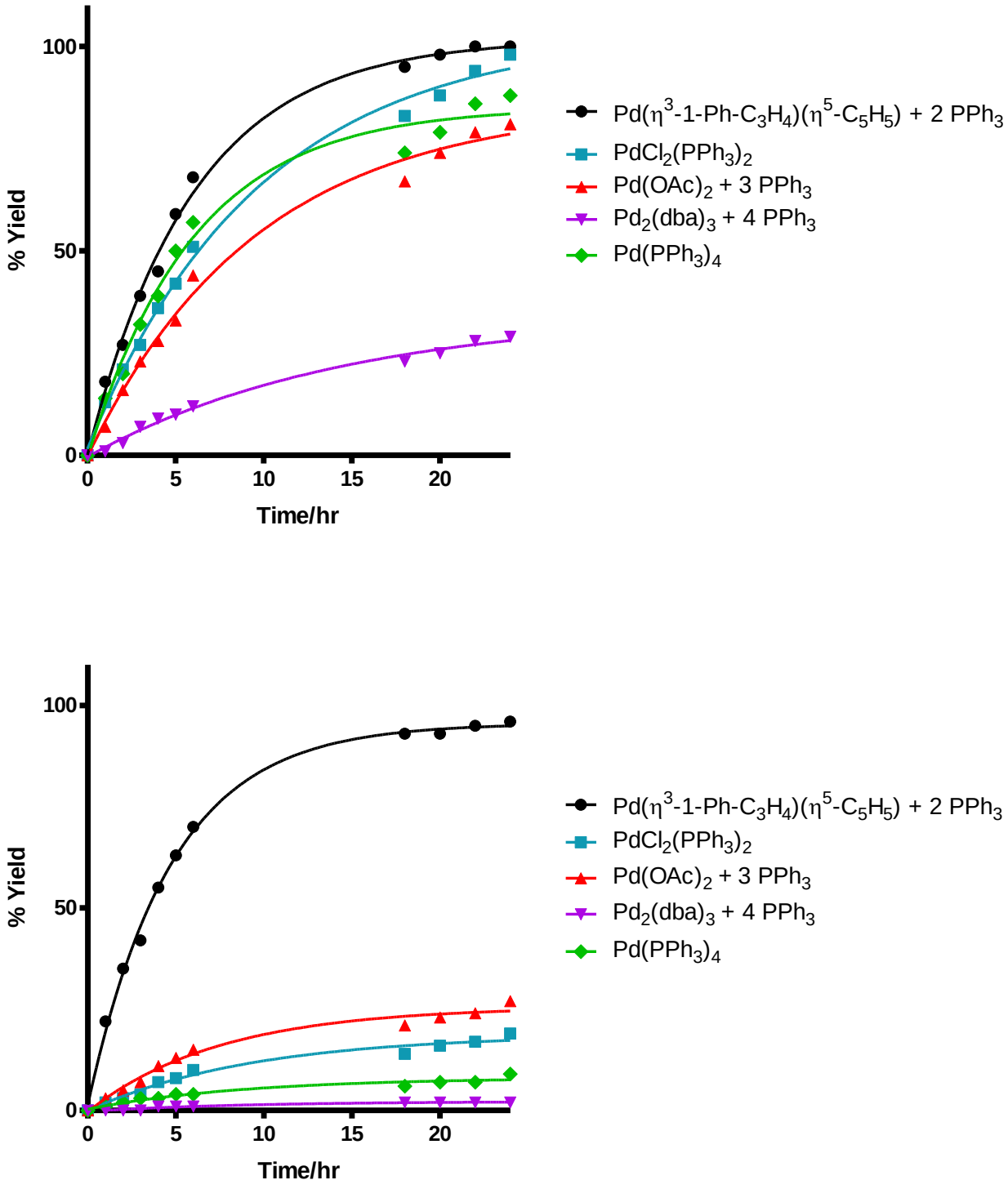

Figure 19. Comparing the effectiveness of the precatalysts used for eq. 1 using 5 mol % precatalyst at 50 °C in the presence of CuI (top) and absence (bottom).

With the success of initial reactions being proof that Pd(η^3-1-Ph-C_3H_4)(η^5-C_5H_5) is a viable precatalyst for Sonogashira reactions, the conditions were manipulated to test the effect of a lowered precatalyst loading. Further literature searching suggested 5 mol % catalyst to be quite high, and therefore a more accepted 1 mol % was employed as suggested by several other research groups[3,4,24-26] while all other reaction conditions remained unchanged from previous attempts. Reactions were carried out using 1 mol % precatalyst loadings according to subsection 2.3.1.3 with the results displayed in Figure 20.

The reduced catalyst concentration did not have a drastic effect on the overall conversion to the desired compound, diphenylacetylene. The trends observed when 5 mol % precatalyst was used remained constant for 1 mol % precatalyst as can be seen when comparing Figures 19 and 20 as no noticeable differences in the yield to diphenylacetylene were observed in the presence and absence of CuI. The reduced precatalyst loading provided a more direct comparison to work done by Shirakawa *et al*.[4] as they developed a copper-free system which produced an 81 % yield to diphenylacetylene using 1 mol % $Pd(OAc)_2$ and PPh_3 at 80 °C. When compared to the copper-free system in this study, Pd(η^3-1-Ph-C_3H_4)(η^5-C_5H_5) produced yields greater than 95 % after the same reaction time and at a lower temperature, demonstrating the superiority compared to not only other common precatalysts but also systems reported within the literature.

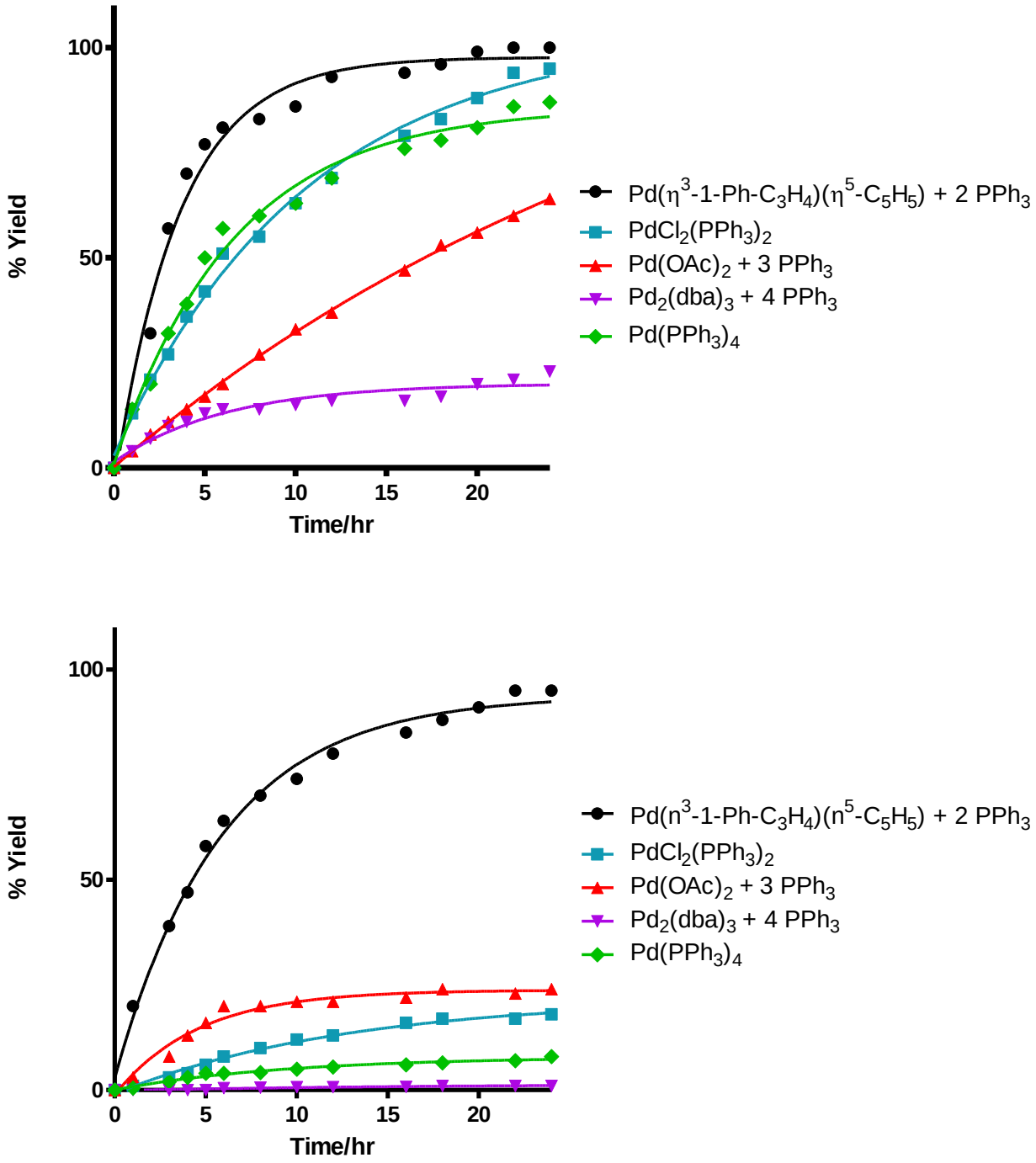

Figure 20. Comparing the effectiveness of the precatalysts used for eq. 1 using 1 mol % precatalyst at 50 °C in the presence of CuI (top) and absence (bottom).

Results obtained using the system of $PdCl_2(PPh_3)_2$ with the addition of two equivalence of PPh_3 as described in Table 1 are not displayed in Figures 19 and 20. The results obtained for the system using additional equivalence of phosphine for the conversion to diphenylacetylene were within 5 % of the system using only $PdCl_2(PPh_3)_2$. It was initially believed that additional equivalents of phosphine were required to reduce $PdCl_2(PPh_3)_2$ to produce the active species. It was later found that this was not necessary as suggested by the literature,[11,12] and therefore excess free PPh_3 was not added to $PdCl_2(PPh_3)_2$ in later reactions. Also to be noted is the exclusion of error bars on all plots. All reactions were repeated to ensure accuracy of the results, but the inclusion of error bars on the graphs resulted in the plots becoming cluttered and extremely difficult to distinguish.

Initial reaction conditions in subsections 2.3.1.1 and 2.3.1.2 were kept mild as it was hypothesized reactions would proceed quickly and be difficult to monitor and to compare any differences. As a result, quantitative yields were not observed in most cases. The literature has shown temperature to be directly correlated to overall yield in cross-coupling reactions,[23] and therefore an increase in temperature for eq. 1 will increase the rate of all reactions independent of the precatalyst. The next series of reactions was performed according to subsection 2.3.1.4 to determine the effect of temperature on the reaction in eq. 1, with the results displayed in Figure 21.

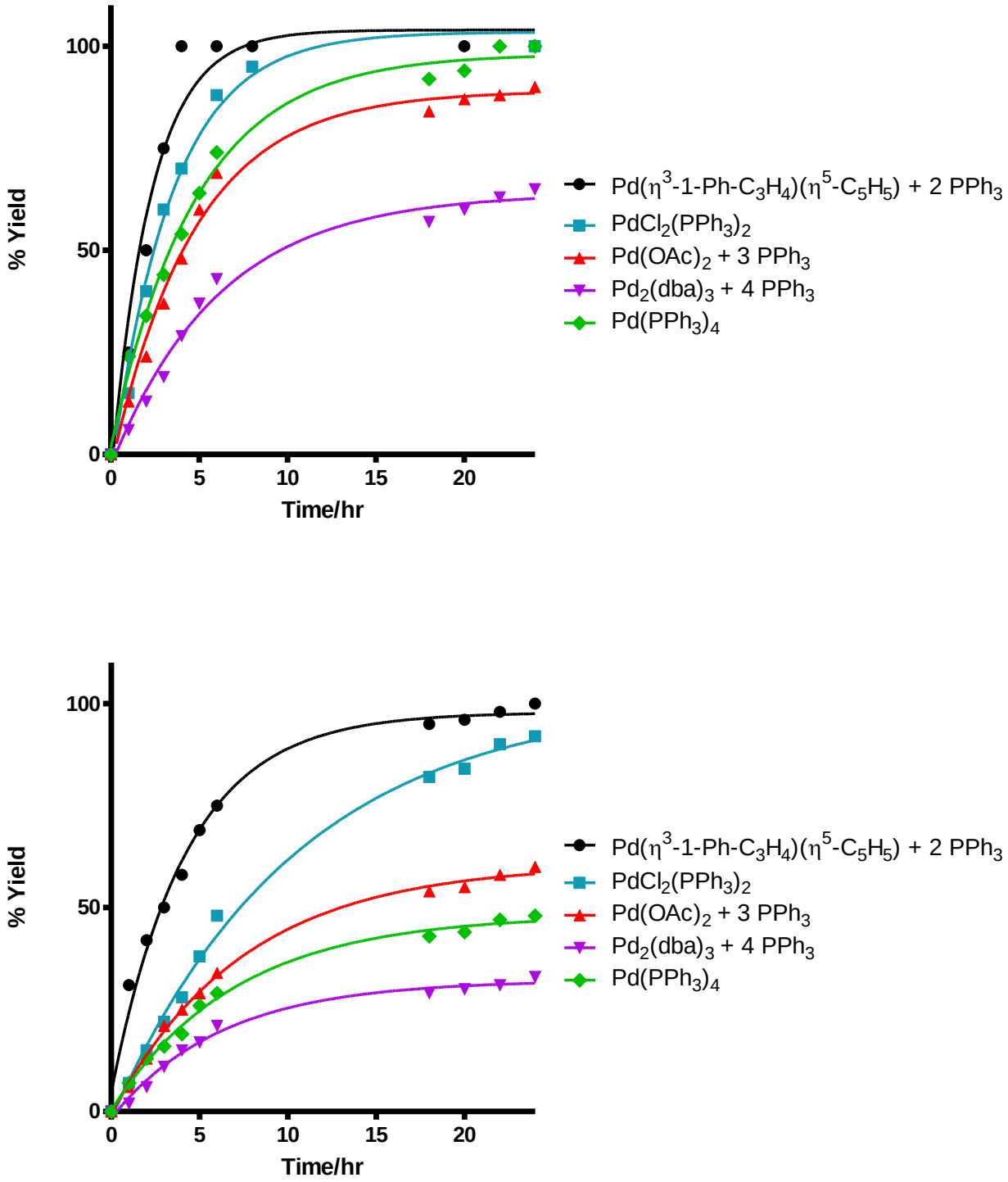

Figure 21. Comparing the efficiency of the precatalysts used for eq. 1 at 100 °C using 1 mol % precatalyst in the presence of CuI (top) and absence (bottom).

The increase in temperature drastically increased the rate of reaction in all cases as can be seen in comparing Figures 21 and 20 and is in agreement with reports by Panda and Sarkar[25]. Once again, this series of reactions followed the trend observed in Figures 19 and 20, that the effectiveness of $Pd(\eta^3\text{-}1\text{-}Ph\text{-}C_3H_4)(\eta^5\text{-}C_5H_5)$ was equal to or better than other commonly used precatalysts for the given reaction.

The next series of reactions was carried out to determine the effect of the phosphine used for eq. 1. The phosphine, L, is generally required to produce the active species, PdL_2 and therefore it is conceivable that altering the phosphine may have a large effect on the reaction. Results reported by Hundertmark *et al*.[26] suggest PBu^t_3 to be a more effective phosphine than PPh_3 for Sonogashira cross-coupling reactions. The Hundertmark system used 3 mol % $PdCl_2(MeCN)_2$ with 2 equivalents of phosphine for the coupling of bromoanisole with phenylacetylene. Results obtained when PBu^t_3 was used were greater than 90 % whereas when PPh_3 was used the percent yield to the desired compound was less than 5 %.[26] With that, the reactions done according to subsection 2.3.1.3 using 1 mol % precatalyst were repeated using PBu^t_3 as Hundertmark *et al*.[26] state increased yields when it was used in place of PPh_3. Trials using $PdCl_2(PPh_3)_2$ and $Pd(PPh_3)_4$ were not repeated. Reactions were performed according to subsections 2.3.2.1 and 2.3.2.2 with the initial series completed at 50 °C, the results are displayed bellow in Figure 22.

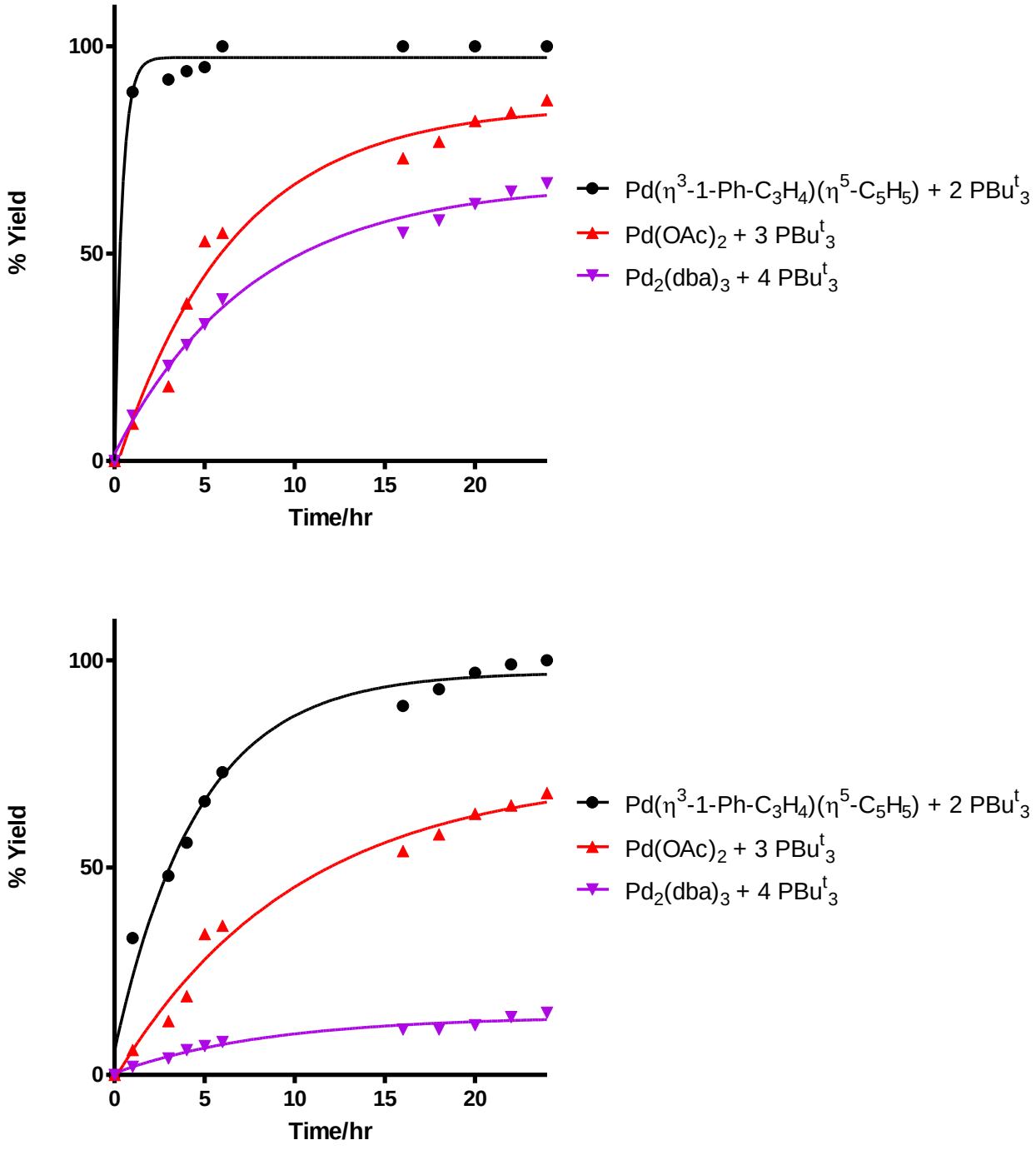

Figure 22. Monitoring the effect of the use of PBu^t_3 in place of PPh_3 for eq. 1 at 50 °C while still comparing the efficiency of the precatalysts. Presence of CuI (top), absence (bottom).

As can be seen in Figure 22, the relative rates of reaction are significantly increased, but the trend observed in Figures 20 and 21, demonstrating that Pd(η^3-1-Ph-C_3H_4)(η^5-C_5H_5) is a more effective precatalyst in the presence and absence of CuI for eq. 1, remained constant. The results also agree with those obtained by Hundertmark *et al*.[26] showing increased yields and faster reaction rates with the use of PBu^t_3 rather than PPh_3. Interestingly, the use of 1 mol % of Pd(η^3-1-Ph-C_3H_4)(η^5-C_5H_5) with two equivalents of PBu^t_3 produced better conversions as compared to the 3 mol % $Pd(PhCN)_2Cl_2$ with two equivalents of PBu^t_3 system also used in the Hundertmark *et al*. study[26], further supporting the hypothesis of the increased effectiveness of Pd(η^3-1-Ph-C_3H_4)(η^5-C_5H_5). To continue the initial investigation of the phosphine effect, reactions were repeated at 100 °C with the results displayed in Figure 23.

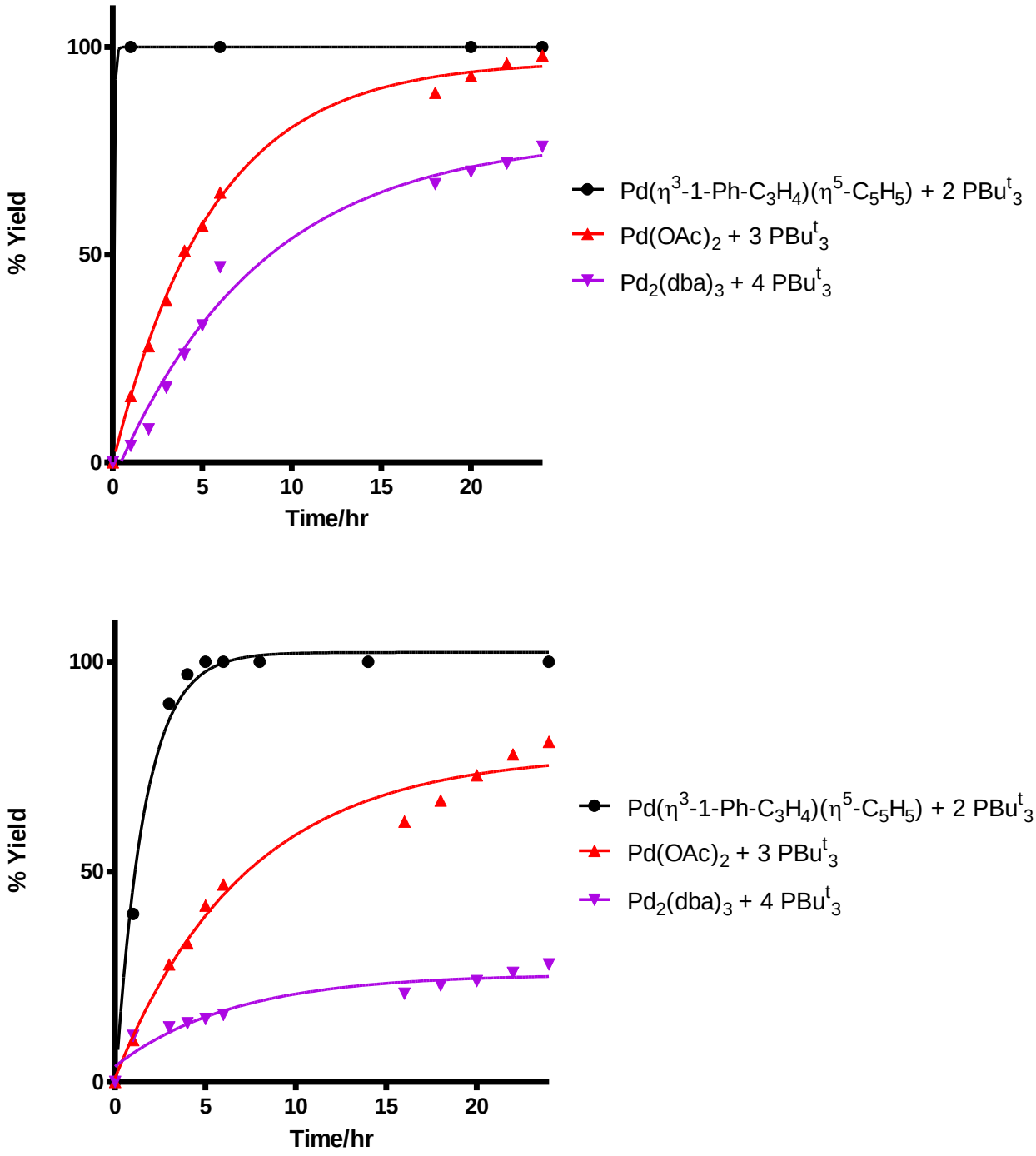

Figure 23. Monitoring the effect of the use of PBu^t_3 in place of PPh_3 for eq. 1 at 100 °C while still comparing the efficiency of the precatalysts. Presence of CuI (top), absence (bottom).

A system involving Pd_2dba_3 with the addition of PPh_3 or PBu^t_3 was reported by Dubbaka and Vogel.[28] The trend observed in their study shows an increase in the rate of reaction with the increase in temperature as well as using PBu^t_3 in place of PPh_3. Although their study involved coupling different substrates, the trend observed in this study when reactions were carried out using Pd_2dba_3 and PBu^t_3 supported their findings. The results obtained using $Pd(\eta^3\text{-}1\text{-}Ph\text{-}C_3H_4)(\eta^5\text{-}C_5H_5)$ and PBu^t_3 produced higher yields as compared to the Pd_2dba_3 system and also agree with the trend observed by Dubbaka and Vogel, demonstrating PBu^t_3 to be a more effective phosphine than PPh_3.

All results obtained to this point were very positive and suggested that $Pd(\eta^3\text{-}1\text{-}Ph\text{-}C_3H_4)(\eta^5\text{-}C_5H_5)$ is a more effective precatalyst for eq. 1. The results also suggest that the reaction can be optimized to produce quantitative yields more quickly and under relatively mild reaction conditions. To further the investigation of $Pd(\eta^3\text{-}1\text{-}Ph\text{-}C_3H_4)(\eta^5\text{-}C_5H_5)$ as a precatalyst for Sonogashira reactions, eq. 1 was optimized to obtain an optimal set of reaction conditions to be implemented as standard conditions for the coupling of a variety of substrates. The literature suggests the rate of reaction to be solvent, temperature, base and phosphine dependent,[3,4,10,22-28] and therefore some of these conditions were varied to optimize eq. 1. The solvent effect using $Pd(\eta^3\text{-}1\text{-}Ph\text{-}C_3H_4)(\eta^5\text{-}C_5H_5)$ for eq. 1 was investigated first according to procedures stated in subsections 2.3.3.1 and 2.3.3.2 with results displayed in Figures 24 and 25.

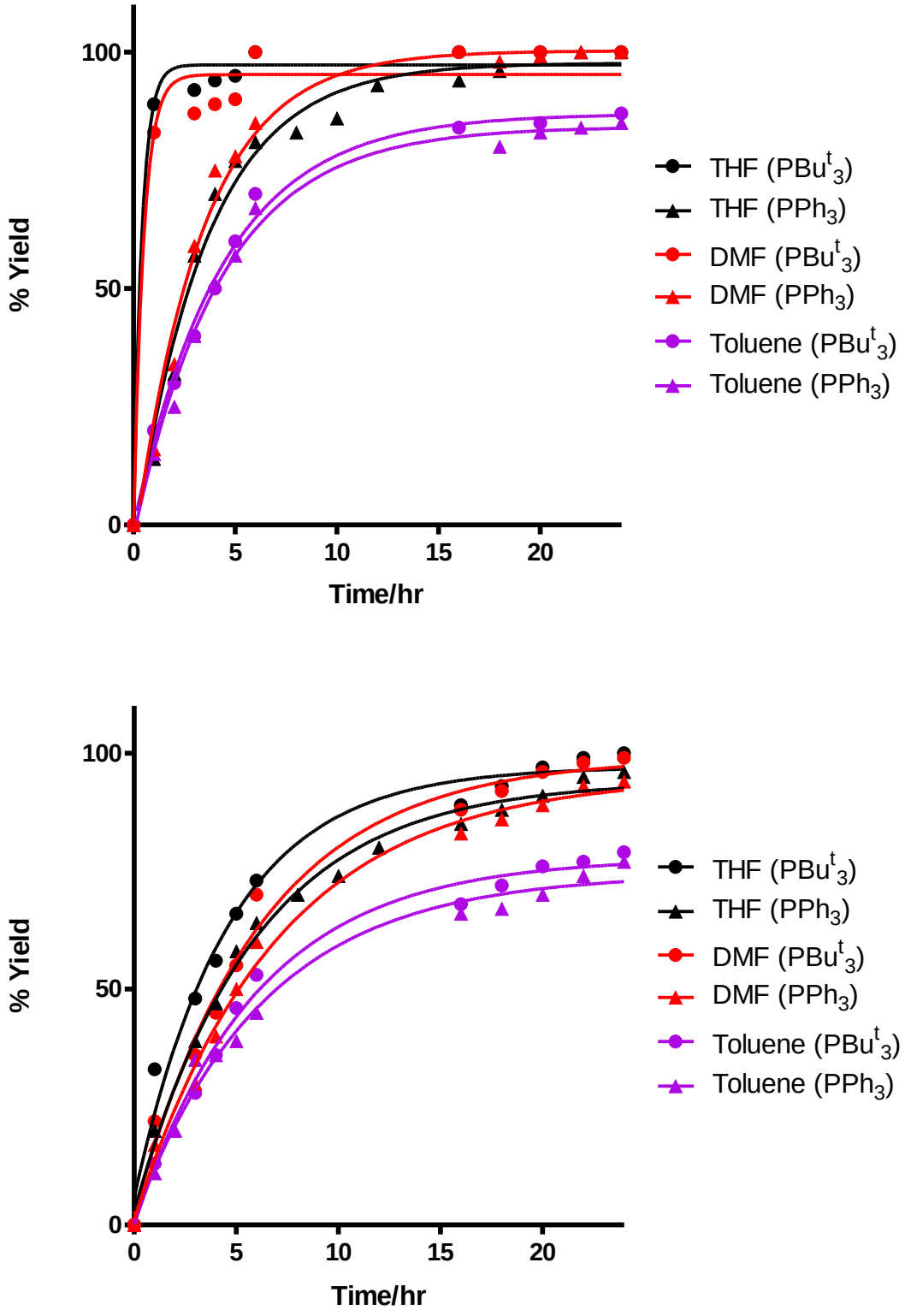

Figure 24. Comparing the effect of solvent variation on eq. 1 using PPh_3 and PBu^t_3 at 50 °C in the presence of CuI (top) and absence (bottom).

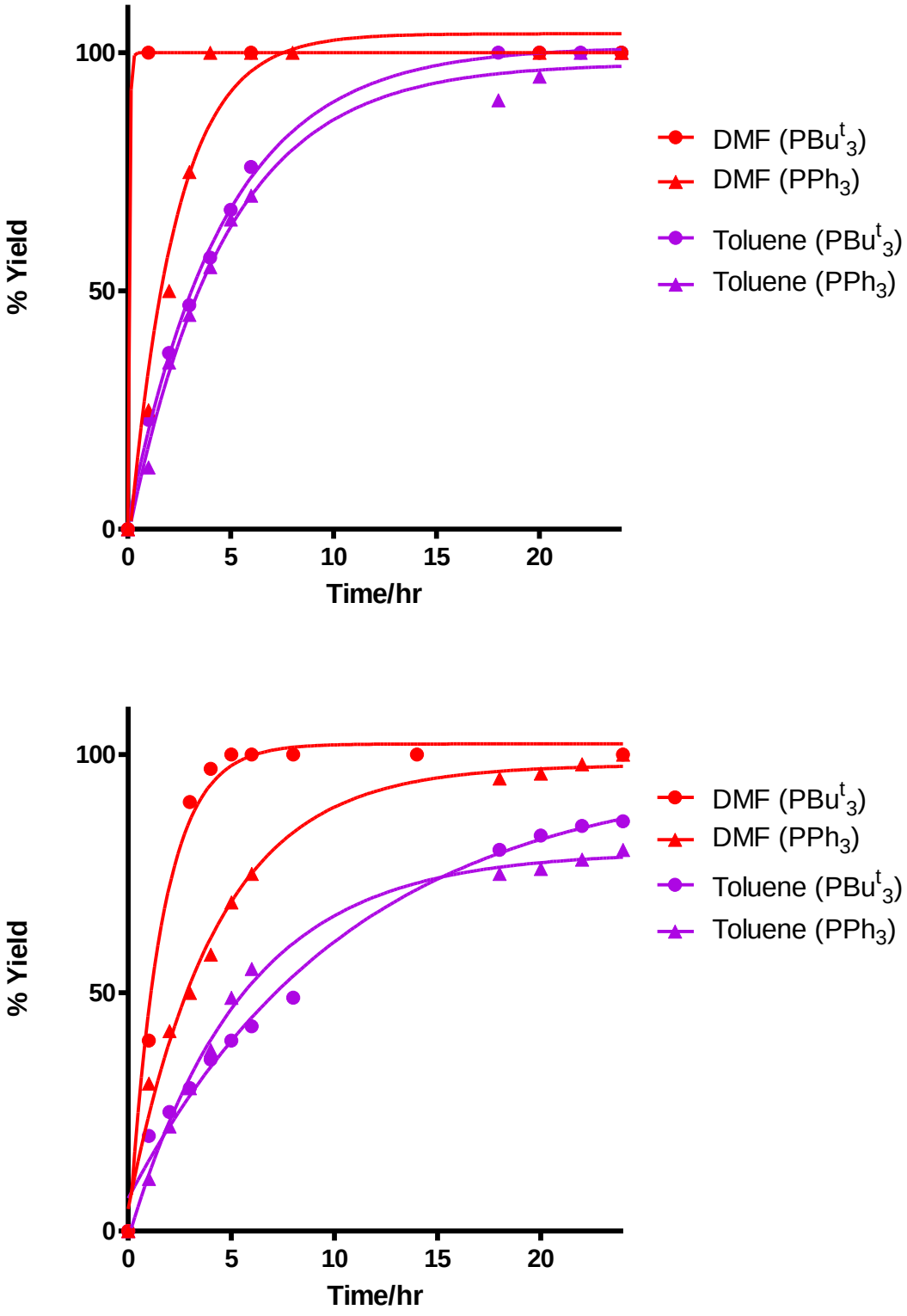

Figure 25. Comparing the effect of solvent variation on eq. 1 using PPh_3 and PBu^t_3 at 100 °C in the presence of CuI (top), absence (bottom).

As can be seen in Figures 24 and 25, variation of the solvent further confirmed the improved efficiency of PBu^t_3 for eq. 1 as in all cases it produced greater yields after 24 h or produced quantitative yields in shorter reaction times as compared to PPh_3. The effect of solvent variation on eq. 1 for a system co-catalyzed by $PdCl_2(PPh_3)_2$ and $AuCl(PPh_3)$ was reported by Panda and Sarkar.[25] Their results show DMF > THF >> toluene for the production of diphenylacetylene. Results obtained from subsection 2.3.3.2 when THF and DMF were used agree with results obtained by Panda and Sarkar, suggesting similar reactivities with THF being more limited due to a significantly lower boiling point. Also to be noted is the decrease in reactivity when toluene was used as the solvent which also supports observations made by Panda and Sarkar.[25]

With the dramatic improvement due to the substitution of phosphine, the next series of reactions was carried out to identify the most effective phosphine for eq. 1. Significant amounts of data can be found in this area with several groups reporting results using a wide variety of phosphines from small to bulky as well as monodentate and bidentate.[41] Although the reaction conditions were not identical in all literature cases, trends suggest a reactivity order of bulky monodentate phosphines > bidentate > small monodentate phosphines.[11,44] Reactions for the phosphine comparison were carried out only using $Pd(\eta^3\text{-}1\text{-}Ph\text{-}C_3H_4)(\eta^5\text{-}C_5H_5)$ as the precatalyst according to procedures in subsection 2.3.3.3 with results displayed in Figures 26 and 27.

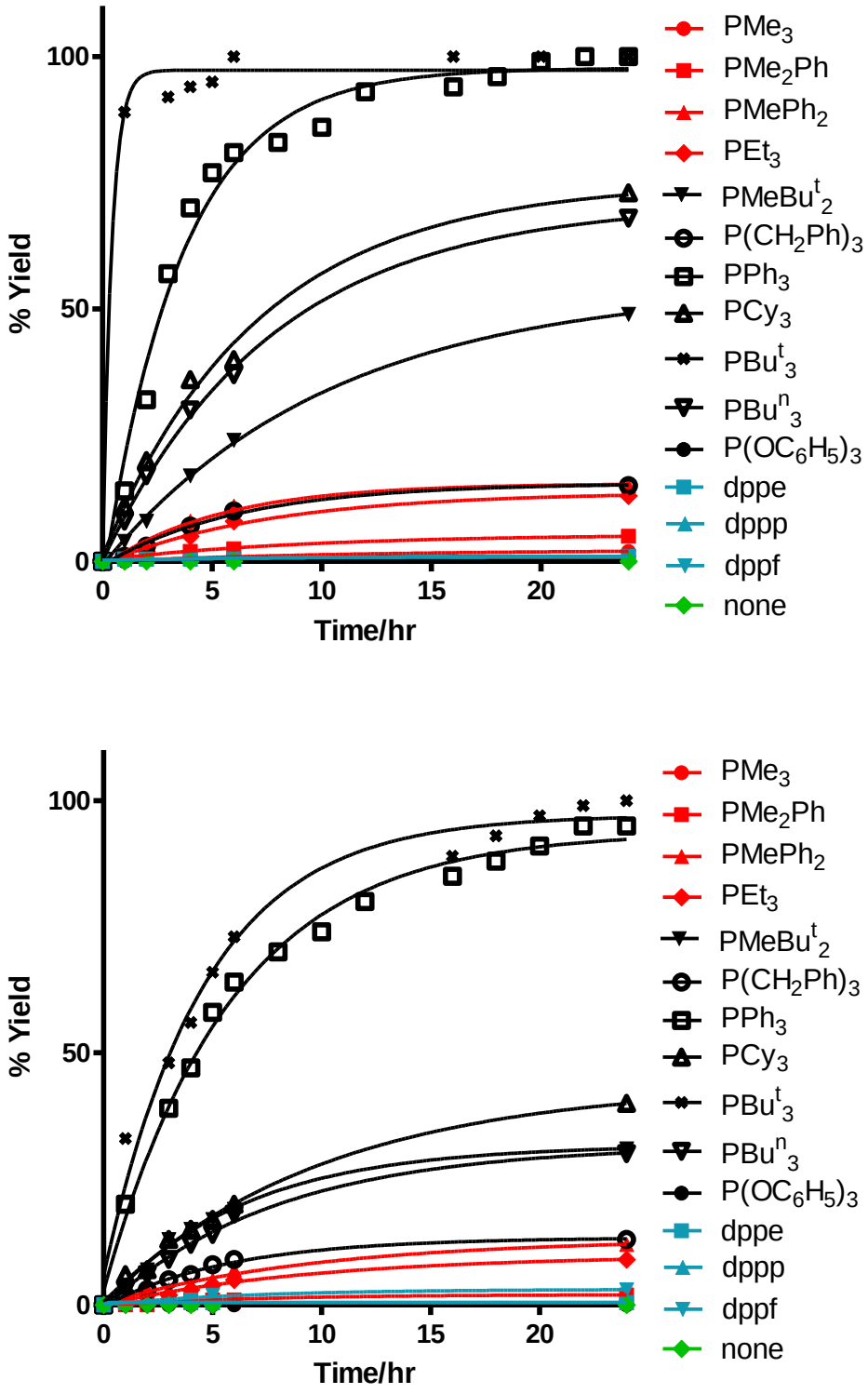

Figure 26. Comparing the effect of phosphine variation on eq. 1 using 1 mol % Pd(η^3-1-Ph-C_3H_4)(η^5-C_5H_5) at 50 °C in the presence of CuI (top) and absence (bottom). Small phosphines (red), bulky phosphines (black), chelating phosphine (blue).

It was initially hypothesized that the reactions would proceed quickly and be difficult to compare any differences. Thus, the reaction conditions were kept mild to ensure slower reactions and therefore obtain comparable results. The phosphine comparisons were initially performed at 50 °C and the results are displayed above in Figure 26. The results agree partially with trends stated in literature,[44] that small phosphines do not work well for cross-coupling reactions. PMe_3, PEt_3 and other smaller phosphines produced low conversions in both the presence and absence of CuI while bulky monodentate phosphines produced the highest yields.[44] Contrary to literature findings, bidentate phosphines produced the lowest yields, a result possibly caused by the mild reaction conditions utilized in this reaction series. After testing a wide variety of phosphines (small, bulky, chelating), PBu^t_3 remained the most effective with PPh_3 being a close second in order of activity for eq. 1. The investigation was continued by repeating the comparisons at 100 °C to increase the activity of the system and be certain of the activity order of phosphines tested. The reactions were performed according to subsection 2.3.3.3 with the results of the phosphine comparison at 100 °C in the presence of $Pd(\eta^3\text{-}1\text{-}Ph\text{-}C_3H_4)(\eta^5\text{-}C_5H_5)$ displayed in Figure 27.

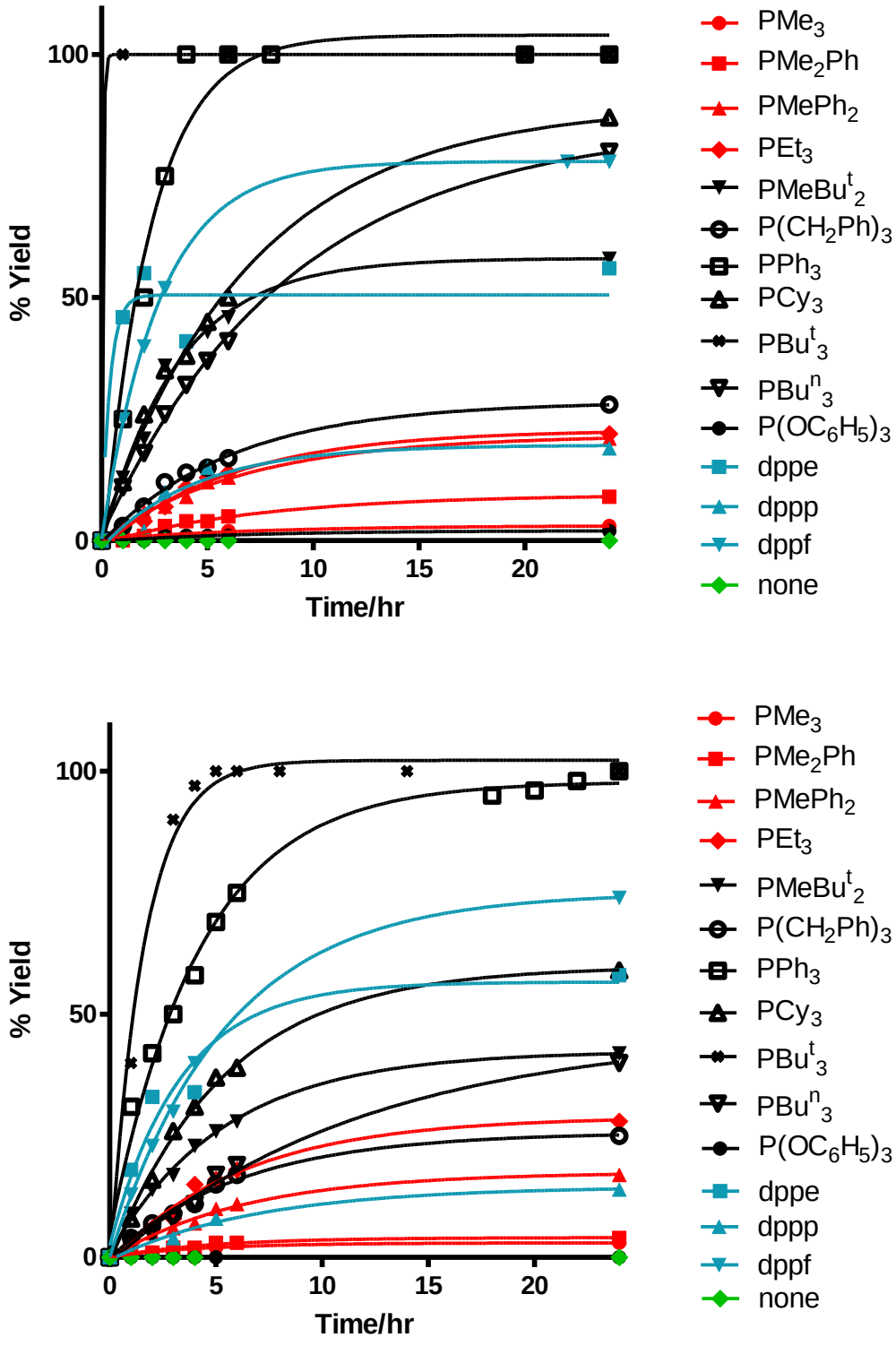

Figure 27. Comparing the effect of phosphine variation on eq. 1 using 1 mol % Pd(η^3-1-Ph-C_3H_4)(η^5-C_5H_5) at 100 °C. Small phosphines (red), bulky phosphines (black), chelating phosphine (blue). Presence of CuI (top), absence (bottom).

As can be seen in Figure 27, the trends observed at elevated temperature completely agree with trends stated in the literature that small phosphines are less effective then bulky monodentate phosphines with bidentate phosphines being intermediate.[44] Once again, PBu^t_3 proved to be the superior phosphine for eq. 1 and was found to be the optimal phosphine independent of other reaction conditions. The dramatic improvement of the chelating phosphines is believed to be due to the increased temperature as this observation agrees with literature findings stating that chelating phosphines produce modest yields at elevated temperatures.[11,44] At 50 °C the chelating phosphines exhibited very little activity, but at 100 °C dppf proved to be one of the more effective phosphines in the presence and absence of CuI. Although a drastic improvement, the dppf system still did not compare to that of PBu^t_3 and the best conditions were determined to be 1 mol % Pd(η^3-1-Ph-C_3H_4)(η^5-C_5H_5) with two equivalents of PBu^t_3 in DMF at 100 °C.

The literature has shown that variation of the halide group has an effect on the difficulty of the cross-coupling reaction to proceed and the general order of reactivity of the sp^2 species is aryl iodide > aryl bromide >>> aryl chloride.[11] The more difficult reaction of coupling chlorobenzene with phenylacetylene to produce diphenylacetylene (eq. 2) was investigated using the optimal reaction conditions previously determined. The investigation was performed according to subsection 2.4.1.1 using chlorobenzene, a less reactive, more difficult substrate as compared to bromobenzene, with the results shown in Figure 28.

$$C_6H_5Cl + C_6H_5C{\equiv}CH \longrightarrow C_6H_5C{\equiv}CC_6H_5 + HCl \quad \text{(eq. 2)}$$

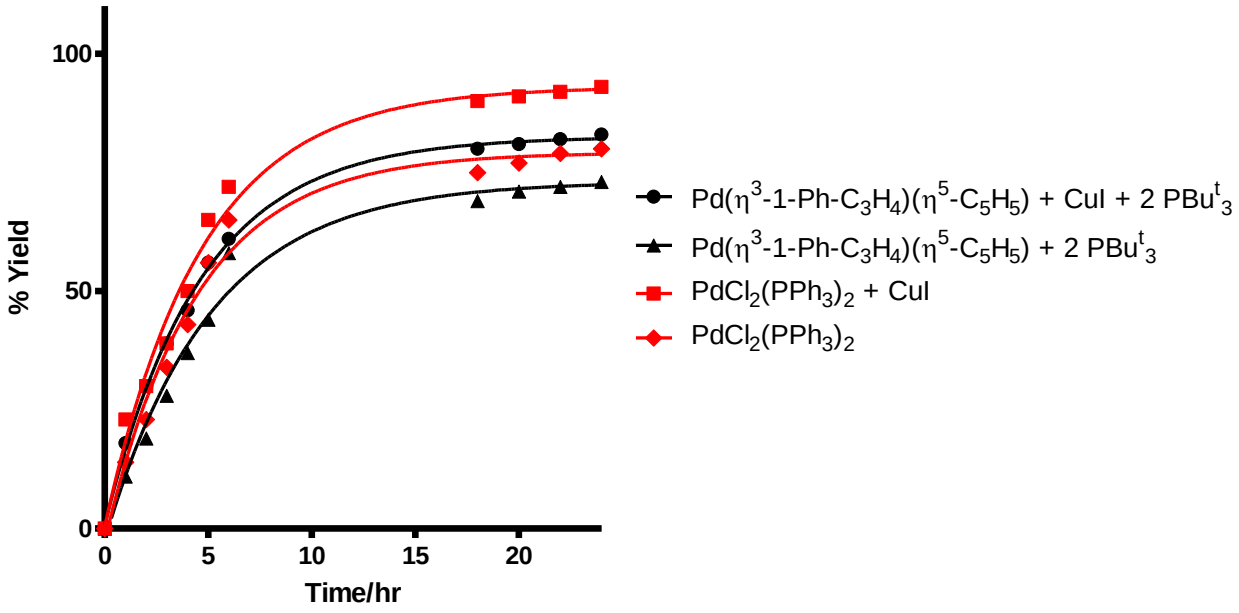

Figure 28. Monitoring the rate of conversion to diphenylacetylene for the more difficult reaction of coupling chlorobenzene and phenylacetylene using the optimal reaction conditions previously determined.

The reactions were run in parallel to compare $Pd(\eta^3\text{-}1\text{-}Ph\text{-}C_3H_4)(\eta^5\text{-}C_5H_5)$ with the most effective commonly used precatalyst, $PdCl_2(PPh_3)_2$. As can be seen in Figure 28, the trends observed for eq. 1 were not carried over to the substrate variation, eq.2. Although $Pd(\eta^3\text{-}1\text{-}Ph\text{-}C_3H_4)(\eta^5\text{-}C_5H_5)$ provided modest conversions, $PdCl_2(PPh_3)_2$, proved to be more effective precatalyst for eq. 2 under all reaction conditions tested.

The substrate variation was extended to include the coupling reaction of bromoanisole with phenylacetylene to produce 4-(phenylethynyl)anisole (eq. 3).

$$MeOC_6H_5Br + C_6H_5C{\equiv}CH \longrightarrow MeOC_6H_5C{\equiv}CC_6H_5 + HBr \quad \text{(eq. 3)}$$

Bromoanisole was chosen because it is a more difficult substrate for cross-coupling reactions as it is a deactivated organohalide.[12] The deactivation is due to the methoxy group donating electron density into the phenyl ring and making it more difficult for the substrate to

oxidatively add to a metal centre.[12] The reactions were once again carried out using both Pd(η^3-1-Ph-C_3H_4)(η^5-C_5H_5) and $PdCl_2(PPh_3)_2$ to provide a direct comparison of the efficiency of the precatalyst. The reactions were carried out according to subsection 2.4.1.2 with the results shown in Figure 29.

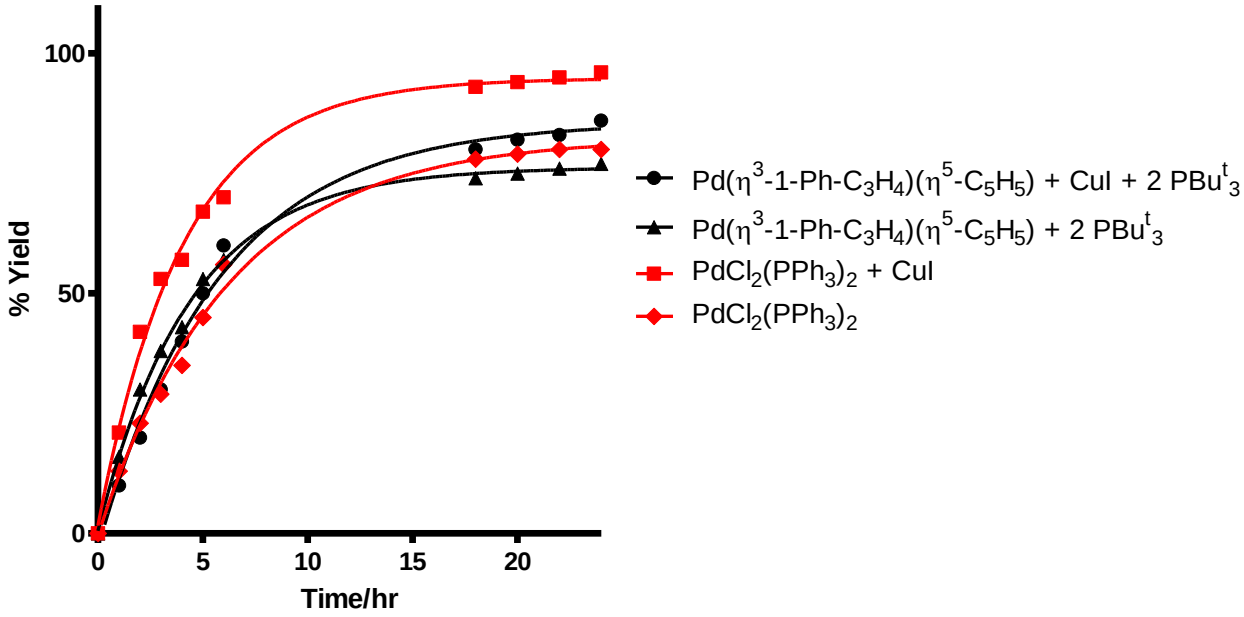

Figure 29. Monitoring the rate of conversion to 4-(phenylethynyl)anisole for the more difficult reaction of coupling bromoanisole and phenylacetylene using the optimal conditions previously determined.

Once again the reactivity trend observed for eq. 1 was not observed for the reaction of bromoanisole coupling with phenylacetylene. Although Pd(η^3-1-Ph-C_3H_4)(η^5-C_5H_5) produced modest conversions to the desired product, $PdCl_2(PPh_3)_2$ proved to be a more efficient precatalyst for eq. 3, producing higher conversions in the presence and absence of CuI.

The results obtained from subsections 2.4.1.1 and 2.4.1.2 show that Pd(η^3-1-Ph-C_3H_4)(η^5-C_5H_5) is not always the best precatalyst for some Sonogashira cross-coupling reactions. The next series of reactions was performed to investigate the potential reasoning behind the increased effectiveness of $PdCl_2(PPh_3)_2$

3.2 Investigation of $PdCl_2(PPh_3)_2$ and Possible Intermediates

Although Norton *et al*. showed Pd(η^3-1-Ph-C_3H_4)(η^5- C_5H_5) quantitatively generates the active Pd(0)L_2 species in the presence of phosphine, there is also potential for the formation of a less active Pd(0)L_3 species at increased temperatures. The reduction pathway of $PdCl_2(PPh_3)_2$ to produce the active species is still unclear. It is presumed that the less active tris palladium species is not formed because there is no free phosphine in the system, hence the reason for the increased reactivity. It seems possible that the acetylide species $Pd(PPh_3)_2(acetylide)_2$ may be an intermediate in the production of the active species. The acetylides could reductively eliminate from the intermediate to produce the homocoupled product and the active Pd(0)L_2 species (Figure 30).

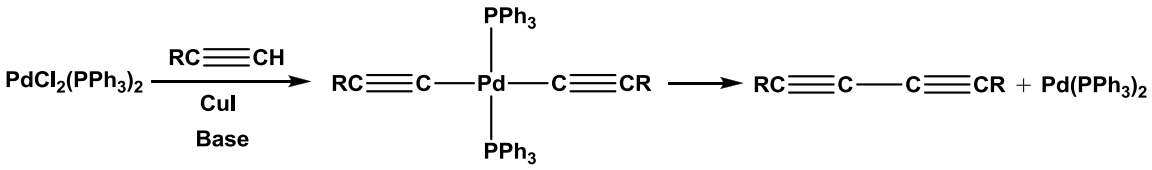

Figure 30. Potential pathway for the production of active species from $PdCl_2(PPh_3)_2$ in the presence of phenylacetylene showing the Pd-diacetylide intermediate

This intermediate, *trans*-$Pd(PPh_3)_2(C{\equiv}CPh)_2$, was synthesized according to methods described by D'Amato *et al*.[41] The synthetic procedure supports the possibility of *trans*-$Pd(PPh_3)_2(C{\equiv}CPh)_2$ being an intermediate in the generation of $Pd(PPh_3)_2$ from $PdCl_2(PPh_3)_2$ as it is synthesized from a 2:1 ratio of phenylacetylene to $PdCl_2(PPh_3)_2$. Their study involved the synthesis of Pt(II) and Pd(II) complexes to be used as polymerization catalysts and had not investigated the possibility of *trans*-$Pd(PPh_3)_2(C{\equiv}CPh)_2$ being an intermediate in the generation of active species for cross-coupling reactions.

A thermal analysis was carried out at various temperatures to determine the stability of the complex and determine if it is a plausible intermediate during the generation of active species from $PdCl_2(PPh_3)_2$. Reactions were carried out according to procedures stated in subsection 2.4.2.1 with results displayed in Figure 31.

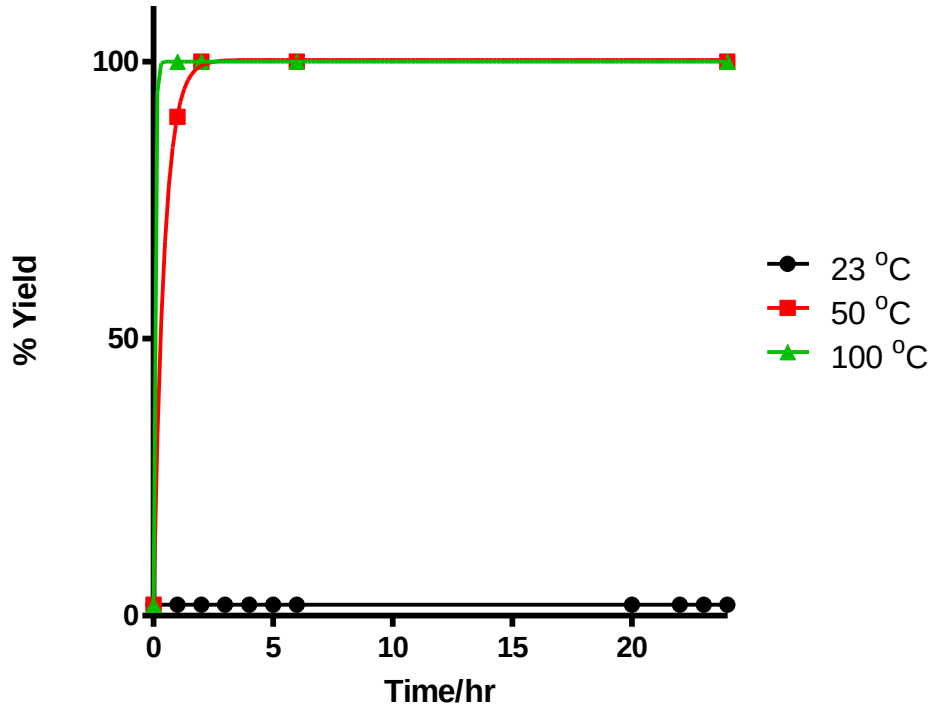

Figure 31. Monitoring the reductive elimination of diphenyldiacetylene from $Pd(PPh_3)_2(C{\equiv}CPh)_2$ at various temperatures.

The results obtained suggest this pathway to be a viable mechanism for the formation of active Pd(0) species, $Pd(PPh_3)_2$, from $PdCl_2(PPh_3)_2$. The production of diphenyldiacetylene was monitored on the assumption that a quantitative yield of diphenyldiacetylene suggests a quantitative yield of the active specie $Pd(PPh_3)_2$. At room temperature the compound remained intact after 24 h of stirring in DMF as no diphenyldiacetylene was produced. When the temperature was elevated to 50 °C or 100 °C, quantitative yields of diphenyldiacetylene were observed within 1 h as displayed in Figure 31. The quantitative yield was achieved more quickly

at 100 °C, a similarity to the quantitative generation of the desired product for cross-coupling reactions. These results provide a plausible rationale for the generation of active species from $PdCl_2(PPh_3)_2$, but do not prove the mechanism. $Pd(PPh_3)_2(C{\equiv}CPh)_2$ was therefore employed as the precatalyst for eq. 1 according to subsection 2.4.2.2 with the yield to diphenylacetylene displayed in Figure 32.

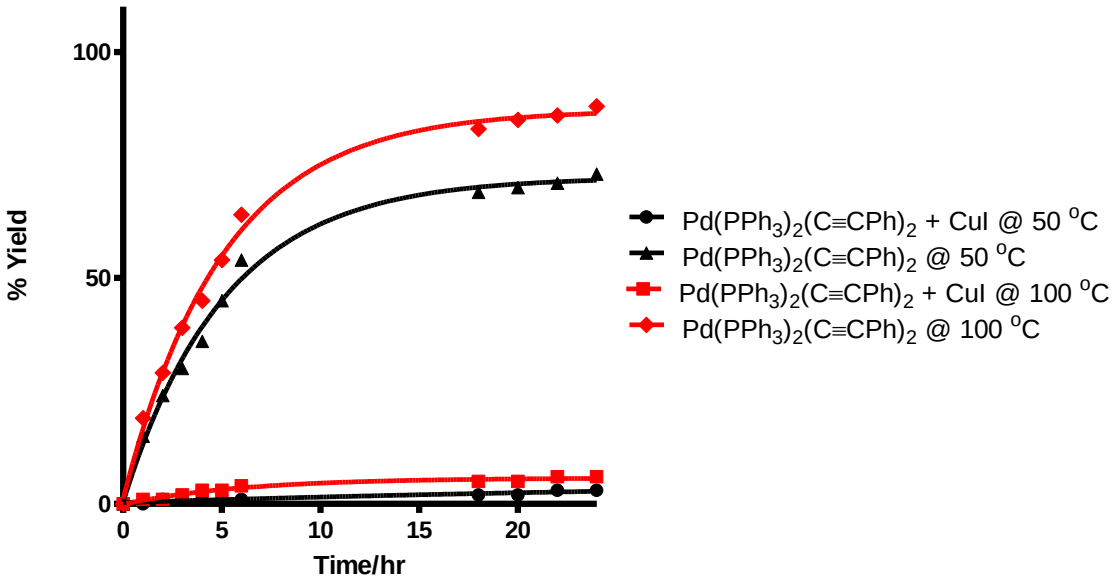

Figure 32. Testing $Pd(PPh_3)_2(C{\equiv}CPh)_2$ as a precatalyst for eq. 1 by monitoring the production of diphenylacetylene.

$Pd(PPh_3)_2(C{\equiv}CPh)_2$ was tested as a precatalyst for eq. 1 at 50 °C and 100 °C in the presence and absence of CuI. Results displayed in Figure 32 show the ability of $Pd(PPh_3)_2(C{\equiv}CPh)_2$ to act as a precatalyst for eq. 1 and suggest it is a viable intermediate for the generation of active species from the commonly used precatalyst, $PdCl_2(PPh_3)_2$. Surprisingly, the reaction produced higher yields when CuI was omitted from the reaction. This observation, worthy of further study, suggests that $Pd(PPh_3)_2(C{\equiv}CPh)_2$ plays a mechanistic role in the overall catalytic cycle.

3.3 Summary and Conclusion

This thesis has furthered the study performed by Norton *et al.*[38] by demonstrating the ability of $Pd(\eta^3\text{-}1\text{-}Ph\text{-}C_3H_4)(\eta^5\text{-}C_5H_5)$ to not only oxidatively add aryl halides but also produce desired compounds in significant yields for Sonogashira cross-coupling reactions. This thesis reports the superior ability of $Pd(\eta^3\text{-}1\text{-}Ph\text{-}C_3H_4)(\eta^5\text{-}C_5H_5)$ to catalyze a simple Sonogashira reaction as compared to other commonly used precatalysts. The cross-coupling reaction between bromobenzene and phenylacetylene to produce diphenylacetylene was monitored while reaction conditions were varied. Under all reaction conditions tested, $Pd(\eta^3\text{-}1\text{-}Ph\text{-}C_3H_4)(\eta^5\text{-}C_5H_5)$ produced quantitative yields more quickly as compared to the commonly used Pd-precatalysts ($PdCl_2(PPh_3)_2$, $Pd(PPh_3)_4$, $Pd_2(dba)_3$ and $Pd(OAc)_2$).

Initial reactions were performed to directly compare the efficiency of the precatalyst employed for a given Sonogashira reaction in the presence and absence of CuI. The reaction conditions were kept relatively mild as it was anticipated that the reactions may all proceed quickly and therefore be difficult to differentiate and to draw conclusions. Under the mild reaction conditions of 50 °C and 1 mol % precatalyst, $Pd(\eta^3\text{-}1\text{-}Ph\text{-}C_3H_4)(\eta^5\text{-}C_5H_5)$ was proven to be the most effective precatalyst, producing a quantitative yield in the presence of CuI and producing yields approximately 70 % greater than the other precatalysts tested in the absence of CuI. The ability for a system to produce significant yields in the absence of CuI for Sonogashira reactions is a highly desirable quality as it reduces the potential for the unwanted formation of the homocoupled product.

As $Pd(\eta^3\text{-}1\text{-}Ph\text{-}C_3H_4)(\eta^5\text{-}C_5H_5)$ was demonstrated to be an effective precatalyst, reaction conditions were optimized for the cross-coupling reaction of bromobenzene and phenylacetylene (eq. 1). It was determined a quantitative yield could be achieved within 1 h in the presence of CuI and 3 h in the absence when reactions were carried out at 100 °C with 1 mol % $Pd(\eta^3\text{-}1\text{-}Ph\text{-}$

$C_3H_4)(\eta^5\text{-}C_5H_5)$ using PBu^t_3 in DMF. A variety of phosphines were tested for eq. 1 with PBu^t_3 determined to be the most effective, and the reactivity order was determined to be bulky monodentate > chelating > small monodentate > no phosphine.

The optimal reaction conditions were employed for the more difficult Sonogashira cross-coupling reactions of coupling chlorobenzene and phenylacetylene as well as coupling bromoanisole with phenylacetylene. The more difficult reactions were carried out using $Pd(\eta^3\text{-}1\text{-}Ph\text{-}C_3H_4)(\eta^5\text{-}C_5H_5)$ as well as $PdCl_2(PPh_3)_2$ to provide a direct comparison of the efficiency of the precatalysts employed. In both reactions $Pd(\eta^3\text{-}1\text{-}Ph\text{-}C_3H_4)(\eta^5\text{-}C_5H_5)$ was capable of producing the desired product, but $PdCl_2(PPh_3)_2$ produced greater yields and proved to be the more effective precatalyst. The decreased activity of Pd $\eta^3\text{-}1\text{-}Ph\text{-}C_3H_4)(\eta^5\text{-}C_5H_5)$ was hypothesized to be caused by the formation of a less active $Pd(0)L_3$ species. In the case of $PdCl_2(PPh_3)_2$, a $Pd(0)L_3$ species would not be capable of forming but rather a Pd-diacetylide intermediate may be formed leading to the reductive elimination of the homocoupled product to produce the active catalytic species. The hypothesized intermediate, $Pd(PPh_3)_2(C{\equiv}CPh)_2$, was synthesized and tested as a precatalyst for eq. 1. Results obtained in the absence of CuI showed conversion to the desired product as well as a small amount of homocoupled product suggesting $Pd(PPh_3)_2(C{\equiv}CPh)_2$ to be a viable intermediate for the generation of active species from $PdCl_2(PPh_3)_2$.

Appendix A

Calibration Curves and Sample GC Spectra

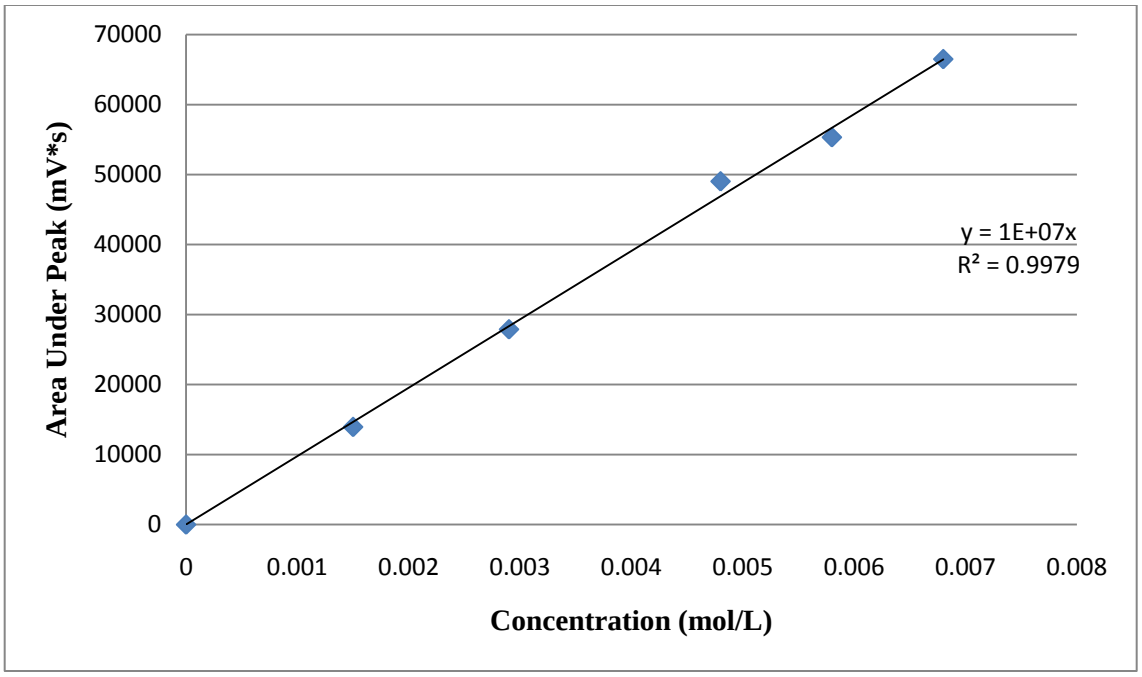

Figure 33. Diphenylacetylene calibration curve.

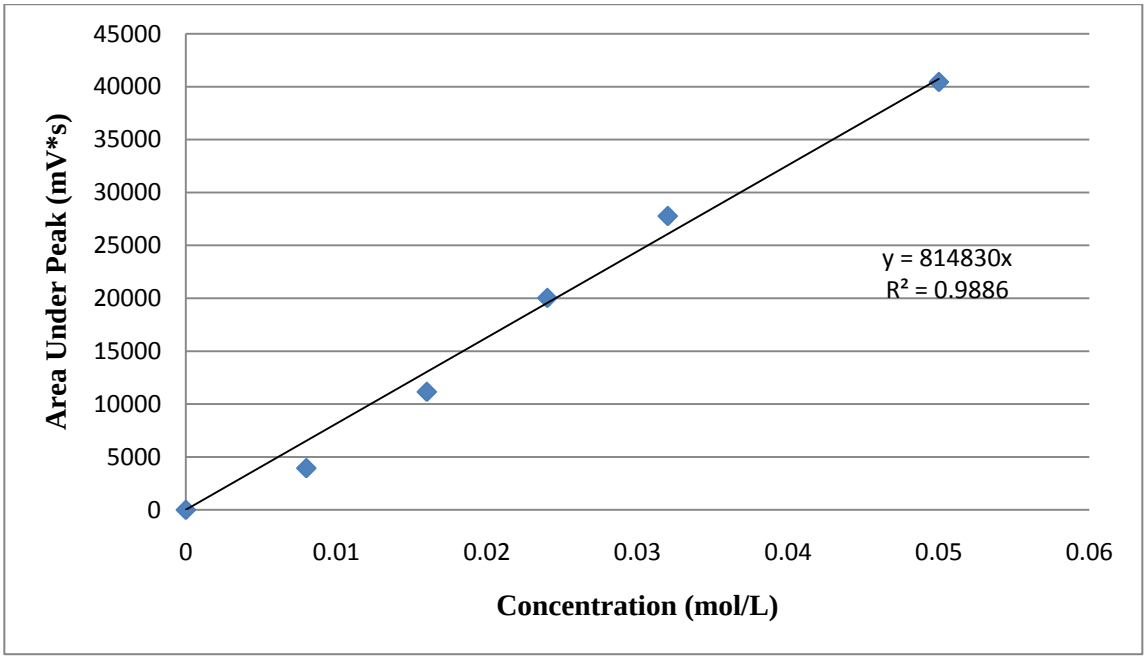

Figure 34. Diphenyldiacetylene calibration curve.

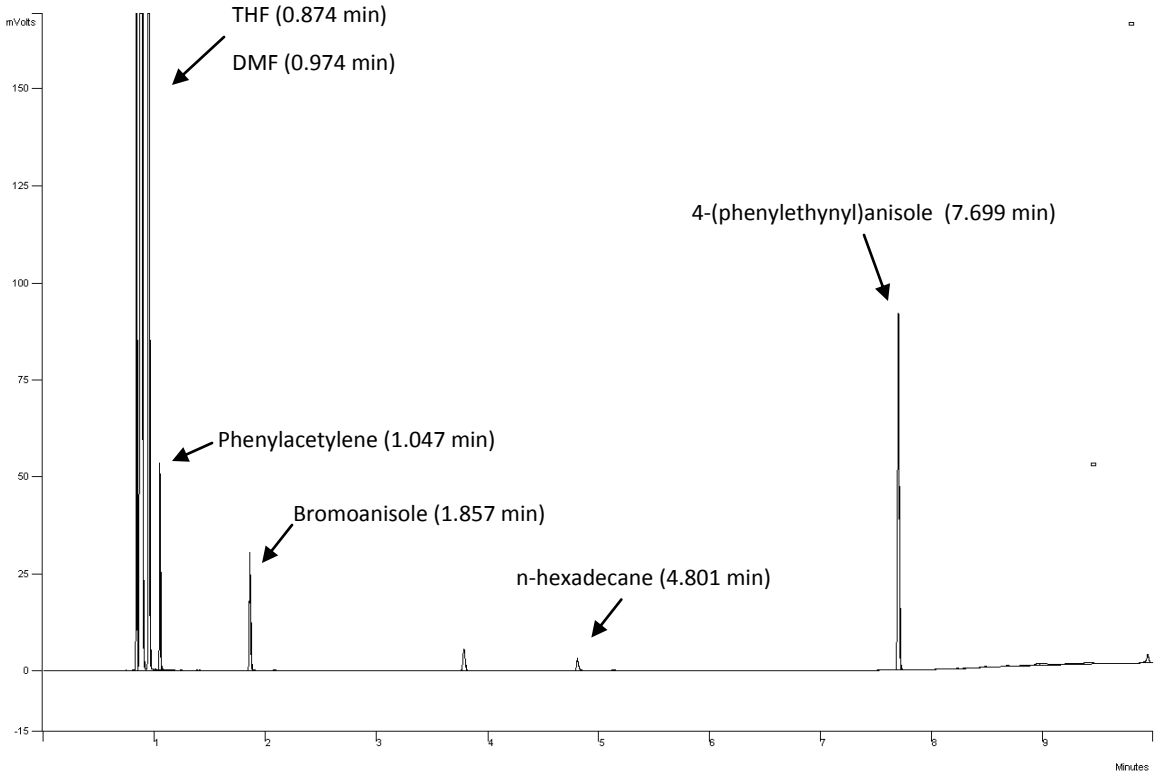

Figure 35. Sample GC spectrum for the cross-coupling reaction of bromoanisole and phenylacetylene to produce 4-(phenylethynyl)anisole.

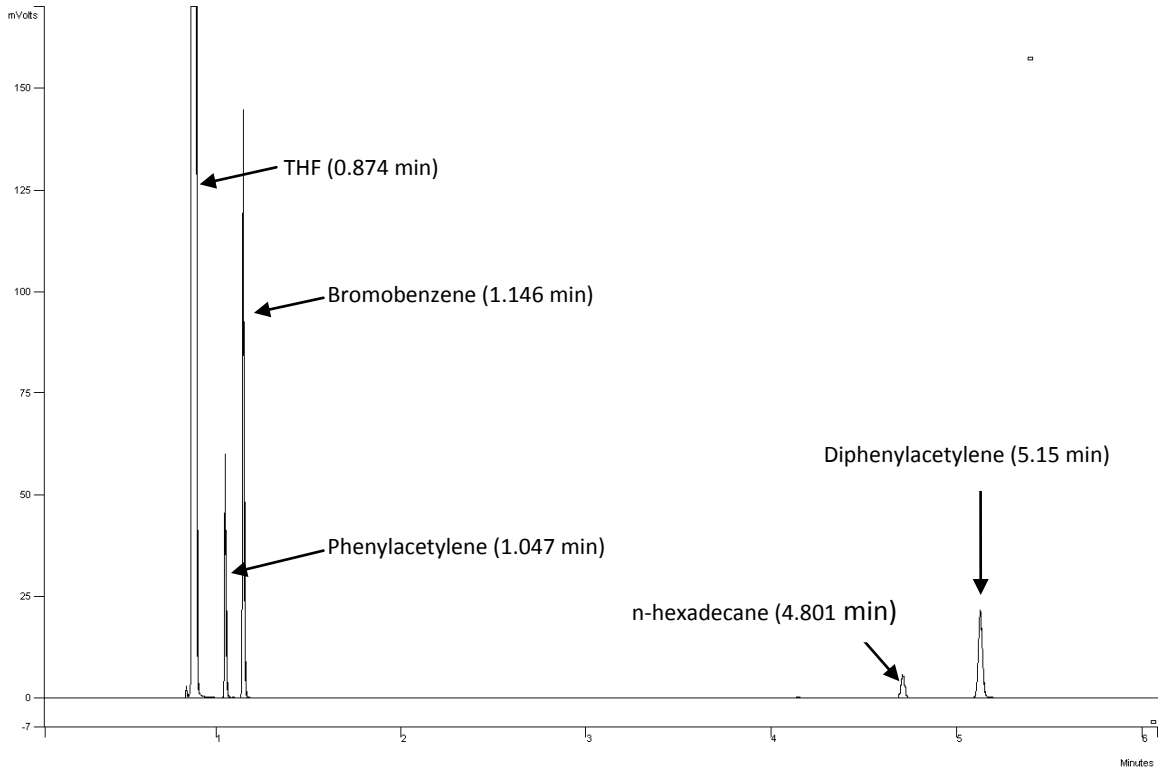

Figure 36. Sample GC spectrum for the cross-coupling reaction of bromobenzene and phenylacetylene to produce diphenylacetylene.

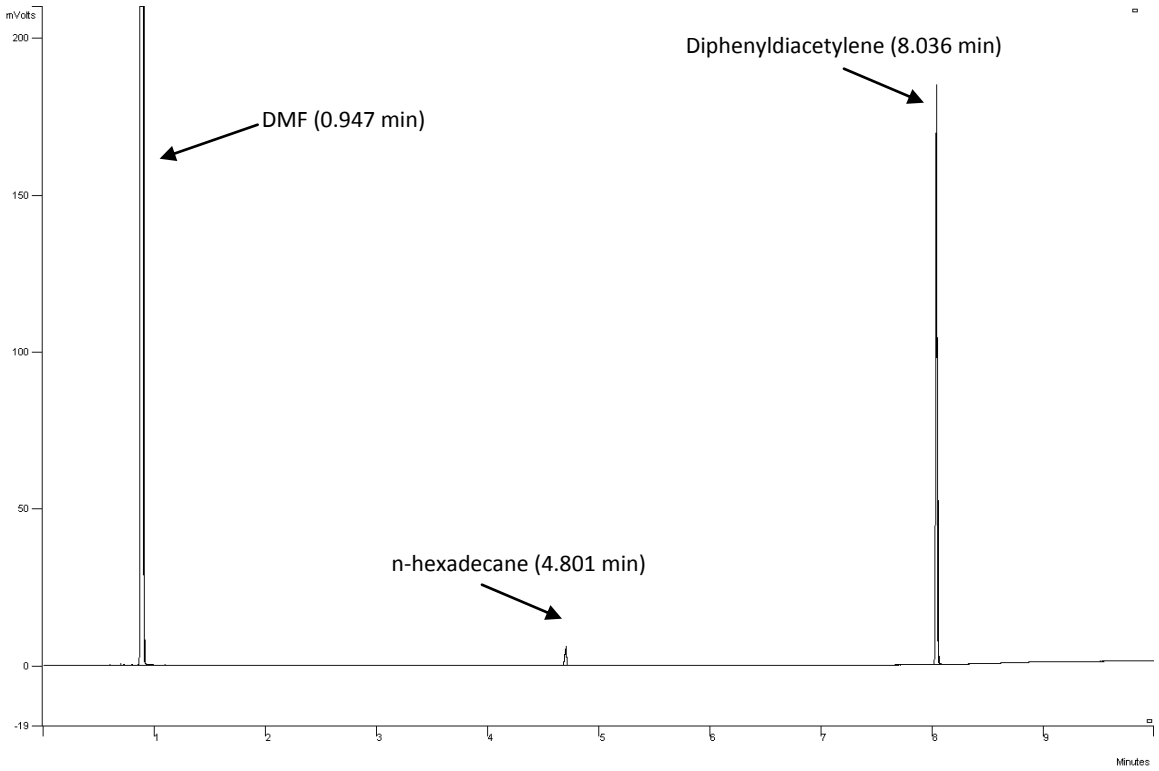

Figure 37. Sample GC Spectrum for the reductive elimination of $Pd(PPh_3)_2(C{\equiv}CPh)_2$ to produce diphenyldiacetylene and active species.

Part 2: Ester Hydrogenation Reactions

Chapter 1

Introduction

1.1 General History of Hydrogenation Reactions

Hydrogenation reactions can be dated back to the early 1800's, but the hydrogenation process is considered to have been discovered by Paul Sabatier in 1897 when he found that the introduction of nickel metal facilitated the addition of hydrogen to molecules of gaseous hydrocarbons.[45] Sabatier was awarded the Nobel Prize in 1912 for his discovery which has now been studied in great depth with a wide variety of functional groups able to be hydrogenated including alkenes, alkynes, aldehydes, ketones and esters.[45]

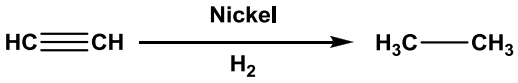

Figure 38. Hydrogenation of C_2H_2 based on methods developed by Paul Sabatier.

In contrast to the hydrogenation of ketones and aldehydes, the hydrogenation of esters to the corresponding alcohols is a problematic reaction.[46] Esters are a stable class of compounds and, with a few exceptions, are reduced with difficulty and have been shown to survive most catalytic hydrogenations. The decreased reactivity of the ester group is believed to be caused by a decreased electrophilicity at carbon, a higher basicity at oxygen, and the lower acidity of the ester group compared to ketones.[47-49]

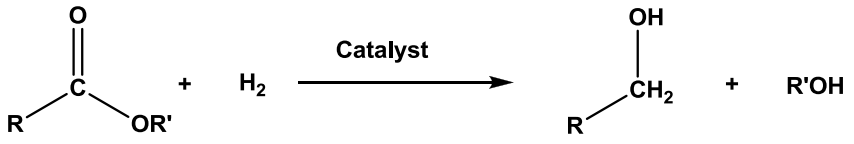

Figure 39. General reaction for ester hydrogenation.

Tradition procedures for the reduction of esters use stoichiometric amounts of metal hydride reagents (e.g. $LiAlH_4$) to obtain alcohols from esters with many environmentally hazardous metal bi-products formed.[50,51] The reduction of esters to the corresponding alcohols is an important reaction in organic synthesis and therefore the catalytic hydrogenation of esters to alcohols, which generates no waste, is environmentally and economically attractive.

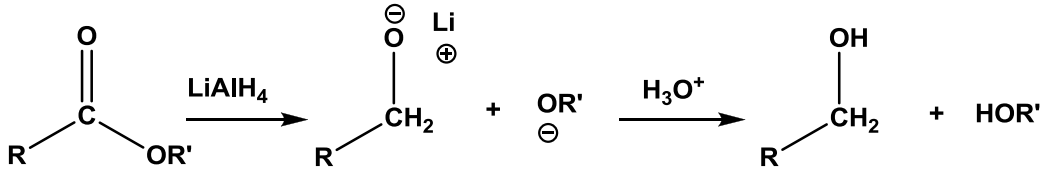

Figure 40. Traditional procedure for ester reduction to produce alcohols using stoichiometric amounts of $LiAlH_4$.

Ruthenium complexes have been employed as catalysts in a wide variety of hydrogenation reactions such as the hydrogenation of alkynes, aldehydes, and ketones.[46] More recent studies have demonstrated the ability of a variety ruthenium complexes to catalyze ester hydrogenations, a much "greener" method compared to traditional methods [47-51,53-58] Heterogeneous hydrogenation of some esters is practiced at relatively high temperatures (200-300 °C) and high hydrogen pressures (200-300 atm) using transition-metal catalysts.[52] Homogeneous systems capable of hydrogenating esters are very scarce,[51,53-58] and are mostly limited to activated esters. In these systems large amounts of additives such as an organic base, inorganic acids, salts, zinc, and fluorinated alcoholic solvents are needed to obtain high conversions of esters into alcohols. The exact functions of the additives are not known, but the additives are believed to aid in the generation of the active catalyst as well as activate the ester carbonyl functionality by coordinating to it rendering it more prone to attack by the catalyst.[50]

Hydrogenation reactions, in general, involve splitting molecular hydrogen, most commonly achieved by the reaction of dihydrogen gas with a transition metal complex.[45] The splitting can occur through two different pathways with the initial intermediate being the same in

both cases, an η^2-dihydrogen-metal complex (Figure 41).[52] The intermediate can then undergo an oxidative addition reaction where the H-H bond is split homolytically to give, when starting with a six-coordinate dihydrogen complex, a seven coordinate dihydride product. Alternatively, if there is a suitable base present, the dihydrogen bond can be split heterolytically to give a six-coordinate metal hydride product and a protonated base.

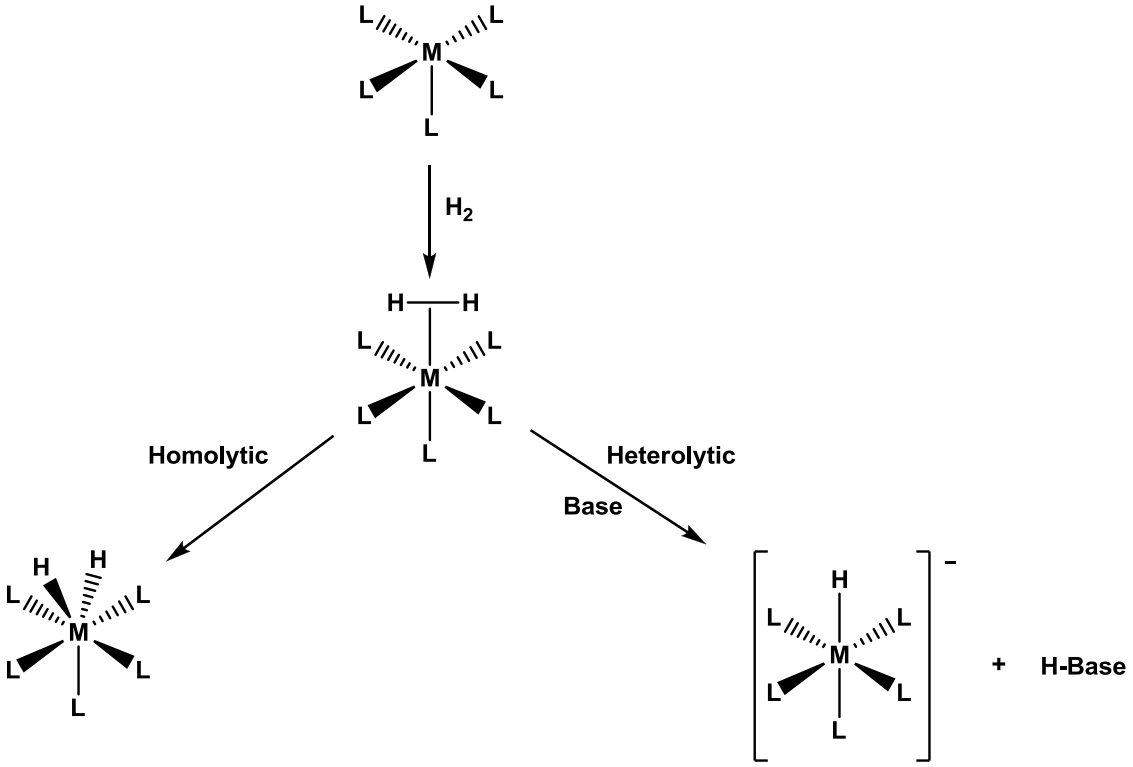

Figure 41. Two reaction pathways for H_2 splitting in the presence of a transition metal.

Both pathways have been demonstrated to occur in separate successful hydrogenation systems.[53-55] These intermediates are considered to be the active catalytic species and have been shown to partake in the catalytic cycle for hydrogenation of functional groups such as alkenes, alkynes, aldehydes, ketones and esters.[45] Although harsh reaction conditions were required for the efficient conversion of the ester to the corresponding alcohols, Grey *et al*.[53] have described an anionic ruthenium hydride complex capable of hydrogenating alkenes, ketones, and esters (Figure 42).

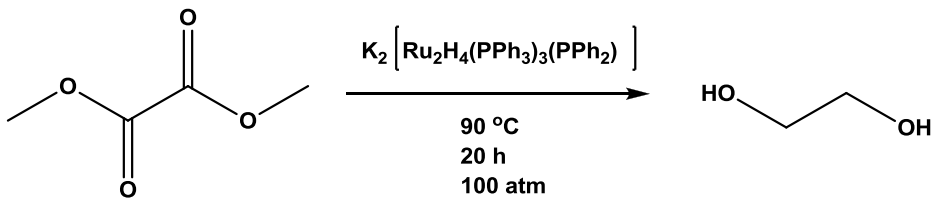

Figure 42. Catalytic hydrogenation of DMO (dimethyl oxalate) to ethylene glycol in the presence of an anionic ruthenium complex.

A study by Matteoli *et al*.[54,55] describes a system capable of catalytically hydrogenating DMO (dimethyl oxalate) to ethylene glycol involving the homolytic cleavage of H_2, and therefore a neutral ruthenium complex (Figure 43).

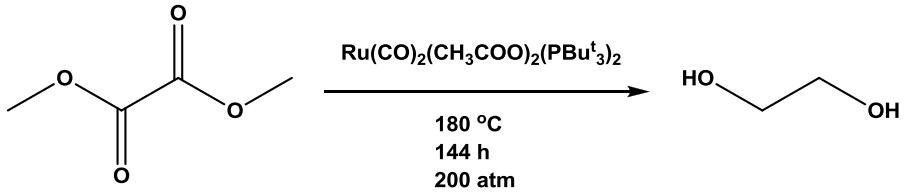

Figure 43. Catalytic hydrogenation of DMO to ethylene glycol in the presence of a neutral ruthenium complex.

1.2 Catalytic Systems Capable of Ester Hydrogenation

Successful systems capable of hydrogenating a variety of substrates are scarce with very few found in the literature.[51,53-58] Teunissen and Elsevier[51] reported a system involving $Ru(acac)_3$ ($acac^-$ = acetylacetonate) with triphos ($MeC(CH_2PPh_2)_3$), which effectively catalyzed the hydrogenation of five different esters. The most difficult reaction reported was the hydrogenation of the deactivated ester benzylbenzoate to benzyl alcohol at 120 °C under 84 atm of H_2. The system used fluorinated alcohols as solvents and an excess of triethylamine to produce a 97 % conversion of the ester with a 95 % selectivity to the desired alcohol (Figure 44).

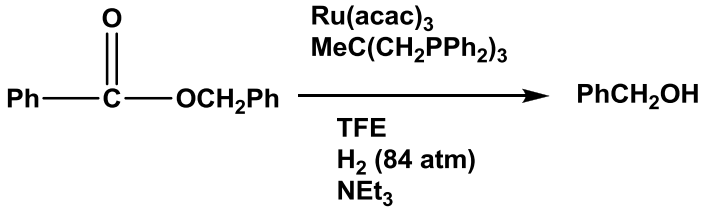

Figure 44. Elsevier and Teunissen's system for the hydrogenation of benzylbenzoate to benzyl alcohol.

Normura *et al*.[58] reported that $Ru(acac)_3$ with excess $P(n\text{-}C_8H_{17})_3$ in the presence of zinc in polar solvents at 200 °C and 10 atm of H_2 was capable of hydrogenating methyl phenylacetate to 2-phenylethanol. The yields obtained were consistently greater than 85 % and varied due to the length of reaction as well as the solvent and additive used (Figure 45).

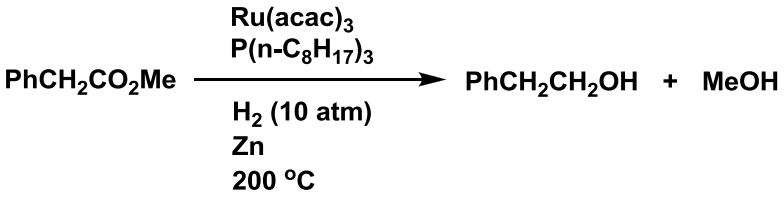

Figure 45. Catalytic system developed by Normura *et al*. for the hydrogenation of methyl phenylacetate to 2-phenylethanol and methanol.

Although both groups were successful in hydrogenating non-activated esters (i.e. esters in which there is no electron withdrawing group adjacent to the carbalkoxy group), the reaction conditions were far from mild and therefore on an industrial scale the systems would not be attractive environmentally or economically.

Recent studies by Teunissen and Elsevier[56] have furthered the investigation of the promising $Ru(acac)_3$/ligand system by performing a ligand comparison to optimize the system. As the active catalyst is generated *in situ*, it was hypothesized that the ligands attached to the metal centre may have a large effect on the conversion of the ester as well as on the selectivity to the

desired alcohols. Results obtained show phosphines to be much more active than nitrogen ligands which have been proven to be successful for other hydrogenation reactions. It was also determined that polydentate phosphines are often favoured over monodentate phosphines and generally produce higher conversions and with higher selectivity to the desired alcohols.[51,56] Reactions were also carried out using $Ru(acac)_3$ in the absence of phosphines. Conversions of the ester were minimal and it was found that the inclusion of phosphines is essential to obtain high conversions. The literature suggests the phosphines aid in the reduction of the Ru(III) species to produce the active catalyst, a Ru(II) speices.[51,56-58,60]

Saudan *et al*.[59] describe a system capable of hydrogenating methyl benzoate to produce benzyl alcohol in 97 % yields using relatively mild reaction conditions as compared to the systems developed by Normura *et al*. and Teunissen and Elsevier. The only negative aspect of the system developed by Saudan *et al*. is the complex ruthenium catalyst (**I**) required to obtain significant conversions to the desired alcohols.

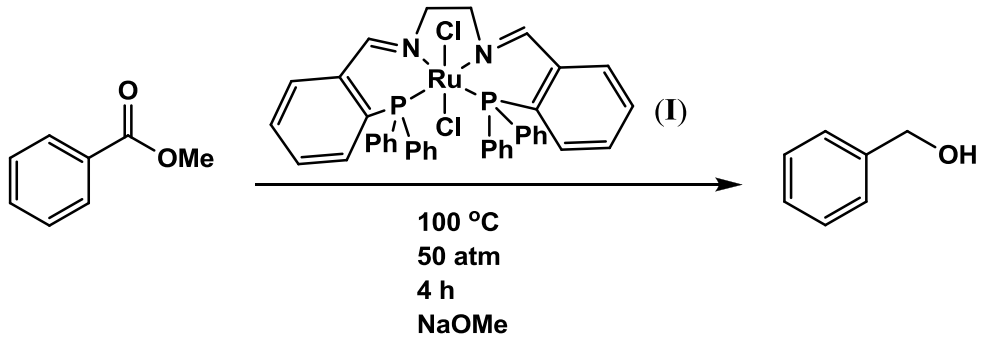

Figure 46. Catalytic hydrogenation of methyl benzoate to benzyl alcohol using the system developed by Saudan *et al.*

1.3 The Reaction Mechanism

As can be seen in Figure 47, the first step in the catalytic cycle is the production of the active catalyst which is believed is believed to be a Ru(II) complex generated *in situ*

through the reduction of the ruthenium complex by molecular hydrogen and other additives.[51,56,58] As the active species is generated *in situ*, the exact structure of the active catalyst is unknown and has made advancements in the area of catalytic ester hydrogenation difficult. For the $Ru(acac)_3$/phosphine systems, the literature suggests the phosphines and H_2 aid in the reduction of the Ru(III) species to produce the active catalyst, a Ru(II) species (Figure 47).[51,56-58,60]

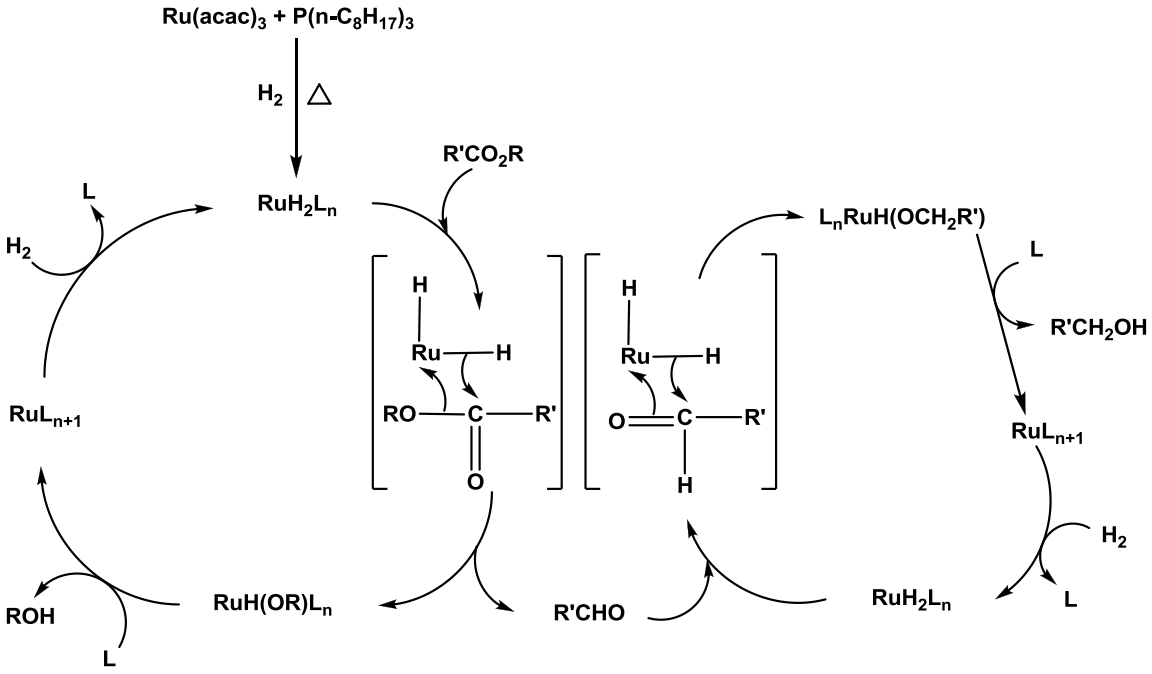

Figure 47. Generally accepted catalytic cycle for ester hydrogenation reactions using the $Ru(acac)_3$/phosphine systems.

1.4 Research Aims

1.4.1 Synthesis of $Ru(acac)_2(phosphine)_{1-2}$ Complexes

The $Ru(acac)_3$/phosphine systems developed by Normura *et al*.[58] and Teunissen and Elsevier[51,56] have proven that the catalytic hydrogenation of a variety of esters is possible in modest yields. The objective of this thesis is to improve upon their systems by employing $Ru(acac)_2(phosphine)_{1-2}$ species with the hypothesis of obtaining increased conversions to the

desired alcohols. The catalyst would be a Ru(II) species prior to reactions rather than generated *in situ* and therefore may increase rates of reaction. Also to be investigated is the potential of decreasing reaction conditions as compared to those reported in literature while maintaining or increasing yields to the desired alcohols.

The literature suggests the active species to be a Ru(II) compound formed from the reduction of the starting material by phosphine ligands.[51,56-58,60] It is hypothesized that pre-forming the $Ru(acac)_2(phosphine)_{1-2}$ species may increase conversions to the desired alcohols and reduce reaction conditions for ester hydrogenation reactions. The Ru(II) complexes will be generated through a simple one step reaction in which zinc acts as a reducing agent.[62,63]

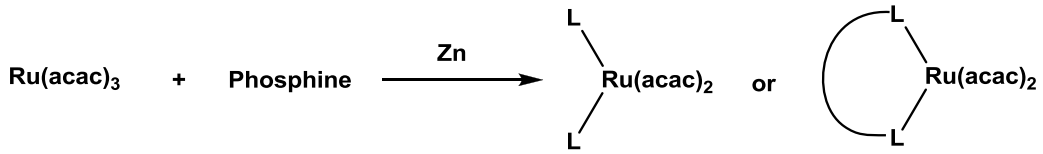

Figure 48. Proposed reaction pathway for the formation of Ru(II) species.

1.4.2 Reactivity Tests – Potential as an Ester Hydrogenation Catalyst

Once synthesized, the $Ru(acac)_2(phosphine)_{1-2}$ complexes will be tested as precatalysts for a standard ester hydrogenation reaction. The preformed Ru(II) species will be compared to systems which the active species is generated *in situ* from the reduction of $Ru(acac)_3$ by phosphine ligands. The most successful result obtained by Normura *et al*.[58] and Elsevier and Teunissen[51,56] will be repeated to ensure proper function of our autoclave as well as provide a direct comparison of the efficiency of the catalysts under identical conditions. Attempts will be made to hydrogenate methyl benzoate to methanol and benzyl alcohol, the standard reaction (Figure 49), with the aim of demonstrating an increased rate of conversion with the use of $Ru(acac)_2(phosphine)_{1-2}$ species. Reaction conditions such as solvent and additional reagents will

be varied in attempts to increase yields to the desired alcohols while maintaining mild reaction conditions.

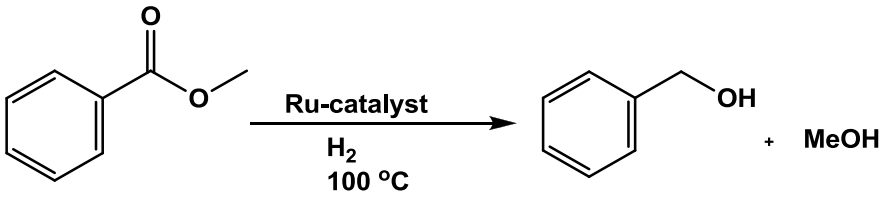

Figure 49. Standard ester hydrogenation reaction to be investigated.

Chapter 2

Experimental

2.1.1 General Synthetic and Analytical Methods

All reactions were carried out in air unless otherwise stated. Hydrogenation reactions were performed using a Parr 5511 25 mL split ring high pressure compact reactor. Syntheses of potential catalysts were performed in air using wet reagents. Specific reagents such as air sensitive phosphines were handled in a dry, deoxygenated argon or nitrogen atmosphere using standard Schlenk line techniques or an MBraun Labmaster glove box.

NMR spectra were obtained on a Bruker AV300 spectrometer. ^{31}P NMR spectra were run at 121.5 MHz with a delay of 2 seconds and are referenced with respect to external 85% H_3PO_4. ^{1}H NMR data are referenced to TMS via the residual proton signals of the deuterated solvents.

GC analyses were conducted on a Varian 3900 GC equipped with a CP-8400 autosampler, a CP-1177 injector, a FID detector and a Varian WCOT Fused Silica column (CP-Sil 8CB, 25 m x 0.32 mm ID, DF = 0.52). The GC method used was a total of 14 minutes with the column oven initially set at 40 °C. The temperature of the column oven was held at 40 °C for 3 minutes before being increased at a rate of 20 °C/minute to 200 °C. Lastly, the column oven was increased at a rate of 100 °C/minute to 300 °C and held for 2 minutes to condition the column at the end of ever run. The injector port and FID detector were set to 250 °C.

GC-MS analyses were conducted on an Agilent Technologies 6850 GC-MS with an Agilent 6850 autosampler, an E.I. detector and a Varian capillary column (30 m x 0.25 mm ID). The method used was the same as the GC method.

2.1.2 Chemical Supplies

All chemicals were purchased from Sigma-Aldrich or Strem and used without purifications, unless otherwise stated. Deuterated solvents were purchased from Cambridge Isotope Laboratories and stored over activated 4 Å molecular sieves. $RuCl_3 \cdot 3H_2O$ was obtained on a loan from Johnson Matthey and was used as obtained. PCy_3 was purchased from Strem and was stored and used in the glovebox. Bidentate phosphines such as dppp and dppf were also purchased from Strem but were used directly on the bench top without any purification. Triphos and PPh_3 were obtained from Strem and the latter was recrystallized from EtOH. Esters such as methyl benzoate and dimethyl oxalate were purchased from Sigma-Aldrich and used as obtained. Solvents were purchased from Fischer Scientific and were used as obtained. Other reagents such as acetylacetone, zinc dust and potassium-tert-butoxide were purchased from Sigma-Aldrich and used as obtained. An ultra high purity 5.0 hydrogen gas cylinder was purchased from Praxair and used as the hydrogen source for all hydrogenation reactions.

2.2 Preparation of Reagents

2.2.1 Synthesis of $Ru(acac)_3$

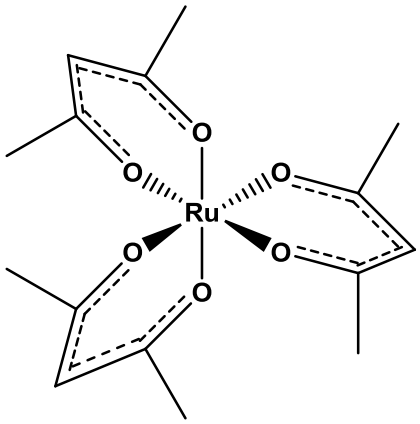

This compound was prepared according to the procedure described by Knowles *et al.*[61] $RuCl_3 \cdot 3H_2O$ (0.23 g, 0.0011 mol) was dissolved in 10 mL of acetylacetone. $KHCO_3$ (0.28 g, 0.0028 mol) was added to the round bottom flask and the mixture was refluxed for 4 h. The

solution was filtered and evaporated to dryness to yield a crude product which was recrystallized from dichloromethane and hexane resulting in red crystals. Yield: 0.34 g, 78 %. ^{1}H NMR ($CDCl_3$): δ −5.4 (CH_3), −29.6 (CH). Lit.[61]: ^{1}H NMR ($CDCl_3$): δ −5.5 (CH_3), −29.9 (CH).

2.2.2 Synthesis of $Ru(acac)_2(PPh_3)_2$

This compound was synthesized through a modified procedure described by Gupta and Poddar.[62] $Ru(acac)_3$ (0.2 g, 0.0005 mol) was dissolved in EtOH (20 mL). Zinc dust (1 g, 0.015 mol) was added and the mixture was refluxed for 1 h. PPh_3 (0.262 g, 0.001 mol) was added and the reaction was refluxed for an additional 4 h. The colour of the solution changed from bright red to yellow and was filtered to remove zinc dust. Portions of the desired compound remained with the zinc dust therefore it was washed with CH_2Cl_2 (3 x 5 mL) to dissolve the compound. The filtrates were combined and evaporated to dryness to yield a crude product which was recrystallized from dichloromethane and hexanes resulting in bright yellow crystals. Yield: 0.31 g, 75 %. ^{1}H NMR ($CDCl_3$): δ 1.48 (s, CH_3), 5.23 (s, CH), 7.04-7.60 (m, phenyl protons). ^{31}P NMR ($CDCl_3$): δ 53.8.

2.2.3 Synthesis of $Ru(acac)_2$(dppp)

This compound was synthesized through a modified procedure described by Hoshino et *al*.[63] $Ru(acac)_3$ (0.2 g, 0.0005 mol) was dissolved in EtOH (20 mL). Zinc dust (1 g, 0.015 mol) was added and the mixture was refluxed for 1 h. Dppp (0.206 g, 0.0005 mol) was added and the reaction was refluxed for an additional 4 h. The colour of the solution changed from bright red to orange/brown and was filtered to remove zinc dust. Portions of the desired compound remained with the zinc dust therefore it was washed with CH_2Cl_2 (3 x 5 mL) to dissolve the compound. The filtrates were combined and evaporated to dryness to yield a crude product which was recrystallized from dichloromethane and hexanes resulting in orange crystals. Yield: 0.26 g, 71

%. ^{1}H NMR ($CDCl_3$): δ 1.84 (s, CH_3), 2.01-2.52 (m, CH_2), 5.23(CH), 7.04-7.60 (phenyl protons). ^{31}P NMR ($CDCl_3$): δ 48.6.

2.2.4 Synthesis of $Ru(acac)_2(dppf)$

This compound was synthesized through a modified procedure described by Hoshino *et al*.[63] $Ru(acac)_3$ (0.2 g, 0.0005 mol) was dissolved in EtOH (20 mL). Zinc dust (1 g, 0.015 mol) was added and the mixture was refluxed for 1 h. Dppf (0.277 g, 0.0005 mol) was added and the reaction was refluxed for an additional 4 h. The colour of the solution changed from bright red to orange and was filtered to remove zinc dust. Portions of the desired compound remained with the zinc dust therefore it was washed with CH_2Cl_2 (3 x 5 mL) to dissolve the compound. The filtrates were combined and evaporated to dryness to yield a crude product which was recrystallized from dichloromethane and hexanes resulting in bright orange crystals. Yield: 0.35 g, 81 %. ^{1}H NMR ($CDCl_3$): δ 1.88 (s, CH_3), 4.21-4.79 (ferrocene protons), 5.23 (s, CH), 7.04-7.60 (phenyl protons). ^{31}P NMR ($CDCl_3$): δ 52.5.

2.3 General Procedures for Hydrogenation Reactions

A stir bar, precatalyst, solvent, ester and in certain cases other reagents such as Zn and a phosphine were added to a glass insert. The insert was placed in the pressure reactor which was then sealed and clamped in an oil bath which was preheated to the desired reaction temperature, 100 °C. The autoclave was flushed with H_2 three times before being filled to the pressure to be used for the reaction, 68 atm. The reactions were generally run for 18-48 h after which the autoclave was cooled and a sample of the reaction mixture was diluted and run through a GC to determine the percent conversion to the desired alcohols.

2.3.1 Hydrogenation Reactions using $Ru(acac)_3$ and Phosphines

$Ru(acac)_3$ (0.05 g, 0.16 mmol), phosphine (0.96 mmol for monodentate, 0.48 mmol for bidentate, 0.32 mmol for tridentate), solvent (10 mL, THF), ester (16 mmol, methyl benzoate or

dimethyl oxalate) were added to a glass insert containing a stir bar. The insert was sealed within the autoclave which was then clamped in an oil bath (100 °C) and attached to the hydrogen gas cylinder. The autoclave was filled with hydrogen to a pressure of 68 atm. The pressure was then released to 34 atm and filled again to 68 atm. This flushing process was repeated three times and after the autoclave was filled to the desired H_2 pressure, 68 atm. Reaction lengths varied from 18-48 h with the majority being stopped after 24 h. The reaction solution was filtered through a celite plug then a 0.2 mL sample was removed and diluted using a 10 mL volumetric flask. The percent conversion of the ester and the percent yields of the desired alcohols were determined by gas chromatography.

2.3.2 Hydrogenation Reactions using $Ru(acac)_3$, Phosphines, and Reagents

The procedure for 5.3.1 was repeated with the addition of Zn (0.032 g, 0.48 mmol). The reactions were run for the same amount of time and results were again obtained by gas chromatography.

2.3.3 Hydrogenation Reactions using $Ru(acac)_2(Phosphine)_{1-2}$

$Ru(acac)_2(phosphine)_{1-2}$ (0.16 mmol), solvent (10 mL, THF, MeOH, toluene, or diglyme), ester (16 mmol, methyl benzoate or dimethyl oxalate), Zn (0.021 g, 0.32 mmol) and phosphine (2 or 4 eq) in certain cases were added to a glass insert containing a stir bar. The insert was sealed within the autoclave which was then clamped in an oil bath (100 °C) and attached to the hydrogen gas cylinder. The autoclave was filled with hydrogen to a pressure of 68 atm. The pressure was then released to 34 atm and filled again to 68 atm. This flushing process was repeated three times and after the autoclave was filled to the desired hydrogen pressure (68 atm). Reaction lengths varied from 18-48 h with the majority being stopped after 24 h. The reaction solution was filtered through a celite plug then a 0.2 mL sample was removed and diluted using a 10 mL volumetric

flask. The sample was run through a GC to determine the percent conversion of the ester as well as the percent yields of the desired alcohols.

2.3.4 Hydrogenation Reactions using $Ru(acac)_3$/$Ru(acac)_2$dppf

$Ru(acac)_2(phosphine)_{1\text{-}2}$ (0.16 mmol), $Ru(acac)_3$ (0.16 mmol), diglyme (10 mL), methyl benzoate (16 mmol) and Zn (0.021 g, 0.32 mmol) were added to a glass insert containing a stir bar. The insert was sealed within the autoclave which was then clamped in an oil bath (100 °C) and attached to the hydrogen gas cylinder. The autoclave was filled with hydrogen to a pressure of 68 atm. The pressure was then released to 34 atm and filled again to 68 atm. This flushing process was repeated three times and after the autoclave was filled to the desired hydrogen pressure (68 atm). After 24 h, the reaction was stopped and the solution was filtered through a celite plug then a 0.2 mL sample was removed and diluted using a 10 mL volumetric flask. The sample was run through a GC to determine the percent conversion of the ester as well as the percent yields of the desired alcohols.

2.3.5 Hydrogenation Reactions using the ruthenium coated glass insert from 2.3.4

After reactions performed in 2.3.4 the glass insert was coated in ruthenium metal. Diglyme (10 mL), methyl benzoate (16 mmol) and Zn (0.021 g, 0.32 mmol) were added to the coated glass insert and sealed within the autoclave. The reaction was carried out as stated in 2.3.4.

Chapter 3

Results and Discussion

3.1 Results and Discussion of $Ru(acac)_2(phosphine)_{1\text{-}2}$ complexes

The newly synthesized $Ru(acac)_2$dppp and $Ru(acac)_2$dppf species were characterized by ^{31}P and ^{1}H NMR spectroscopy and to further confirm the structures, by X-ray crystallography. $Ru(acac)_2(PPh_3)_2$ has been reported,[62] but the characterization did not include crystallographic data and as a large crystal was obtained during the synthesis, a crystal structure was also obtained to further confirm the structure. Select bond lengths and the crystal structures obtained are displayed below for the three compounds. A complete set of structural data can be found in Appendix B. Elemental analyses were not performed as the compounds showed next to no activity as catalysts and the project was dropped as there seemed to be a discrepancy in the literature.

Table 2. Selected Bond Lengths (Å) for $Ru(acac)_2(PPh_3)_2$.

bond	bond length (Å)	bond	bond length (Å)
Ru(1)-O(3)	2.060(3)	Ru(1)-O(4)	2.096(3)
Ru(1)-O(2)	2.063(3)	Ru(1)-P(1)	2.295(11)
Ru(1)-O(1)	2.096(3)	Ru(1)-P(2)	2.326(11)

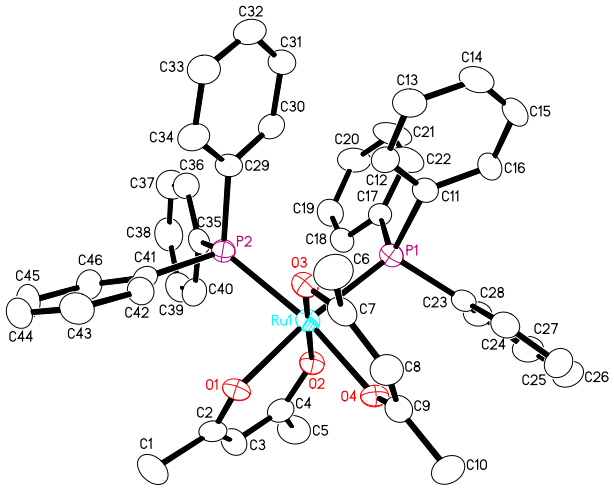

Figure 50. Molecular structure of $Ru(acac)_2(PPh_3)_2$ (50% probability level).

Table 3. Selected Bond Lengths (Å) for $Ru(acac)_2dppp$

bond	bond length (Å)	bond	bond length (Å)
Ru(1)-O(2)	2.0694(17)	Ru(1)-O(1)	2.1065(18)
Ru(1)-O(3)	2.0703(17)	Ru(1)-P(1)	2.2541(7)
Ru(1)-O(4)	2.1030(18)	Ru(1)-P(2)	2.2568(8)

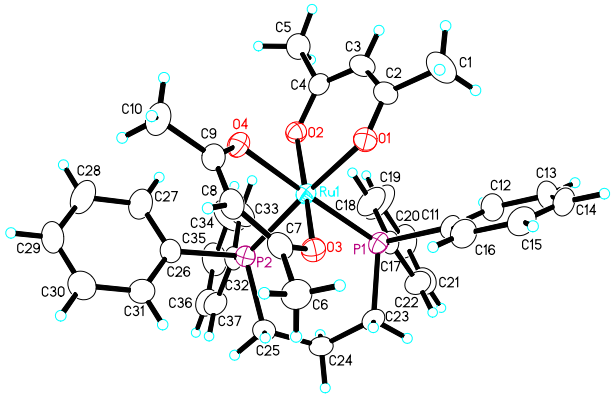

Figure 51. Molecular structure of $Ru(acac)_2dppp$ (50% probability level).

Table 4. Selected bond Lengths (Å) for $Ru(acac)_2dppf$.

bond	bond length (Å)	bond	bond length (Å)
Ru(1)-O(3)	2.0564(19)	Ru(1)-O(2)	2.099(2)
Ru(1)-O(1)	2.0569(19)	Ru(1)-P(1)	2.2731(8)
Ru(1)-O(4)	2.086(2)	Ru(1)-P(2)	2.2843(7)

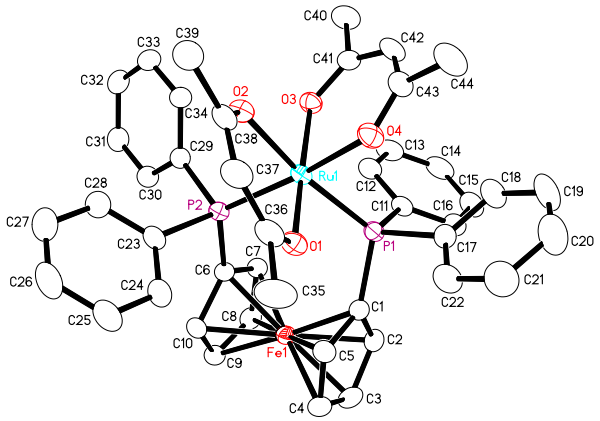

Figure 52. Molecular structure of $Ru(acac)_2dppf$ (50% probability level).

As can be seen in Tables 2, 3, and 4, the larger *trans* effect of the phosphine ligand causes the Ru-O bond opposite it to be slightly longer than other Ru-O bonds which are not *trans* to a phosphine.[64] An example can be seen in Figure 50 as the Ru(1)-O(1) bond is *trans* to a phosphine and has a bond length of 2.096 Å, whereas the Ru(1)-O(1) bond is *trans* to an oxygen and has a smaller bond length of 2.060 Å. The *trans* effect is present again within $Ru(acac)_2$dppp and $Ru(acac)_2$dppf as the Ru-O bond lengths are slightly longer when the bond is *trans* to a phosphine. This bond lengthening, and therefore weakening, is caused by the strong sigma donation from the phosphine to the metal centre, which in turn, weakens the M-L bond opposite to it.[64]

3.2 Results and Discussion of Hydrogenation Reactions

The aim of this research is to probe the nature of the ruthenium-based catalysts in the system developed by Teunissen and Elsevier,[51,56] which was capable of hydrogenating dimethyl oxalate (DMO) to ethylene glycol in 95 % yield. The ruthenium catalyst was generated *in situ* by the reaction of $Ru(acac)_3$ with triphos ($MeC(CH_2PPh_2)_3$) and H_2. The reported reaction was replicated using our autoclave and chemicals to ensure proper function of equipment as well as procedures. The result obtained was within 5 % of the reported conversion of DMO to ethylene glycol. Saudan *et al*.[59] recently reported a series of reactions using a complex ruthenium catalyst, (**I**), for the hydrogenation of methyl benzoate to benzyl alcohol and methanol. Their most significant reaction produced a 99 % conversion of methyl benzoate with a system using (**I**) at 100 °C with a hydrogen pressure of 50 atm. The results showed significant conversions under more mild reaction conditions as compared to the systems developed by Teunissen and Elsevier other then the complexity of the ruthenium catalyst employed.

The initial series of reactions in this study extended the work carried out by Normura *et al.* and Teunissen and Elsevier for ester hydrogenation reactions. The simple $Ru(acac)_3$/phosphine system was employed for the hydrogenation of methyl benzoate, a reaction previously not performed using this system. The aim of the reaction series was to produce similar results as obtained by Saudan *et al.* for the hydrogenation of methyl benzoate. The hydrogenation reactions were carried out according to subsection 2.3.1 in which the phosphine was varied to determine the effect of phosphine on the system with results displayed in Table 5.

Table 5. Hydrogenation of methyl benzoate using $Ru(acac)_3$/phosphine system.

Catalyst	Phosphine (equivalents)	% Conversion of methyl benzoate	% Yield of benzyl alcohol	% Yield of methanol [b]
$Ru(acac)_3$	triphos (2 eq)	54	50	N/I
$Ru(acac)_3$	PPh_3 (6 eq)	5	3	N/I
$Ru(acac)_3$	PCy_3 (6 eq)	0	0	N/I
$Ru(acac)_3$	dppe (3 eq)	24	18	N/I
$Ru(acac)_3$	dppp (3 eq)	25	14	N/I
$Ru(acac)_3$	dppf (3 eq)	30	19	N/I
$Ru(acac)_3$	none	0	0	N/I

a. Conditions: 100 °C, $p(H_2)$ = 68 atm, 24 h, MeOH.

b. N/I = not investigated (difficult to determine the yield of MeOH when MeOH was used as the solvent).

Results obtained for the phosphine variation agreed with the trends observed in the literature for the hydrogenation of DMO. The tridentate phosphine, triphos, produced the largest conversion of methyl benzoate to the desired alcohols while monodentate phosphines produced the lowest yields. The conversion of methyl benzoate was significantly lower as compared to the conversion of DMO but a greater concern was the fact that the system developed by Saudan *et al*. produced larger conversions for the hydrogenation of methyl benzoate.

The overall conversion of methyl benzoate was not significant and it was hypothesized that the reactions may be enhanced through the addition of reagents such as zinc as suggested by

other groups.[58,60,65] The reactions were repeated in the presence of zinc with the goal of obtaining comparable results to those obtained by the system developed by Saudan *et al*. which also uses zinc as a reagent for the hydrogenation of methyl benzoate. The reactions were performed according to subsection 2.3.2 with the results displayed in Table 6.

Table 6. Additive effect. $Ru(acac)_3$/phosphine system with the addition of zinc.

Catalyst	Phosphine (equivalents)	% Conversion of methyl benzoate	% Yield of benzyl alcohol	% Yield of methanol [b]
$Ru(acac)_3$	triphos (2 eq)	73	67	N/I
$Ru(acac)_3$	PPh_3 (6 eq)	17	8	N/I
$Ru(acac)_3$	PCy_3 (6 eq)	3	0	N/I
$Ru(acac)_3$	dppe (3 eq)	34	22	N/I
$Ru(acac)_3$	dppp (3 eq)	39	26	N/I
$Ru(acac)_3$	dppf (3 eq)	45	31	N/I
$Ru(acac)_3$	none	0	0	N/I

a. Conditions: 100 °C, p(H_2) = 68 atm, 24 h, MeOH, Zn (0.01 g).

b. N/I = not investigated (to determine the yield of MeOH when MeOH was used as the solvent).

The results using zinc agreed with results obtained by other groups[58,60] as its presence produced an increase in the conversion of methyl benzoate. However the hydrogenation reactions were still not producing significant conversions or yields to the desired alcohols. The $Ru(acac)_3$/phosphine system has proven to be capable of catalytically hydrogenating certain esters with the extent of conversion depending on the ester to be hydrogenated. As the results from subsections 2.3.1 and 2.3.2 were not significant, the project was taken in a slightly different direction by employing a variation of the catalytic system. The active catalytic species is not known, but the literature suggests it to be a Ru(II) species.[58,60] A series of Ru(II) complexes of the type $Ru(acac)_2(phosphine)_{1-2}$ was therefore synthesized and tested as catalysts for the hydrogenation of methyl benzoate according to subsection 2.3.3 with the results displayed in Table 7.

Table 7. Hydrogenation of methyl benzoate using $Ru(acac)_2(phosphine)_{1-2}$ systems.

Catalyst	% Conversion of methyl benzoate	% Yield of benzyl alcohol	% Yield of methanol [b]
$Ru(acac)_2(PPh_3)_2$	9	0	N/I
$Ru(acac)_2$dppp	7	0	N/I
$Ru(acac)_2$dppf	15	4	N/I

a. Conditions: 100 °C, p(H_2) = 68 atm, 24 h, MeOH, Zn (0.01 g).

b. N/I = not investigated (difficult to determine yield of MeOH when solvent used was MeOH).

As PCy_3 did not produce high yields under the conditions tested it was omitted from this series of reactions. As can be seen in Table 7, the use of $Ru(acac)_2(phosphine)_{1-2}$ species did not increase the efficiency of the system as minimal conversions of methyl benzoate were observed. The preformed Ru(II) species were not effective as precatalysts under the conditions stated and as a result reaction conditions were varied in an attempt to increase conversions and yields.

Several groups have reported that the solvent utilized in hydrogenation reactions has an effect on the amount of conversion of the ester.[51,58,60] The next series of reactions was performed to determine if the variation of solvent could increase conversion of methyl benzoate to the desired alcohols using the new $Ru(acac)_2(phosphine)_{1-2}$ systems. It was hypothesized that finding an optimal solvent may contribute to increased yields of the desired alcohols as suggested by other groups. The reactions performed in subsection 2.3.3 when zinc was present were repeated using a variety of solvents with the results displayed in Table 8, 9 and 10.

Table 8. Solvent effect. $Ru(acac)_2(phosphine)_{1-2}$ systems in THF.

Catalyst	Phosphine (equivalents)	% Conversion of methyl benzoate	% Yield of benzyl alcohol	% Yield of methanol
$Ru(acac)_3$	triphos (2 eq)	70	61	59
$Ru(acac)_2(PPh_3)_2$	-	9	1	0
$Ru(acac)_2$dppp	-	12	3	1
$Ru(acac)_2$dppf	-	16	6	2

a. Conditions: 100 °C, p(H_2) = 68 atm, 24 h, THF, Zn (0.01 g).

Table 9. Solvent effect. $Ru(acac)_2(phosphine)_{1\text{-}2}$ systems in toluene.

Catalyst	Phosphine (equivalents)	% Conversion of methyl benzoate	% Yield of benzyl alcohol	% Yield of methanol
$Ru(acac)_3$	triphos (2 eq)	52	41	37
$Ru(acac)_2(PPh_3)_2$	-	1	0	0
$Ru(acac)_2$dppp	-	2	0	0
$Ru(acac)_2$dppf	-	5	1	0

a. Conditions: 100 °C, p(H_2) = 68 atm, 24 h, toluene, Zn (0.01 g).

Table 10. Solvent effect. $Ru(acac)_2(phosphine)_{1\text{-}2}$ systems in diglyme.

Catalyst	Phosphine (equivalents)	% Conversion of methyl benzoate	% Yield of benzyl alcohol	% Yield of methanol
$Ru(acac)_3$	triphos (2 eq)	76	64	62
$Ru(acac)_2(PPh_3)_2$	-	3	0	0
$Ru(acac)_2$dppp	-	8	2	1
$Ru(acac)_2$dppf	-	24	9	8

a. Conditions: 100 °C, p(H_2) = 68 atm, 24 h, diglyme, Zn (0.01 g).

As can be seen from the results displayed in Tables 8, 9 and 10, variation of the solvent does have an effect on the amount of ester converted with diglyme producing the largest conversions. The systems continued to follow the trend that the preformed Ru(II) species are ineffective for the hydrogenation of methyl benzoate, further nullifying the hypothesis of $Ru(acac)_2(phosphine)_{1\text{-}2}$ systems improving conversions of esters to the desired alcohols.

As the systems developed by Elsevier and Teunissen and Nomura *et al*. required ratios of phosphine:$Ru(acac)_3$ greater than those used to produce the $Ru(acac)_2(phosphine)_{1\text{-}2}$ compounds, it was hypothesized that the $Ru(acac)_2(phosphine)_{1\text{-}2}$ systems may require additional equivalents of phosphine to obtain significant yields to the desired alcohols. With that, a series of reactions was performed according to subsection 2.3.3 with the results displayed in Table 11.

Table 11. Hydrogenation of methyl benzoate using $Ru(acac)_2(phosphine)_{1-2}$ with 4 (monodentate) or 2 (bidentate) additional equivalents of various phosphines.

Catalyst	Phosphine (equivalents)	% Conversion of methyl benzoate	% Yield of benzyl alcohol	% Yield of methanol
$Ru(acac)_2(PPh_3)_2$	PPh_3 (4 eq)	31	13	13
$Ru(acac)_2$dppp	dppp (2 eq)	40	18	16
$Ru(acac)_2$dppf	dppf (2 eq)	49	20	19
$Ru(acac)_3$	$Ru(acac)_2$dppf	88	3	3

a. Conditions: 100 °C, p(H_2) = 68 atm, 24 h, diglyme, Zn (0.01 g).

When comparing Tables 10 and 11, it is evident that the results were improved with the addition of equivalents of phosphine to the $Ru(acac)_2(phosphine)_{1-2}$ systems, further confirming their inability to act as standalone precatalysts for ester hydrogenation reactions. Additional equivalents of phosphine were added to also determine if there was an advantage in starting with a pre-reduced ruthenium species rather than a Ru(III) species. Although the conversion of methyl benzoate was increased, the results obtained did not show any improvement from the previous $Ru(acac)_3$/phosphine systems.

An interesting result was obtained when two ruthenium species ($Ru(acac)_3$ and $Ru(acac)_2$dppf) were combined for a single reaction. A large portion of methyl benzoate was converted not to the desired alcohols as anticipated but rather to an unexpected compound. Rather than hydrogenating the ester functionality, the system hydrogenated the benzene ring and the unexpected product was determined to be methyl cyclohexanecarboxylate through GC-MS. Upon further investigation, ruthenium metal was found coated to the glass insert after the completion of a hydrogenation reaction. The hydrogenation of methyl benzoate was attempted using the ruthenium coated glass insert in the absence of addition catalyst. Methyl cyclohexanecarboxylate was once again obtained suggesting ruthenium metal to be hydrogenating the benzene ring, an observation already stated in the literature.[66]

The overall conversions of methyl benzoate to the desired alcohols using the $Ru(acac)_2(phosphine)_{1-2}$ systems were not promising, as the results obtained showed no

improvement from those stated in the literature. A final series of reactions was performed with the results displayed in Table 12. The series was based on observations made by Abdur-Rashid *et al*.[65] and Takebayashi and Bergens[49] suggesting the presence of $KOBu^t$ to have beneficial effects on catalytic systems for ester hydrogenations.

Table 12. Additive effect. $Ru(acac)_2(phosphine)_{1\text{-}2}$ system with the addition of $KOBu^t$.

Catalyst	Phosphine (equivalents)	% Conversion of methyl benzoate	% Yield of benzyl alcohol	% Yield of methanol
$Ru(acac)_3$	triphos (2 eq)	55	40	39
$Ru(acac)_2(PPh_3)_2$	-	1	0	0
$Ru(acac)_2(PPh_3)_2$	PPh_3 (4 eq)	12	6	8
$Ru(acac)_2$dppp	-	0	0	0
$Ru(acac)_2$dppp	dppp (2 eq)	16	8	9
$Ru(acac)_2$dppf		1	0	0
$Ru(acac)_2$dppf	dppf (2 eq)	31	16	12

a. Conditions: 100 °C, $p(H_2)$ = 68 atm, 24 h, diglyme, $KOBu^t$ (0.01 g).

The reaction trends observed were similar to those obtained in the presence of zinc, but the percent conversion was decreased, suggesting zinc to be a more effective additive.

3.3 Summary and Conclusion

Ester hydrogenation reactions have been catalyzed by a system involving the *in situ* generation of active species from a reaction of $Ru(acac)_3$ with phosphines.[51,56,58] The literature suggests the active species to be a Ru(II) complex[51,56-58,60] and therefore a series of $Ru(acac)_2(phosphine)_{1\text{-}2}$ species were synthesized.

This thesis reports the synthesis and characterization of $Ru(acac)_2(PPh_3)_2$, $Ru(acac)_2$dppf, and $Ru(acac)_2$dppp. These complexes were tested as potential catalysts for the difficult hydrogenation reaction of converting esters into their corresponding alcohols.

This thesis reports the insufficient conversions of the ester while in the presence of the newly synthesized Ru(II) species. Higher conversions of the ester were obtained when additional

equivalents of phosphines were added to the $Ru(acac)_2(phosphine)_{1-2}$ systems. The results obtained with the addition of phosphines demonstrated that there was no benefit in starting with a pre-reduced Ru(II) complex as higher conversions were obtained using the $Ru(acac)_3$/phosphine systems.

Although the literature suggests the active catalyst to be a Ru(II) species generated *in situ*, the Ru(II) complexes synthesized and tested in this report are not the active catalysts. The project was dropped as there seemed to be discrepancies with the literature.

References

1. (a) Tamao, K.; Miyaura, N. *Top. Curr. Chem.*, **2002**, *219*, 1. (b) Echavarren, A. M.; Cardenas, D. J. *Metal Catalyzed Cross-Coupling Reactions*, 2nd ed.; de Mejiere, A.; Diederich, F., Eds.; John Wiley & Sons: New York, 2004; pp 1 – 40. (c) Negishi, E. *Acc. Chem. Res.*, **1982**, *15*, 340. (d) Stanforth, S. P. *Tetrahedron*, **1998**, *54*, 263.
2. Jiang, L.; Buchwald, S. L. *Metal Catalyzed Cross-Coupling Reactions*, 2nd ed.; de Mejiere, A.; Diederich, F., Eds.; John Wiley & Sons: New York, **2004**; pp 699 – 756.
3. Kim, J.H.; Lee, D.H.; Jun, B.H.; Lee, Y.S. *Tet. Lett.*, **2007**, *48*, 7079.
4. Shirakawa, E.; Kitabata, T.; Otsuka, H.; Tsuchimoto, T. *Tetrahedron*, **2005**, *61*, 9878.
5. Ljungdahl, T.; Bennur, T.; Dallas, A.; Emtenas, H.; Martensson, *J. Organometallics*, **2008**, *27*, 2490.
6. Stephens, R.D.; Castro, C.E.; *J. Org. Chem*., **1963**, *28*, 3313.
7. Cassar, L. *J. Org. Chem*., **1975**, *93*, 253.
8. Diek, H.A.; Heck, F.R.; *J. Org. Chem*., **1975**, *93*, 259.
9. Tykwinski, R.R. *Angew. Chem. Int. Ed*. **2003**, *42*, 1566.
10. Sonogashira, K.; Tohda, Y.; Hagihara, N. *Tet. Lett.*, **1975**, *50*, 4467.
11. Doucet, H.; Hierso, J. C. *Angew. Chem. Int. Ed*. **2007**, *46*, 834.
12. Chinchilla, R.; Najera, C. *Chem. Rev.*, **2007**, *107*, 874.
13. (a) Cornils, B.; Herrmann, W.A. *Applied Homogeneous Catalysis with Organometallic Compounds*., Eds.; Wiley-VCH: Weinheim, **1996**. (b) Negishi, E.; de Meijere, A. *Handbook of Organopalladium Chemistry for Organic Synthesis.*, Eds.; Wiley: New York, **2002**. (c) Beller, M.; Bolm, C. *Transition Metals for Organic Synthesis*., Eds.; Wiley-VCH: Weinheim, **2004**.
14. Kotha, S.; Lahiri, K.; Kashinath, D. *Tetrahedron*, **2002**, *58*, 9633.
15. Hills, I. D.; Netherton, M. R.; Fu, G. C. *Angew. Chem. Int. Ed.*, **2003**, *42*, 5749.
16. Amatore, C.; Jutand, A. *J. Organomet. Chem.*, **1999**, *576*, 254.

17. Amatore, C.; Pfluger, F. *Organometallics*, **1990**, *9*, 2278.

18. Casado, A. L.; Espinet, P. *Organometallics*, **1998**, *17*, 954.

19. Crabtree, R. H. *The Organometallic Chemistry of the Transition Metals*, 4th ed.; John Wiley & Sons: New Jersey, **2005**; pp 159 – 181.

20. Bertus, P.; Fecourt, F.; Bauder, C.; Pale, P. *New J. Chem*., **2004**, *28*,12.

21. Miyaura, N.; Suzuki, A. *Chem. Rev.*, **1995**, *95*, 2457.

22. Soheili, A.; Albaneze-Walker, J.; Murry, J.; Dormer, P.G.; Hughs, D.L. *Org. Lett*., **2003**, *5*, 4191.

23. Amatore, C.; Bensalen, S.; Ghalem, S.; Jutand, A. *J. Organomet. Chem*., **2004**, *689*, 4642.

24. Jutand, A. *Pure Appl. Chem*., **2004**, *76*, 565.

25. Panda, B.; Sarkar, T. *Tet. Lett.*, **2010**, *51*, 301.

26. Hundertmark, T.; Littke, A.F.; Buchwald, S.L.; Fu, G.C. *Organic Letters*, **2000**, *2*, 1729.

27. Bohm, V.P.; Herrmann, W.A. *Eur. J. Org. Chem*., **2000**, 3679.

28. Dubbaka, S.R.; Vogel, P. *Adv. Synth. Catal*. **2004**, *346*, 1793.

29. Thorand, S.; Krause, N. *J. Org. Chem*. **1998**, *63*, 8551.

30. Roy, A. H.; Hartwig, J. F. *J. Am. Chem. Soc.*, **2001**, *123*, 1232.

31. Hartwig, J. F. *Inorg. Chem.*, **2007**, *46*, 1936.

32. Amatore, C.; Jutand, A.; Khalil, F.; M'Barki, M. A.; Mottier, L. *Organometallics*, **1993**, *12*, 3168.

33. Fitton, P.; Rick, E. A. *J. Organomet. Chem*., **1971**, *28*, 287.

34. (a) Amatore, C.; Jutand, A.; M'Barki, M. A. *Organometallics*, **1992**, *11*, 3009. (b) Amatore, C.; Carre, E.; Jutand, A.; M'Barki, M. A. *Organometallics*, **1995**, *14*, 1818. (c) Csákai, Z.; Skoda-Földes, R.; Kollár, L. *Inorg. Chim. Acta*, **1999**, *286*, 93.

35. Fiaud, J. C.; De Gournay, A. H.; Larcheeveque, M.; Kagan, H. B. *J. Organomet. Chem.*, **1978**, *154*, 175.

36. Amatore, C.; Jutand, A. *Coord. Chem. Rev.*, **1998**, *178-180*, 511.

37. Amatore, C.; Azzabi, M.; Jutand, A. *J. Am. Chem. Soc*., **1991**, *113*, 8375.

38. Norton, D.M.; Mitchell, E.A.; Botros, N.R.; Jessop, P.G.; Baird, M.C. *J. Org. Chem*., **2009**, *74*, 6674.

39. Lord, M.A.; Mahon, M.F.; Lloyd, M.D.; Threadgill, M.D. *J. Med. Chem*., **2009**, *52*, 868.

40. Tellier, F.; Sauvetre, R.; Norman, J. *J. Organomet. Chem*., **1985**, *292*, 19.

41. D'Amato, R.; Furlani, A.; Colapietro, M.; Portalone, G.; Casalboni, M.; Falconieri, M.; Russo, M.V. *J. Organomet. Chem*., **2001**, *627*, 13.

42. Pietrusewicz, E.; Sienczyk, M.; Oleksyszyn, J. *J. Enzyme Inhibition and Medicinal Chem*., **2009**, *24*, 1229.

43. Ngassa, F. N.; Lindsey, E. A.; Haines, B. E. *Tetrahedron*, **2009**, *65*, 4085.

44. Komaromi, A.; Laszlo, G.; Novak, Z. *Tet. Lett*., **2008**, *49*, 7294Naota, T.; Takaya, H.; Murahashi, S. I. *Chem. Rev.*, **1998**, *98*, 2599.

45. Naota, T.; Takaya, H.; Murahashi, S. I. *Chem. Rev.*, **1998**, *98*, 2599.

46. McAlees, A. J.; McCrindle, R. *J. Chem. Soc.*, **1969**, 2425.

47. Carey, F. A.; Sundberg, R. J. *Advanced Organic Chemistry*, 4th ed., Kluwer Academic/Plenum: New York, **2000.**

48. Burkey, D. J.; Debad, J. D.; Legzdins, P. J. *J. Am. Chem. Soc.*, **1997**, *119*, 1139.

49. Takebayashi, S.; Bergens, S. H. *Organometallics*, **2009**, *28*, 2349.

50. Ege, S. N.; *Organic Chemistry*, D. C. Heath and Company, Lexington, **1989**, p.596.

51. Teunissen, H. T.; Elsevier, C. J. *Chem, Commun.*, **1998**, 1367.

52. Zhang, J.; Leitus, G.; Ben-Davis, Y.; Milstein, D. *Angew. Chem. Int. Ed.*, **2006**, *45*, 1113.

53. Grey, R. A.; Pez, G. P.; Wallo, A. *J. Am. Chem. Soc.*, **1981**, *103*, 7536.

54. Matteoli, U.; Mench, G.; Bianch, M.; Piacenti, F. *J. Mol. Catal.*, **1988**, *44*, 347.

55. Matteoli, U.; Mench, G.; Bianch, M.; Piacenti, F.; Ianelli, S.; Nardelli, M. *J. Organomet. Chem.*, **1995**, 498.

56. Teunissen, H.; Elsevier, C. J. *Chem. Commun*., **1997**, 667.

57. Hara, Y.; Inagaki, H.; Nishimura, S.; Wada, K. *Chem. Lett*., **1992.**

58. Nomura, K.; Ogura, H.; Imanishi, Y. *J. Mol. Catal*., **2002**, *178*, 105.

59. Saudan, L. A.; Saudan, C. M.; Debieux, C.; Wyss, P. *Angew. Chem. Int. Ed.*, **2007**, *46*, 7473.

60. van Engelen, M. C.; Teunissen, H. T.; de Vries, J. G.; Elsevier, C. J. *J. Mol. Cat*., **2006**, *206*, 185.

61. Knowles, T. S.; Howells, M. E.; Howlin, B. J.; Smith, G. W. *Polyhedron*, **1994**, *13*, 2197.

62. Gupta, A. K.; Poddar, R. K. *Indian Journal of Chemistry*, **2000**, *39*, 457.

63. Hoshino, Y.; Yukawa, Y.; Maruyama, T.; Endo, A.; Shimizu, K. *Inorganica Chimica Acta*, **1990**, *174*, 41.

64. Miessler, G. L.; Tarr, D. A. *Inorganic Chemistry* 3rd ed; Pearson Education Inc.: New Jersey, **2004**; pp. 437-440.

65. Abdur-Rashid, K.; Guo, R.; Lough, A. J.; Morris, R. H.; Song, D. *Adv. Synth. Catal*., **2005**, *347*, 571.

66. Wang, H.; Zhao, F. *Int. J. Mol. Sci.*, **2007**, *8*, 628.

Appendix B

Crystal Structure Data

The crystal structure determination was performed by Dr. Ruiyao Wang in the X-ray Crystallography Laboratory at Queen's University. Diffraction intensity data were collected with a Bruker SMART APEX II X-ray diffractometer with graphite-monochromated Mo K_α radiation (λ = 0.71073 Å) controlled with Cryostream Controller 700. The space group was determined from systematic absences in the diffraction data. The structure was solved by direct methods. Full-matrix least-square refinements minimizing the function $\sum w (F_o^2 - F_c^2)^2$ were applied to the compound. All non-hydrogen atoms were refined anisotropically. All of the other H atoms were placed in geometrically calculated positions, with C-H = 1.00(Cp-), 0.95(phenyl-, $acac^-$) and 0.98 Å (CH_3), and refined as riding atoms, with Uiso(H) = 1.5 UeqC(methyl), or 1.2 Ueq(other C). In addition, the methyl groups were refined with AFIX 137, which allowed the rotation of the methyl groups whilst keeping the C-H distances and X-C-H angles fixed.

Crystal Structure of $Ru(acac)_2dppf$

Table 13. Crystal data and structure refinement for $Ru(acac)_2dppf$.

Empirical formula	C44.50 H43 Cl Fe O4 P2 Ru	
Formula weight	896.10	
Temperature	180(2) K	
Wavelength	0.71073 Å	
Crystal system	Triclinic	
Space group	P-1	
Unit cell dimensions	a = 12.7464(6) Å	□= 91.3730(10)°.
	b = 18.1944(9) Å	□= 96.6190(10)°.
	c = 18.6022(9) Å	γ = 107.6050(10)°.
Volume	4076.7(3) $Å^3$	
Z	4	
Density (calculated)	1.460 Mg/m^3	
Absorption coefficient	0.912 mm^{-1}	
F(000)	1836	
Crystal size	0.35 x 0.30 x 0.30 mm^3	
Theta range for data collection	1.56 to 26.00°.	
Index ranges	-15<=h<=15, -22<=k<=22, -22<=l<=22	
Reflections collected	40313	
Independent reflections	15927 [R(int) = 0.0209]	
Completeness to theta = 26.00°	99.4 %	
Absorption correction	Multi-scan	
Max. and min. transmission	0.7715 and 0.7407	
Refinement method	Full-matrix least-squares on F^2	
Data / restraints / parameters	15927 / 36 / 985	
Goodness-of-fit on F^2	1.031	
Final R indices [I>2sigma(I)]	R1 = 0.0339, wR2 = 0.0908	
R indices (all data)	R1 = 0.0392, wR2 = 0.0958	
Largest diff. peak and hole	2.226 and -2.365 $e.Å^{-3}$	

Table 14. Select bond lengths [Å] and angles [°] for $Ru(acac)_2dppf$

Ru(1)-O(3)	2.0564(19)
Ru(1)-O(1)	2.0569(19)
Ru(1)-O(4)	2.086(2)
Ru(1)-O(2)	2.099(2)
Ru(1)-P(1)	2.2731(8)
Ru(1)-P(2)	2.2843(7)
Ru(2)-O(6)	2.0508(19)
Ru(2)-O(8)	2.0685(19)
Ru(2)-O(5)	2.090(2)
Ru(2)-O(7)	2.0956(19)
Ru(2)-P(4)	2.2752(7)
Ru(2)-P(3)	2.2762(8)

O(3)-Ru(1)-O(1)	172.00(8)
O(3)-Ru(1)-O(4)	90.78(8)
O(1)-Ru(1)-O(4)	82.34(8)
O(3)-Ru(1)-O(2)	83.36(8)
O(1)-Ru(1)-O(2)	91.54(8)
O(4)-Ru(1)-O(2)	81.42(8)
O(3)-Ru(1)-P(1)	94.97(6)
O(1)-Ru(1)-P(1)	89.16(6)
O(4)-Ru(1)-P(1)	90.23(6)
O(2)-Ru(1)-P(1)	171.44(6)
O(3)-Ru(1)-P(2)	93.62(6)
O(1)-Ru(1)-P(2)	92.50(6)
O(4)-Ru(1)-P(2)	169.47(6)
O(2)-Ru(1)-P(2)	89.60(6)
P(1)-Ru(1)-P(2)	98.90(3)

O(6)-Ru(2)-O(8)	172.46(8)
O(6)-Ru(2)-O(5)	91.80(8)
O(8)-Ru(2)-O(5)	83.09(8)
O(6)-Ru(2)-O(7)	82.22(8)
O(8)-Ru(2)-O(7)	91.60(8)
O(5)-Ru(2)-O(7)	82.74(8)
O(6)-Ru(2)-P(4)	96.10(6)
O(8)-Ru(2)-P(4)	89.41(6)
O(5)-Ru(2)-P(4)	89.39(6)
O(7)-Ru(2)-P(4)	171.88(6)
O(6)-Ru(2)-P(3)	91.44(6)
O(8)-Ru(2)-P(3)	92.79(6)
O(5)-Ru(2)-P(3)	170.63(6)
O(7)-Ru(2)-P(3)	88.99(6)
P(4)-Ru(2)-P(3)	99.01(3)

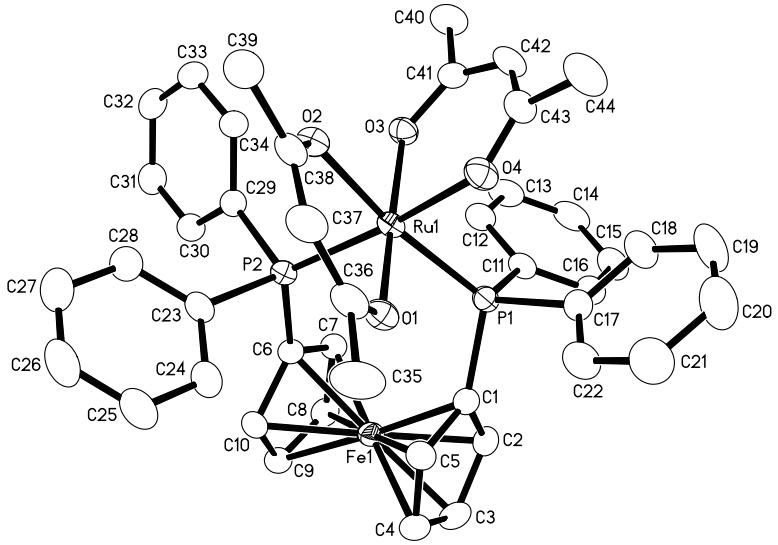

Crystal Structure for $Ru(acac)_2(PPh_3)_2$

Table 15. Crystal data and structure refinement for $Ru(acac)_2(PPh_3)_2$.

Empirical formula	C46 H44 O4 P2 Ru	
Formula weight	823.82	
Temperature	180(2) K	
Wavelength	0.71073 Å	
Crystal system	Triclinic	
Space group	P-1	
Unit cell dimensions	a = 10.4116(4) Å	α= 75.349(2)°.
	b = 10.9543(4) Å	β= 87.491(2)°.
	c = 17.8482(5) Å	γ = 80.996(2)°.
Volume	1945.14(12) $Å^3$	
Z	2	
Density (calculated)	1.407 Mg/m^3	
Absorption coefficient	0.529 mm^{-1}	
F(000)	852	
Crystal size	0.25 x 0.20 x 0.10 mm^3	
Theta range for data collection	1.98 to 26.00°.	
Index ranges	-12<=h<=12, -13<=k<=13, -21<=l<=21	
Reflections collected	15463	
Independent reflections	7554 [R(int) = 0.0579]	
Completeness to theta = 26.00°	98.8 %	
Absorption correction	Multi-scan	
Max. and min. transmission	0.9490 and 0.8791	
Refinement method	Full-matrix least-squares on F^2	
Data / restraints / parameters	7554 / 0 / 482	
Goodness-of-fit on F^2	0.975	
Final R indices [I>2sigma(I)]	R1 = 0.0509, wR2 = 0.1055	
R indices (all data)	R1 = 0.0790, wR2 = 0.1196	
Largest diff. peak and hole	0.837 and -0.808 $e.Å^{-3}$	

Table 16. Select bond lengths [Å] and angles [°] for $Ru(acac)_2(PPh_3)_2$

Ru(1)-O(3)	2.060(3)
Ru(1)-O(2)	2.063(3)
Ru(1)-O(1)	2.096(3)
Ru(1)-O(4)	2.096(3)
Ru(1)-P(1)	2.2953(11)
Ru(1)-P(2)	2.3263(11)
O(3)-Ru(1)-O(2)	172.93(10)
O(3)-Ru(1)-O(1)	85.02(10)
O(2)-Ru(1)-O(1)	90.52(10)
O(3)-Ru(1)-O(4)	91.29(10)
O(2)-Ru(1)-O(4)	82.71(10)
O(1)-Ru(1)-O(4)	83.04(10)
O(3)-Ru(1)-P(1)	94.01(7)
O(2)-Ru(1)-P(1)	89.79(8)
O(1)-Ru(1)-P(1)	173.45(8)
O(4)-Ru(1)-P(1)	90.51(7)
O(3)-Ru(1)-P(2)	87.79(8)
O(2)-Ru(1)-P(2)	97.53(8)
O(1)-Ru(1)-P(2)	87.71(8)
O(4)-Ru(1)-P(2)	170.75(7)
P(1)-Ru(1)-P(2)	98.74(4)

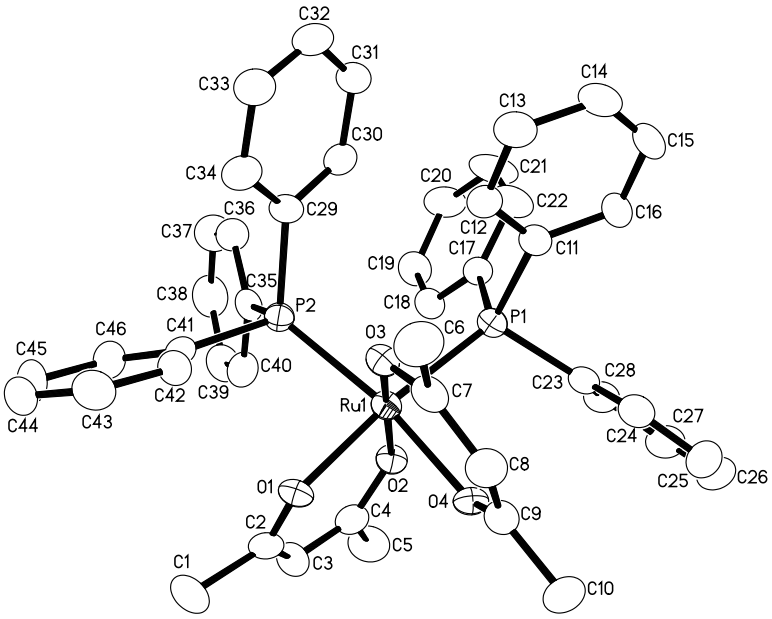
C32
C31
C33
C30
C34
C29
C36
C37
C35
C38
P2
C41
C46
C45
C40
C42
C39
C44
C43
Ru1
O3
C6
C7
P1
C13
C14
C15
C21
C20
C22
C16
C12
C11
C17
C19
C18
C23
C28
C27
C24
C25
C26
C8
O1
O2
O4
C9
C2
C4
C5
C1
C3
C10

Crystal Structure of $Ru(acac)_2dppp$

Table 17. Crystal data and structure refinement for $Ru(acac)_2dppp$

Empirical formula	C37 H40 O4 P2 Ru	
Formula weight	711.70	
Temperature	180(2) K	
Wavelength	0.71073 Å	
Crystal system	Monoclinic	
Space group	P2(1)/n	
Unit cell dimensions	a = 10.5020(10) Å	α= 90°.
	b = 17.5754(16) Å	β= 102.6830(10)°.
	c = 18.1782(17) Å	γ = 90°.
Volume	3273.4(5) $Å^3$	
Z	4	
Density (calculated)	1.444 Mg/m^3	
Absorption coefficient	0.616 mm^{-1}	
F(000)	1472	
Crystal size	0.30 x 0.25 x 0.25 mm^3	
Theta range for data collection	1.63 to 26.00°.	
Index ranges	-12<=h<=12, -21<=k<=21, -22<=l<=22	
Reflections collected	27011	
Independent reflections	6421 [R(int) = 0.0463]	
Completeness to theta = 26.00°	99.7 %	
Absorption correction	Multi-scan	
Max. and min. transmission	0.8612 and 0.8368	
Refinement method	Full-matrix least-squares on F^2	
Data / restraints / parameters	6421 / 0 / 401	
Goodness-of-fit on F^2	1.052	
Final R indices [I>2sigma(I)]	R1 = 0.0333, wR2 = 0.0714	
R indices (all data)	R1 = 0.0463, wR2 = 0.0770	
Largest diff. peak and hole	0.483 and -0.547 $e.Å^{-3}$	

Table 18. Select bond lengths [Å] and angles [°] for $Ru(acac)_2dppp$

Ru(1)-O(2)	2.0694(17)
Ru(1)-O(3)	2.0703(17)
Ru(1)-O(4)	2.1030(18)
Ru(1)-O(1)	2.1065(18)
Ru(1)-P(2)	2.2541(7)
Ru(1)-P(1)	2.2568(8)
O(2)-Ru(1)-O(3)	170.88(7)
O(2)-Ru(1)-O(4)	81.17(7)
O(3)-Ru(1)-O(4)	91.29(7)
O(2)-Ru(1)-O(1)	90.78(7)
O(3)-Ru(1)-O(1)	83.56(7)
O(4)-Ru(1)-O(1)	86.06(7)
O(2)-Ru(1)-P(2)	96.84(5)
O(3)-Ru(1)-P(2)	88.64(5)
O(4)-Ru(1)-P(2)	93.27(5)
O(1)-Ru(1)-P(2)	172.16(5)
O(2)-Ru(1)-P(1)	100.94(5)
O(3)-Ru(1)-P(1)	86.32(6)
O(4)-Ru(1)-P(1)	176.16(5)
O(1)-Ru(1)-P(1)	90.69(5)
P(2)-Ru(1)-P(1)	89.67(3)

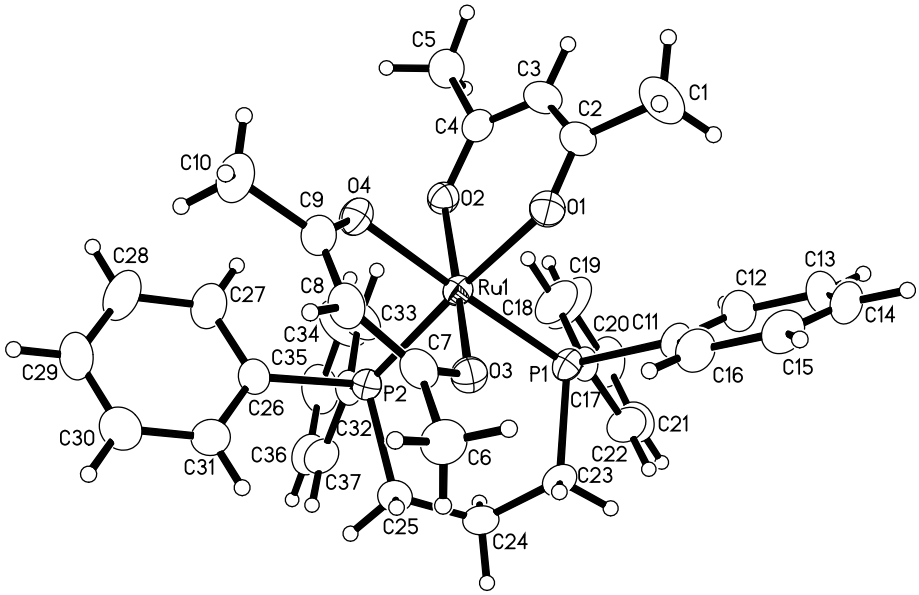
C5
C3
C1
C2
C4
C10
O4
C9
O2
O1
C28
C27
C8
Ru1
C19
C18
C20
C11
C12
C13
C14
C33
C34
C7
C35
O3
P1
C16
C15
C29
P2
C17
C26
C21
C32
C30
C6
C22
C36
C31
C37
C23
C25
C24

Appendix C.

Calibration Curves and a Sample GC Spectrum

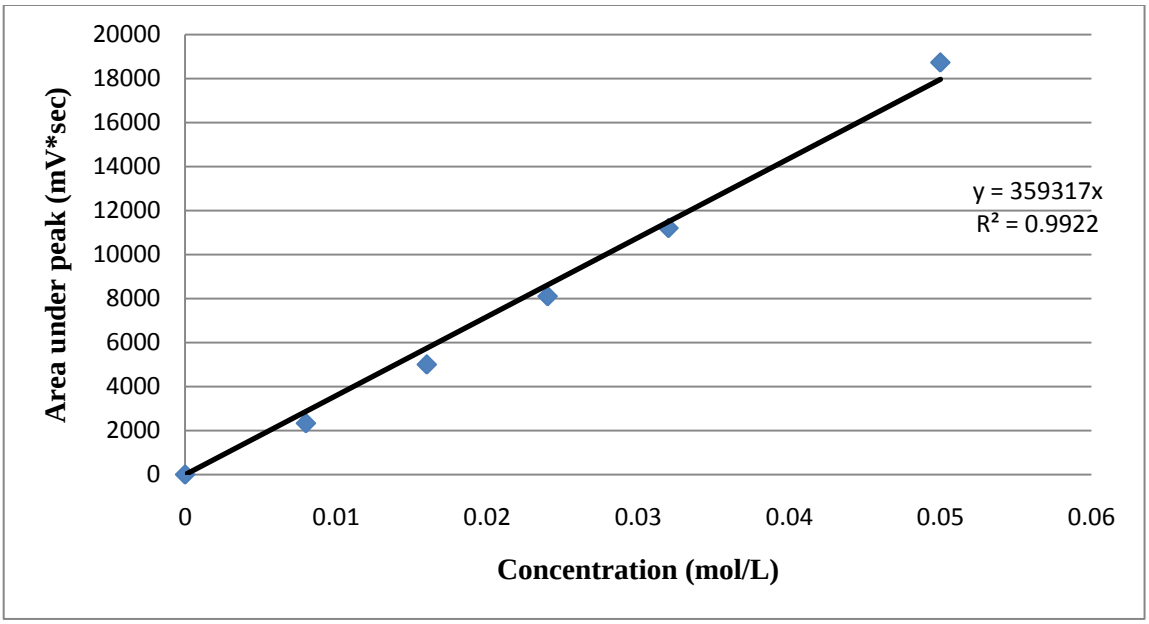

Figure 53. Benzyl alcohol calibration curve.

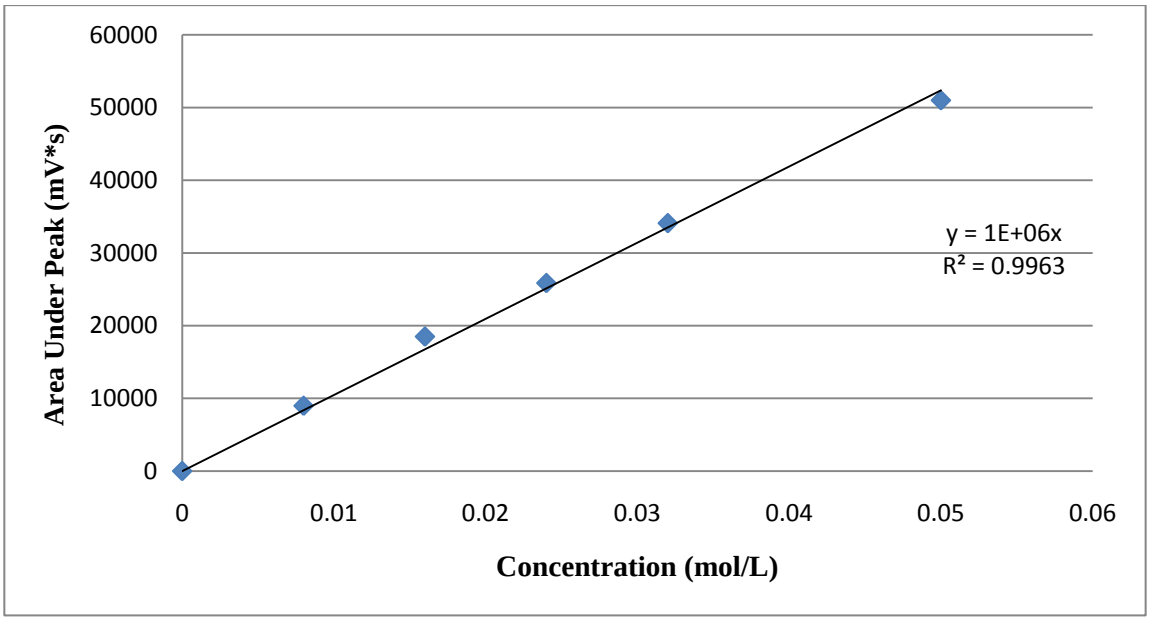

Figure 54. Methanol calibration curve.

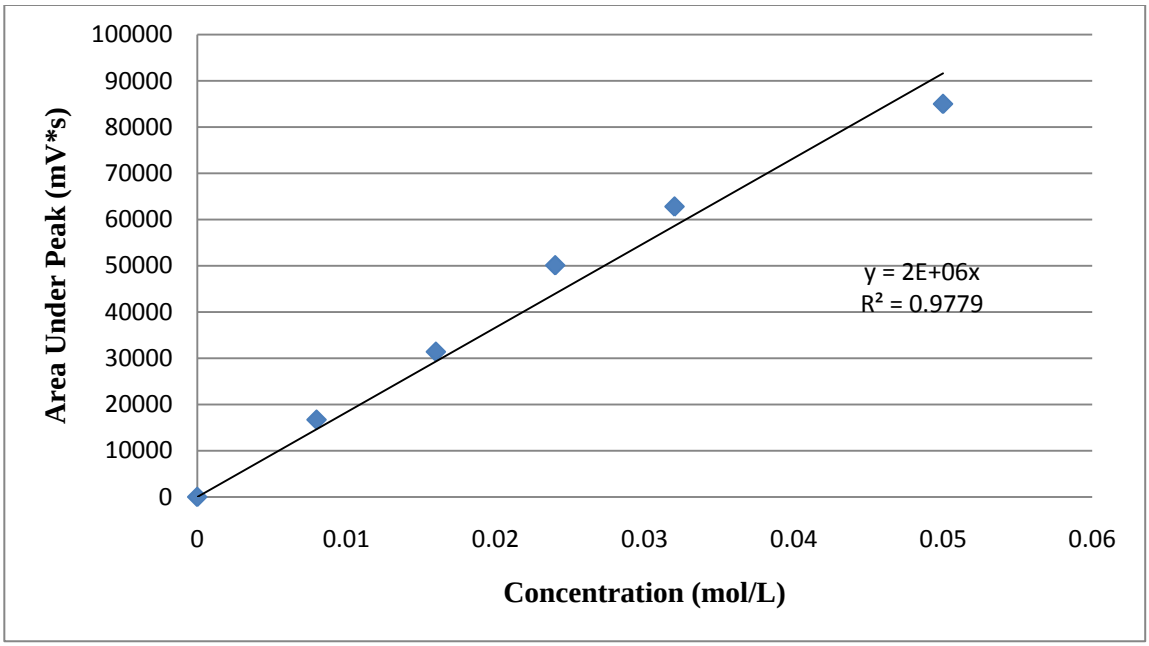

Figure 55. Methyl benzoate calibration curve.

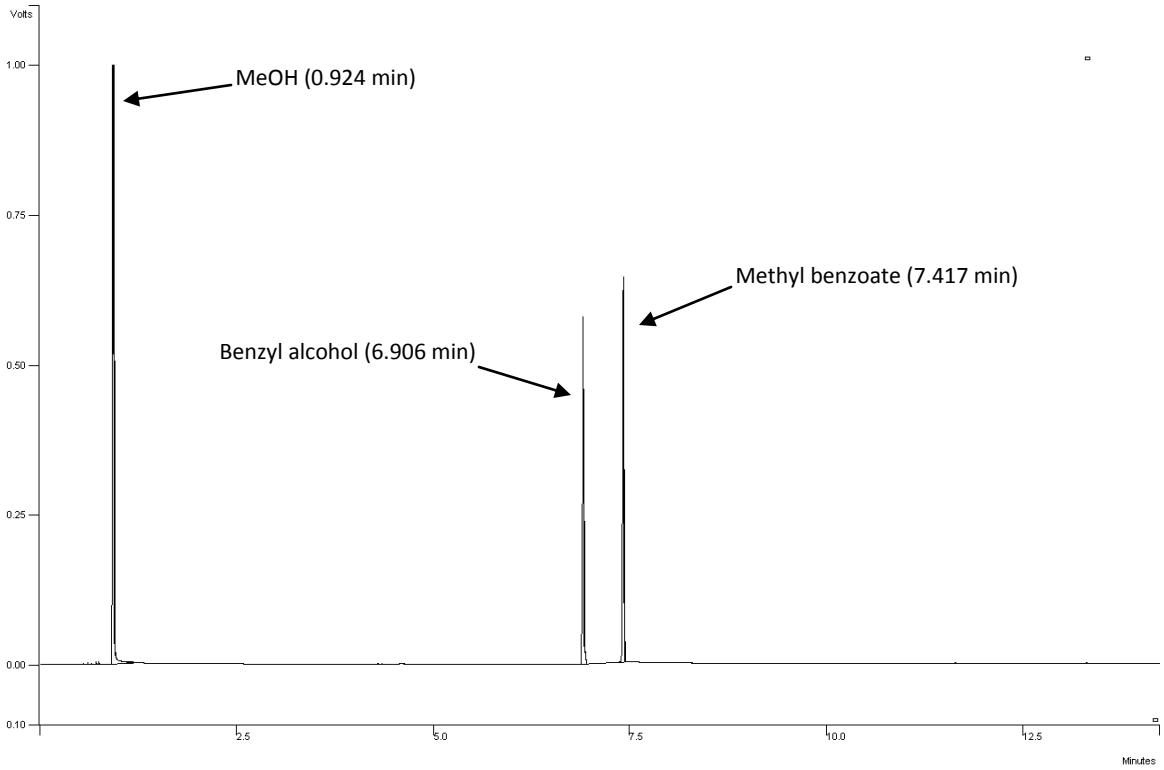

Figure 56. Sample GC spectrum for the hydrogenation of methyl benzoate to produce benzyl alcohol and methanol.

Appendix D

NMR Spectra

NMR Spectra for $Ru(acac)_2(PPh_3)_2$ (^{31}P top and ^{1}H bottom)

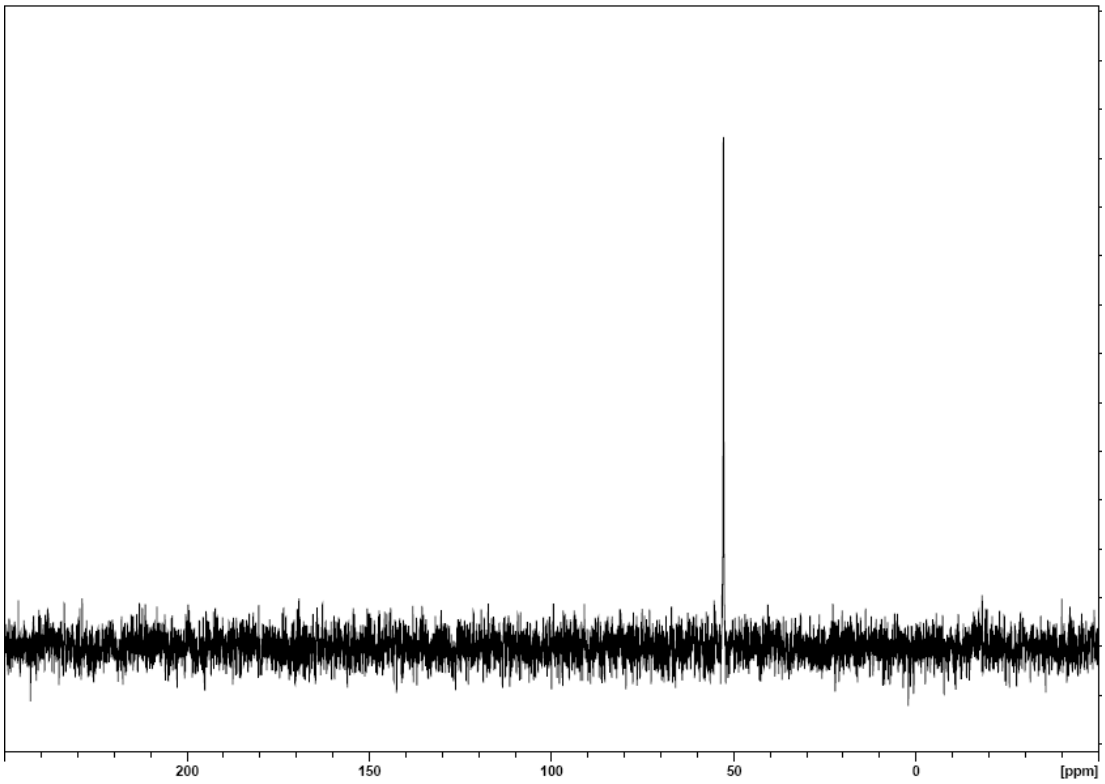

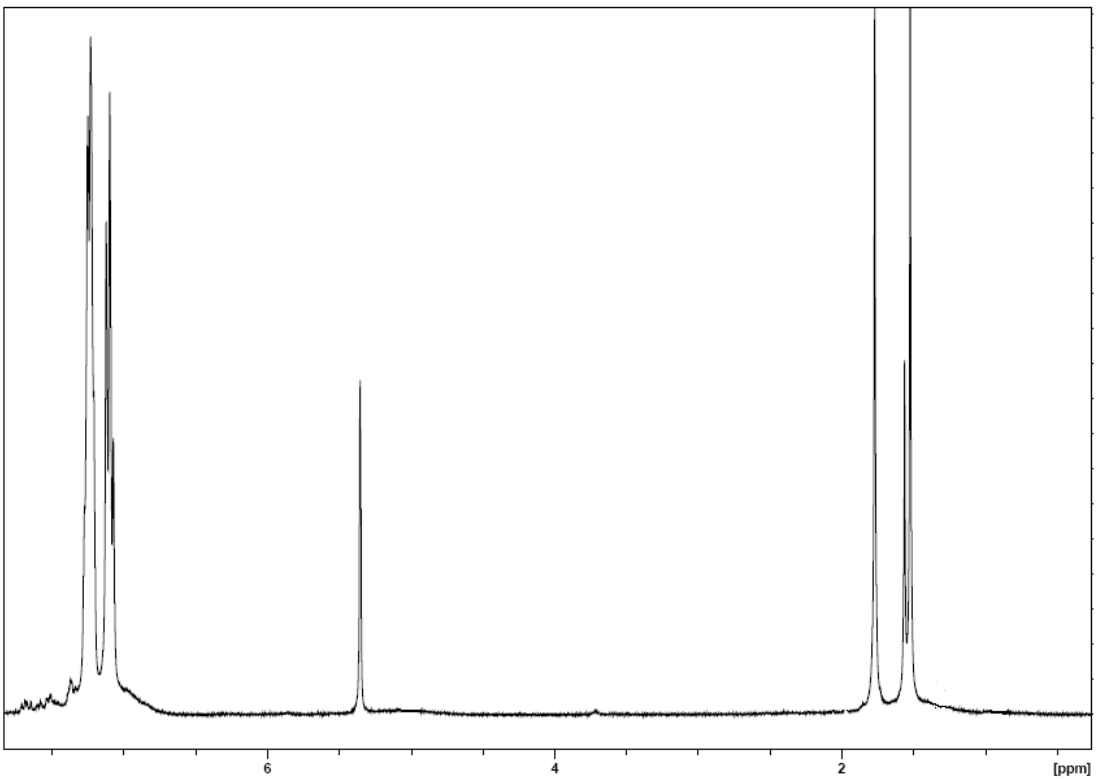

NMR Spectra of $Ru(acac)_2dppp$ (^{31}P top and ^{1}H bottom)

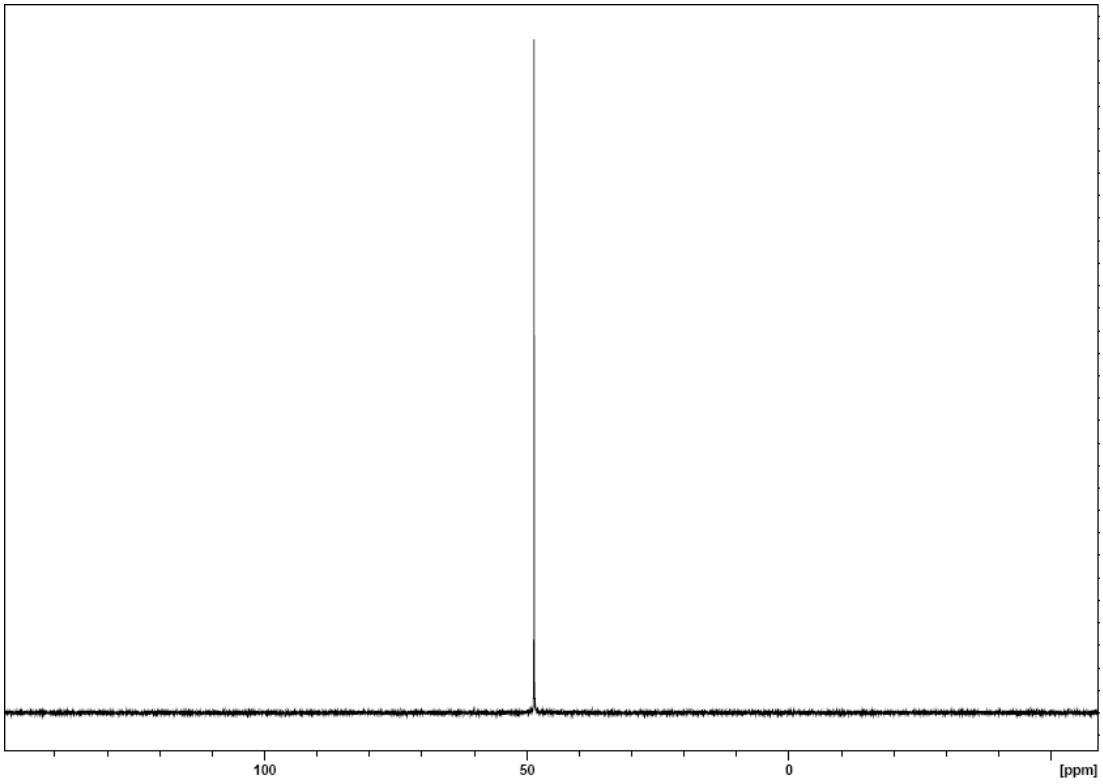

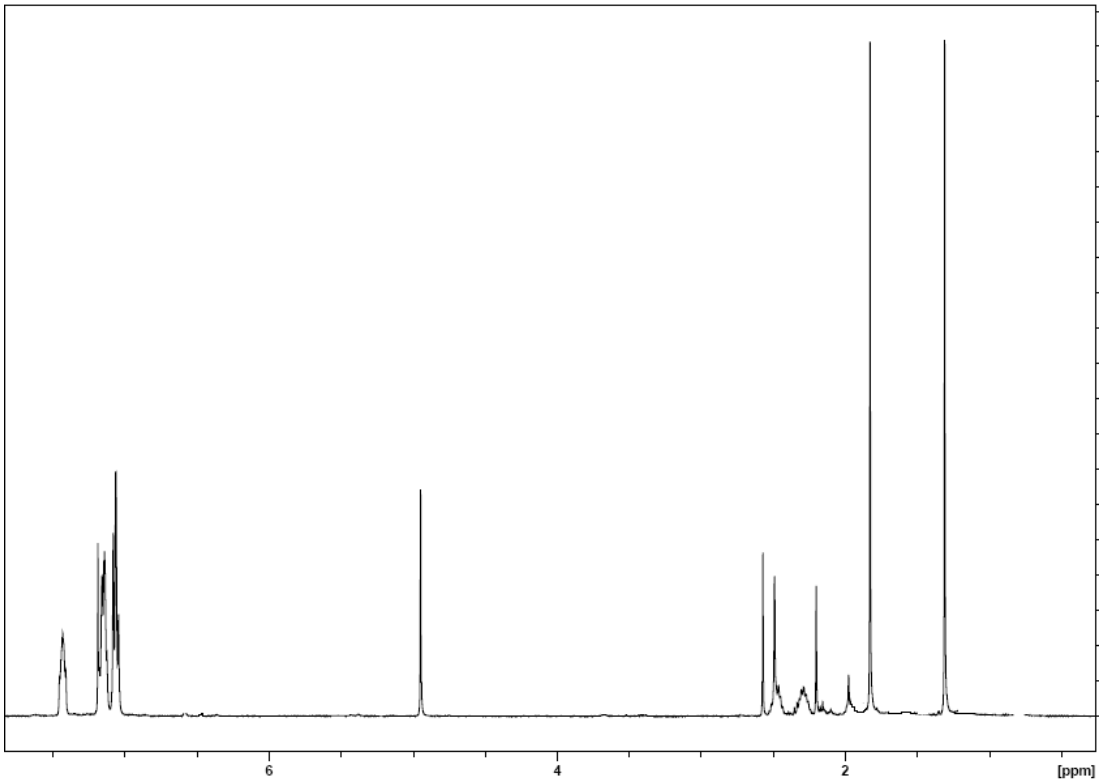

NMR Spectra for $Ru(acac)_2dppf$ (^{31}P top and ^{1}H bottom)

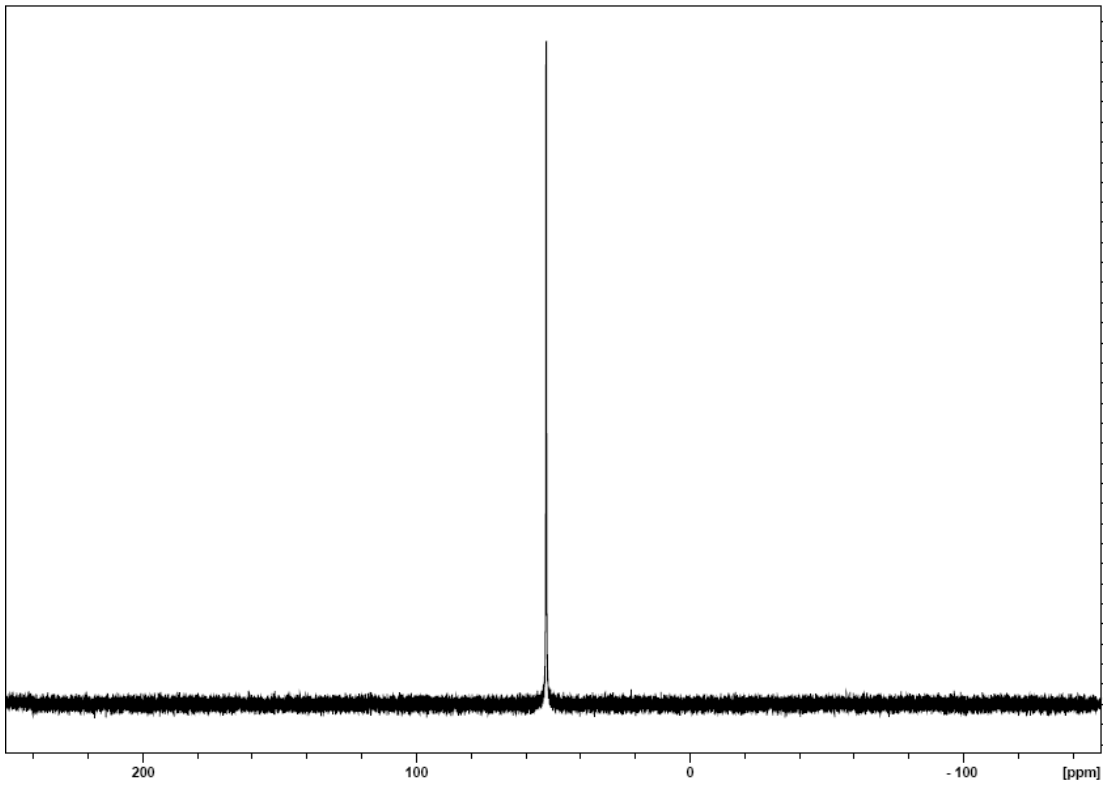

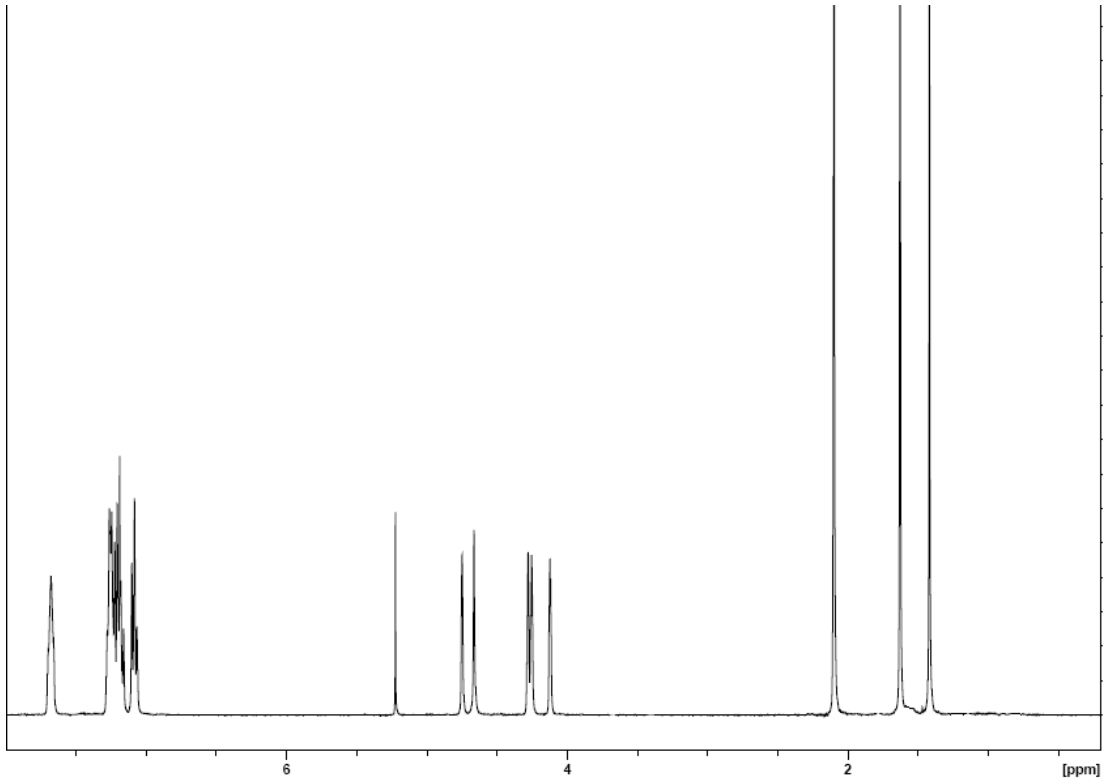

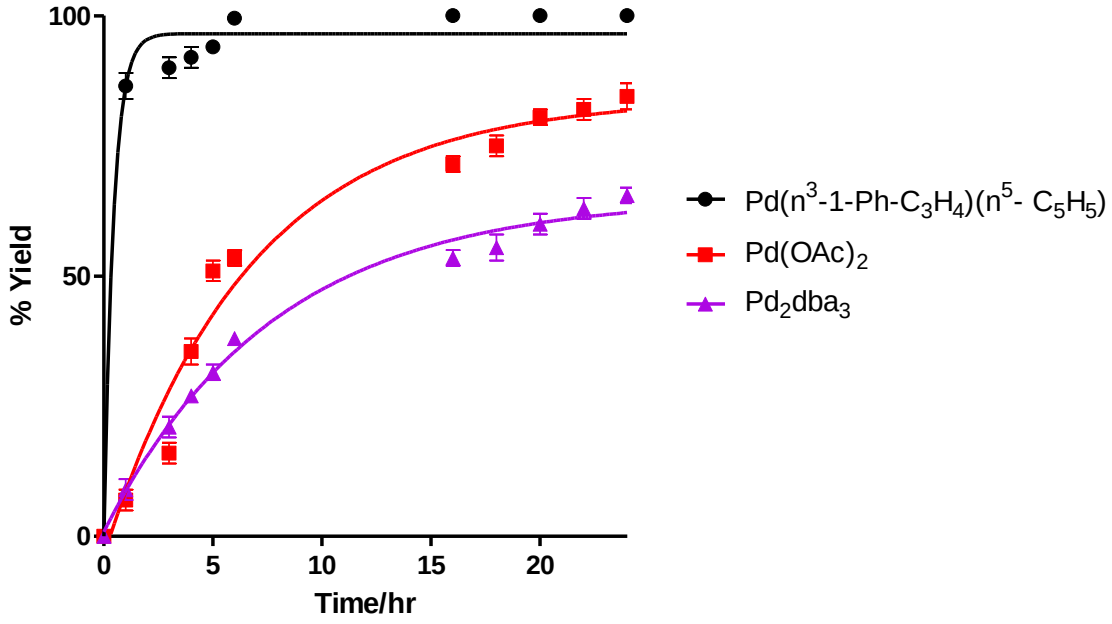

Figure 57. Sample of a plot for eq. 1 showing error bars associated with the precatalysts.